THE UNIVERSITY OF OKLAHOMA

GRADUATE COLLEGE

# KINETIC STUDY OF THE FORMATION OF CYCLOHEXENE FROM ETHYLENE AND BUTADIENE AT ELEVATED PRESSURES AND TEMPERATURES

A DISSERTATION

SUBMITTED TO THE GRADUATE FACULTY

in partial fulfillment of the requirements for the degree of

DOCTOR OF PHILOSOPHY

BY

JOSEPH L. SKINNER

Norman, Oklahoma

1962

KINETIC STUDY OF THE FORMATION OF CYCLOHEXENE FROM ETHYLENE AND BUTADIENE AT ELEVATED PRESSURES AND TEMPERATURES

APPROVED BY

DISSERTATION COMMITTEE

ABSTRACT

Kinetic Study of the Formation of Cyclohexene from Ethylene and Butadiene at Elevated Pressures and Temperatures

The effect of pressure on the rate of a chemical reaction is a phenomenon which has been of interest for many years. However, essentially no kinetic data at elevated pressures have been reported for homogeneous, noncatalyzed gaseous reactions. To obtain a better understanding of the effect of pressure on homogeneous, noncatalytic, gaseous (fluid) systems the Diels-Alder reaction of ethylene with butadiene to form cyclohexene was investigated. The objectives were: (1) to design and construct an efficient continuous flow reactor for use at pressures up to 5,000 lb./sq.in. and temperatures up to 900°F, and (2) to utilize this equipment in making a comprehensive kinetic study to determine the effect of pressure on the reaction rate constant.

The first part of the dissertation covers both the theoretical and practical aspects of high-pressure, high-temperature design for thick-walled vessels. The actual construction and subsequent operation of the experimental

equipment are presented in detail, with particular emphasis on the more difficult operating problems and their solution.

The second part of the dissertation is concerned with the effect of pressure on the reaction rate constant, explained in terms of the two rate theories, for the formation of cyclohexene from ethylene and butadiene. The experimental reaction rate constants are presented in terms of both activities and concentrations and when expressed in terms of activities are in agreement with the absolute reaction rate theory.

## ACKNOWLEDGMENT

The author wishes to thank the staff of the Chemical Engineering Department for their advice and suggestions. In particular, appreciation is extended to Dean C. M. Sliepcevich, Chairman of the author's Doctoral Committee, for his valuable suggestions, patience, encouragement, and interest throughout the course of this work.

The author is indebted to Mr. F. Maginnis of the Research Instrument Company for his valuable help in solving the pumping problems.

Appreciation is extended to Messrs. D. Finn and J. Lott for their help in the use of the IBM 650 computer and to Messrs. K. Bishop and P. Gallier for their help in the use of the Donner 3100 analog computer. The figures were prepared by Mr. J. Samaska. The excellent job of typing by Mrs. Carolyn Staton is appreciated.

The author wishes to thank the Phillips Petroleum Company for supplying the ethylene and Esso Research Laboratories for supplying the butadiene required for this work.

Financial support was received from the Continental Oil Company. The major sponsor of the project has been the National Science Foundation.

Joseph L. Skinner

TABLE OF CONTENTS

LIST OF TABLES

LIST OF ILLUSTRATIONS

# KINETIC STUDY OF THE FORMATION OF CYCLOHEXENE FROM ETHYLENE AND BUTADIENE AT ELEVATED PRESSURES AND TEMPERATURES

## CHAPTER I

## INTRODUCTION

The effect of pressure on the rate of a chemical reaction is a phenomenon which has been of interest for many years. Previous studies have covered a wide range of reactions in both homogeneous and catalyzed liquid systems and in catalyzed gaseous systems. However, except for one system (1) no kinetic data at elevated pressures have been reported for homogeneous, noncatalyzed, gaseous reactions. To obtain a better understanding of the effect of pressure on homogeneous, non-catalytic, gaseous (fluid) systems the Diels-Alder reaction of ethylene with butadiene to form cyclohexene was selected for investigation at elevated pressures and temperatures.

In general, the rate of a chemical reaction in a homogeneous gaseous system is affected in two ways by increased pressure. One is the increase in the activity of the reactants with increased pressure and the other is

the effect of pressure on the reaction rate constant itself. The latter effect is of primary interest in this study.

The objectives of this investigation were: (1) to design and construct an efficient continuous flow reactor system for use at pressures up to 5,000 lb./sq.in. and up to 900°F, and (2) to utilize this equipment in making a comprehensive kinetic study to determine the effect of pressure on the reaction rate constant.

# CHAPTER II

## DESCRIPTION OF EXPERIMENTAL EQUIPMENT

The equipment was designed so that the reaction between ethylene and butadiene would take place continuously, at constant pressure and temperature, in a tubular reactor. A schematic flow diagram of the experimental equipment is shown in Figure 1. A 1.5-cubic feet Autoclave Engineers high pressure vessel (1) was used as the feed reservoir for ethylene at 5,000 lb./sq.in. Water was pumped into the bottom of the high pressure ethylene reservoir with a Sprague, air-operated, liquid pump (2) to maintain the ethylene at a constant 5,000 lb./sq.in. as it was used during a run. The ethylene feed from the high pressure reservoir passed in succession through a dryer (3), filter (4), and an excess surge check valve (5). The dryer was an Autoclave Kuentzel Bomb, 1-inch I.D. by 15-inches long, filled with Dri-Rite desiccant. The excess surge check valve was used in the system as a safety device to stop the flow of ethylene in case of a rupture downstream. The ethylene flowed through a coiled capillary tube (6) which was used as a metering device. A Barton differential

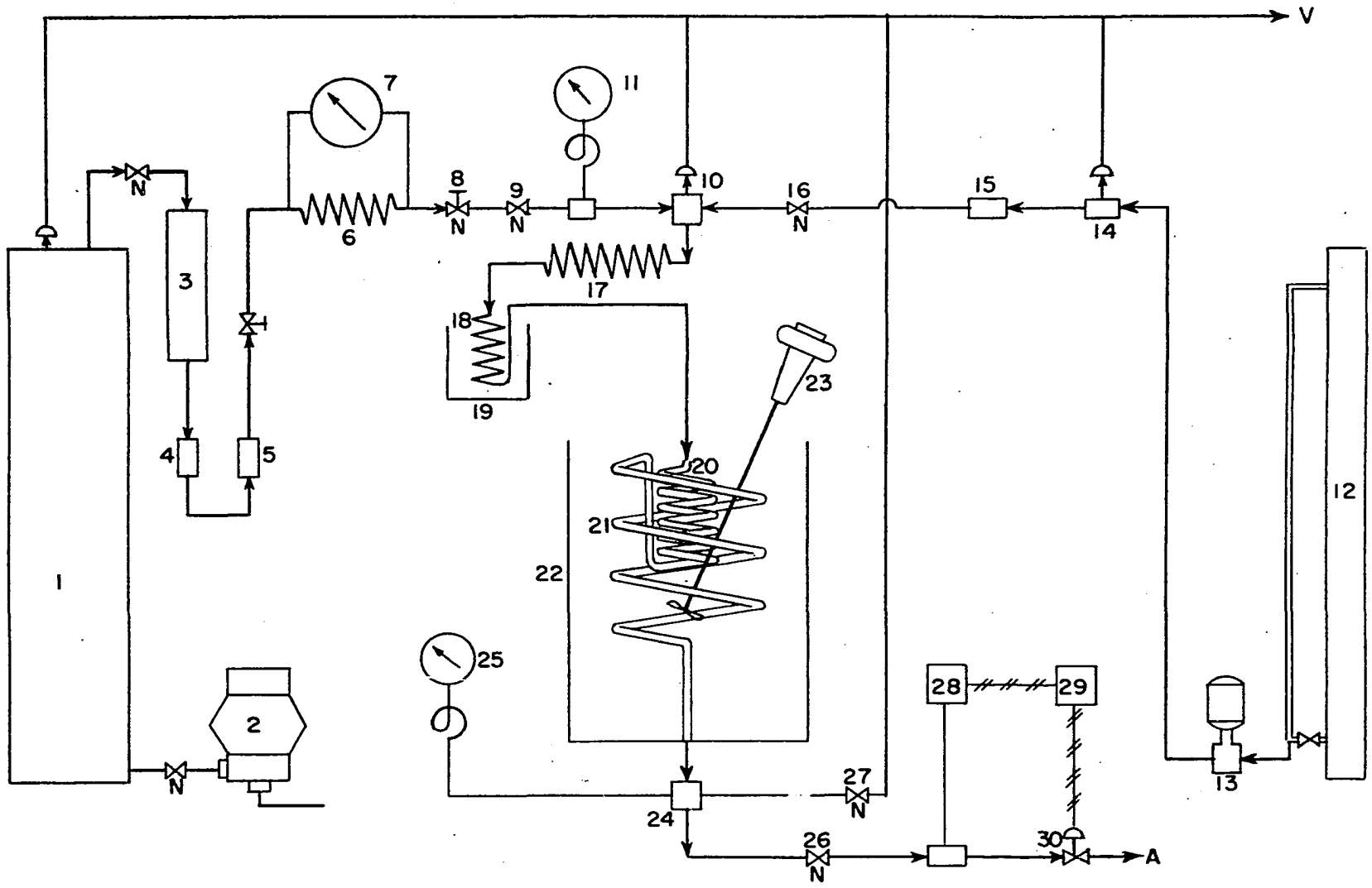


Figure 1 - Flow Diagram of Experimental Equipment

pressure gauge (7) measured and indicated the pressure drop across the coiled capillary which by calibration yielded the ethylene flow rate. The ethylene flow rate was controlled with an Autoclave 1/8-inch metering valve having a 2-degree tapered stem (8). A standard needle valve (9) was located down-stream for shut-off control since the metering valve should be used only for metering. The ethylene from the needle valve entered a cross-type safety head assembly (10) where it was mixed with the liquid butadiene feed. The rupture disk in the safety head assembly was connected to the vent line which was vented to the outside. A pressure gauge with a 0-5,000 lb./sq.in. pressure range (11) was connected between the shut-off needle valve and the safety head assembly so that the ethylene pressure could be determined prior to mixing with the butadiene and to entering the reactor.

The butadiene feed reservoir (12) for the high-pressure liquid pump was constructed from a 2-inch I.D. by 5-foot long copper tube. The tube was fitted with a sight glass over its entire length. The butadiene flow rate was low enough so that the sight glass alone was used as the reservoir when the flow rate of the butadiene was determined during each run. The high pressure liquid pump was a Hills-McCanna "U" type proportioning pump (13). A nitrogen pressure of 60 lb./sq.in. gauge was maintained on the liquid butadiene in order to prevent any vaporization in the pump

cylinder during the pumping cycle. A rupture disk assembly (14) was located immediately downstream from the high pressure liquid pump. The butadiene then passed through a twin seal check valve (15) and standard needle valve (16) before it entered the cross-type safety head assembly (10) and mixed with the ethylene.

The mixed feed passed through a mixing coil (17) where the pulsation effect of the liquid butadiene due to the pumping action was dissipated before it entered the low temperature preheater. The mixing coil consisted of a 6-foot long coil of 1/16-inch I.D. 304 stainless tubing. The low temperature preheater (18) consisted of an 8-foot long 1/16-inch I.D. stainless steel tube coiled and immersed in a hot oil bath (19). The oil bath was heated with a 500-watt immersion heater and was maintained at 400°F by means of a Fenwal Thermoswitch. The mixed feed from the low temperature preheater flowed to the high temperature preheater (20) and hence to the large reactor (21). The preheater was formed from an 8-foot long 1/16-inch I.D. 304 stainless stell tube coiled into a 3-inch diameter coil. The large reactor consisted of approximately 40-feet of 1/4-inch O.D. by 1/8-inch I.D. 304 stainless steel tubing coiled into a 6-inch diameter coil. The outlet end of the high temperature preheater was connected to the inlet end of the reactor within the liquid salt pot and both the high temperature preheater and reactor were immersed in the liquid

salt bath (22). A small reactor, consisting of 60 feet of 1/8-inch O.D. by 1/16-inch I.D. 304 stainless steel tubing, was also coiled and immersed in the liquid salt bath. The small reactor when in use was connected directly to the low temperature preheater. The salt pot, 8-inches I.D. by 20-inches long, was filled with Thermo-Quench heat treating nitrate-nitrite base salt obtained from the Park Chemical Company. The salt melted at approximately 300°F. A "Lightnin" air-driven portable mixer (23) was mounted above the salt pot and supplied the necessary agitation for maintaining a uniform temperature within the liquid salt bath as well as maintaining a high heat transfer coefficient to the reactor and preheater coils.

The salf pot was heated by four 500-watt Chromalox strip heaters elements mounted vertically on the outside of the salt pot. Two-inch thick Kaylo high temperature pipe insulation was used to insulate around the outside of the salt pot. The heat input to the heaters was controlled with a Powerstat variable transformer. The temperature within the salt pot was controlled very accurately by means of a Bayley Precision Temperature Controller. The Bayley controller utilizes a resistance thermometer with an electronic bridge circuit and has a stated control accuracy of $\pm$ .001°C. The Bayley controller controlled the power input by on-off control to a small 175-watt immersion heater located within the salt pot. Temperature control of

considerably better than ± 1°F was maintained within the salt pot at all times. The actual temperature within the salt bath was obtained by a Leeds and Northrup 8662 precision potentiometer from a chromel-alumel thermocouple mounted in a thermocouple well located in the top of the salt pot.

The outlet end of the reactor extended through the bottom of the salt pot. A 1/16-inch I.D. stainless steel tube connected the reactor outlet to a cross (24). A pressure gauge (25) with a 0-7,500 lb./sq.in. range was connected to the cross in order to determine the pressure within the reactor. The remaining two outlets from the cross were connected to two standard needle valves (26, 27). One of these needle valves was connected directly to a vent line and the other one to a Research Control Valve (30). The Research Control Valve was part of the back pressure regulator system which controlled the pressure in the reactor. The back pressure regulator system was composed of a Series 650 Metagraphic, pneumatic pressure transmitter (28) obtained from the Bristol Company, a M-58 Consotrol pneumatic controller (29) obtained from the Foxboro Company, and a Research Control Valve (30) obtained from Research Controls, Inc. With this back pressure regulator system the operating pressure in the reactor could be accurately controlled (± 20 lb./sq.in.) at any pressure from 200 to 5,000 lb./sq.in. In normal operation the products from the

reactor passed through the Research Control Valve to the analysis section. The other needle valve (27) was used only when it became necessary to vent or flush out the system.

A flow diagram for the analysis section is shown in Figure 2. The reactor products after expanding through the Research Control Valve passed through a cold water condenser (1) maintained at approximately 50°F. The liquid products were collected in a 50 ml. graduated receiver (2). The gaseous product passed overhead from the liquid receiver to a 1 liter mixing flask (3). From the mixing flask the gas product passed through a sample fitting (4) where gas samples were obtained for chromatographic analysis. The mixing flask was inserted between the liquid receiver and sample point in order that a more representative gas sample could be obtained. The gaseous product then passed through a water saturator (5) to a "Precision" wet-test meter (6), where it was metered. From the wet-test meter the gaseous product was vented to the outside.

All of the apparatus shown in Figure 1, except for the butadiene reservoir, the two high pressure liquid pumps, the pressure transmitter and the controller, were located behind a steel and wood barricade. The barricade was constructed from 1/4-inch steel plate backed by a 1-inch thick wood layer. The wood layer was separated from the steel plate by a 2-inch air space. A door consisting of a heavy rope blast mat provided an entrance to the barricaded

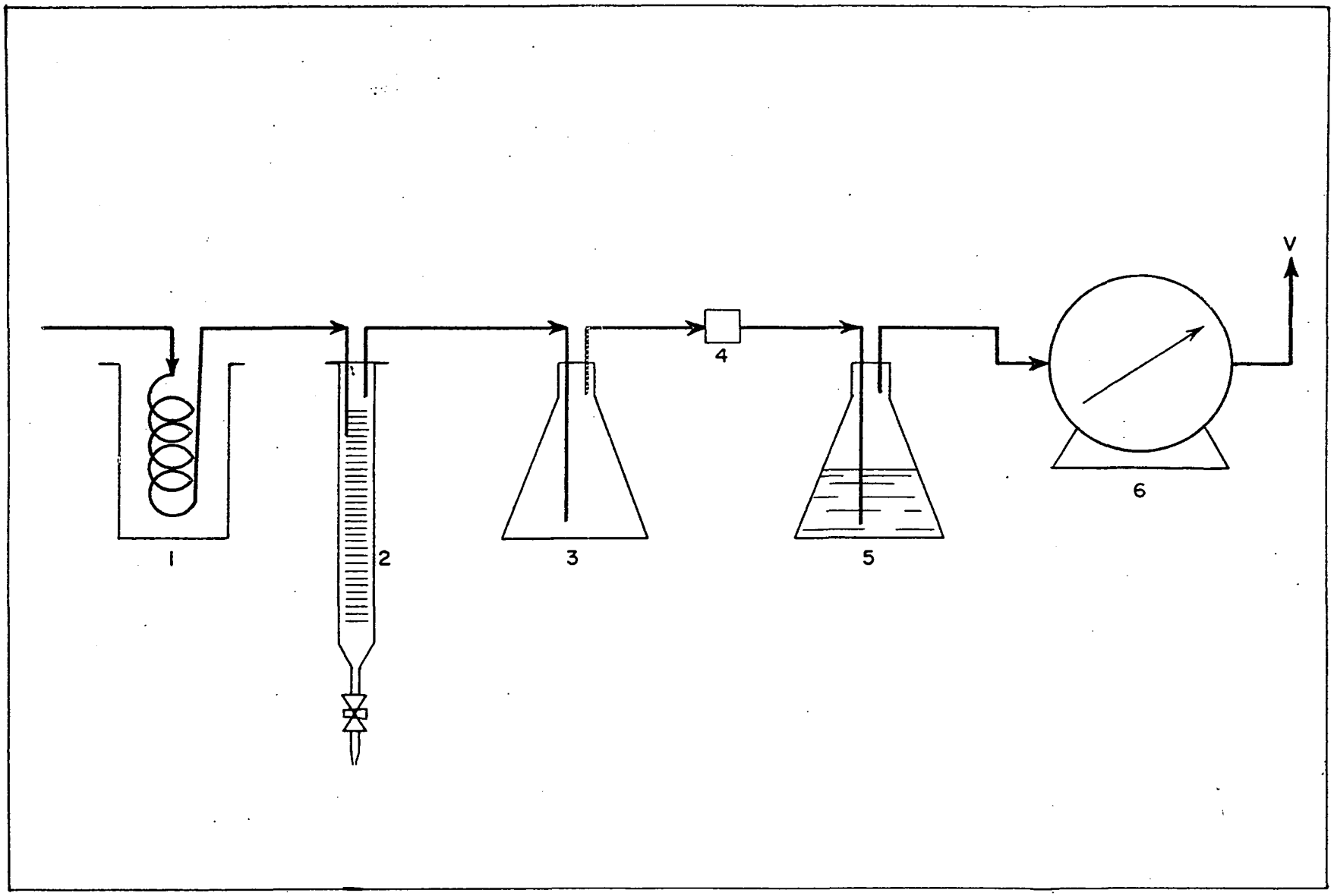


Figure 2 - Flow Diagram of Analysis Section

area.

Figure 3 shows a front view of the barricade. All the valves have extensions through the barricade so that all required operations could be performed without going behind the barrier. Holes were cut in the barricade above eye-level so that the Barton differential pressure gauge and the standard pressure gauges could be read easily from in front of the barrier. The flow diagram of the equipment was marked on the front of the barricade with colored scotch tape as shown in Figure 3. Figure 4 shows the heavy rope blast mat access door.

Figure 5 shows all associated equipment located outside of the barricaded area. Pictured in the upper left is a Leeds and Northrup Micromax multipoint temperature recorder which was used to moniter the temperatures at several points in the system. Located below the temperature recorder are the wet-test meter, product condenser, Bayley Precision Temperature Controller, gas sample fitting, graduated liquid receiver, gas-mixing flask and water saturator. The panel board contains the powerstats for controlling the power input to the various heaters and the switch for the Hills-McCanna liquid butadiene pump. The Foxboro Consotrol pneumatic controller is shown mounted on the upper left corner of the panel board. The Bristol Metographic pressure transmitter is mounted on the back of the panel board immediately behind the Foxboro controller,

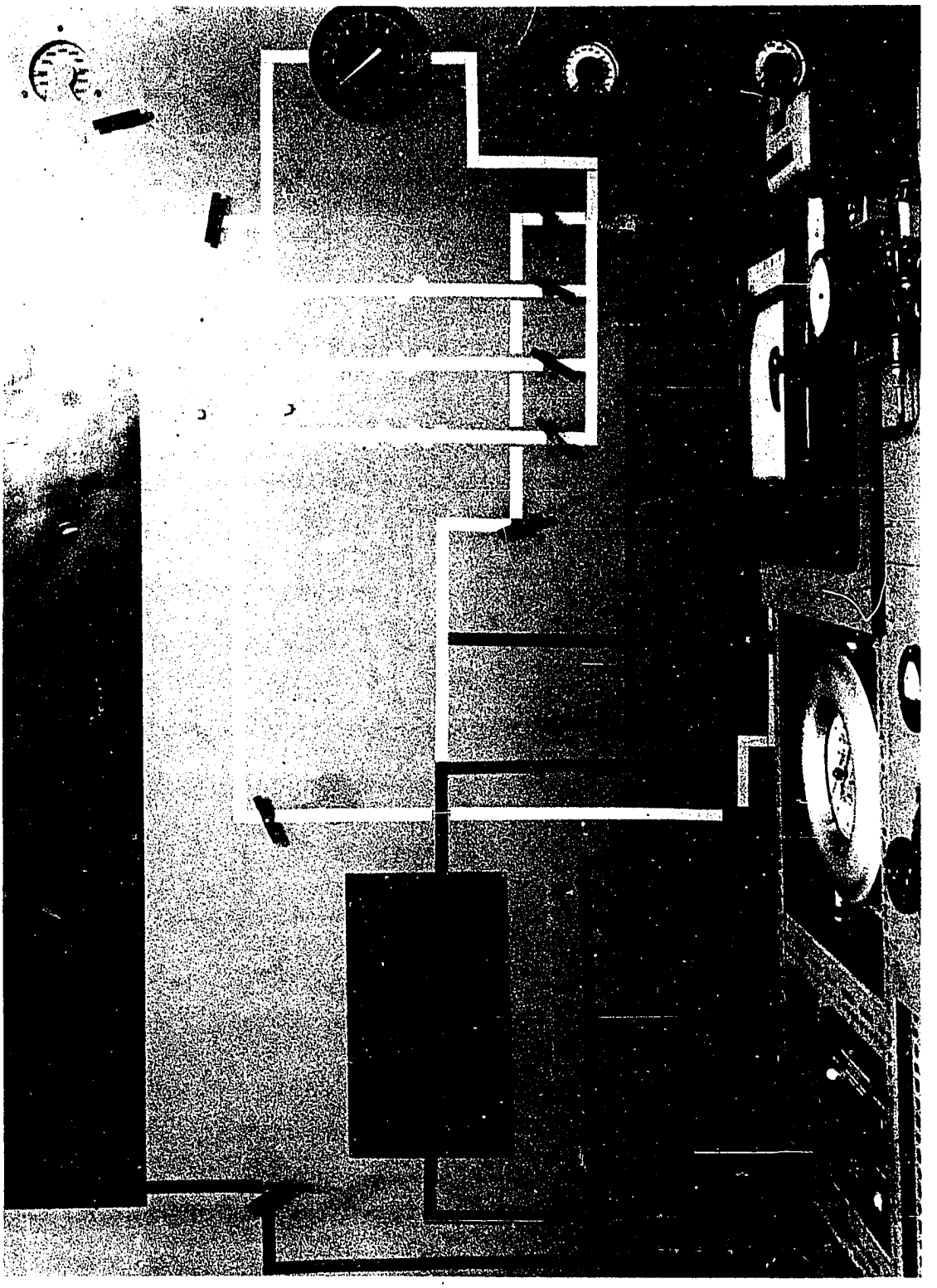

Figure 3 - Front View of Barricade

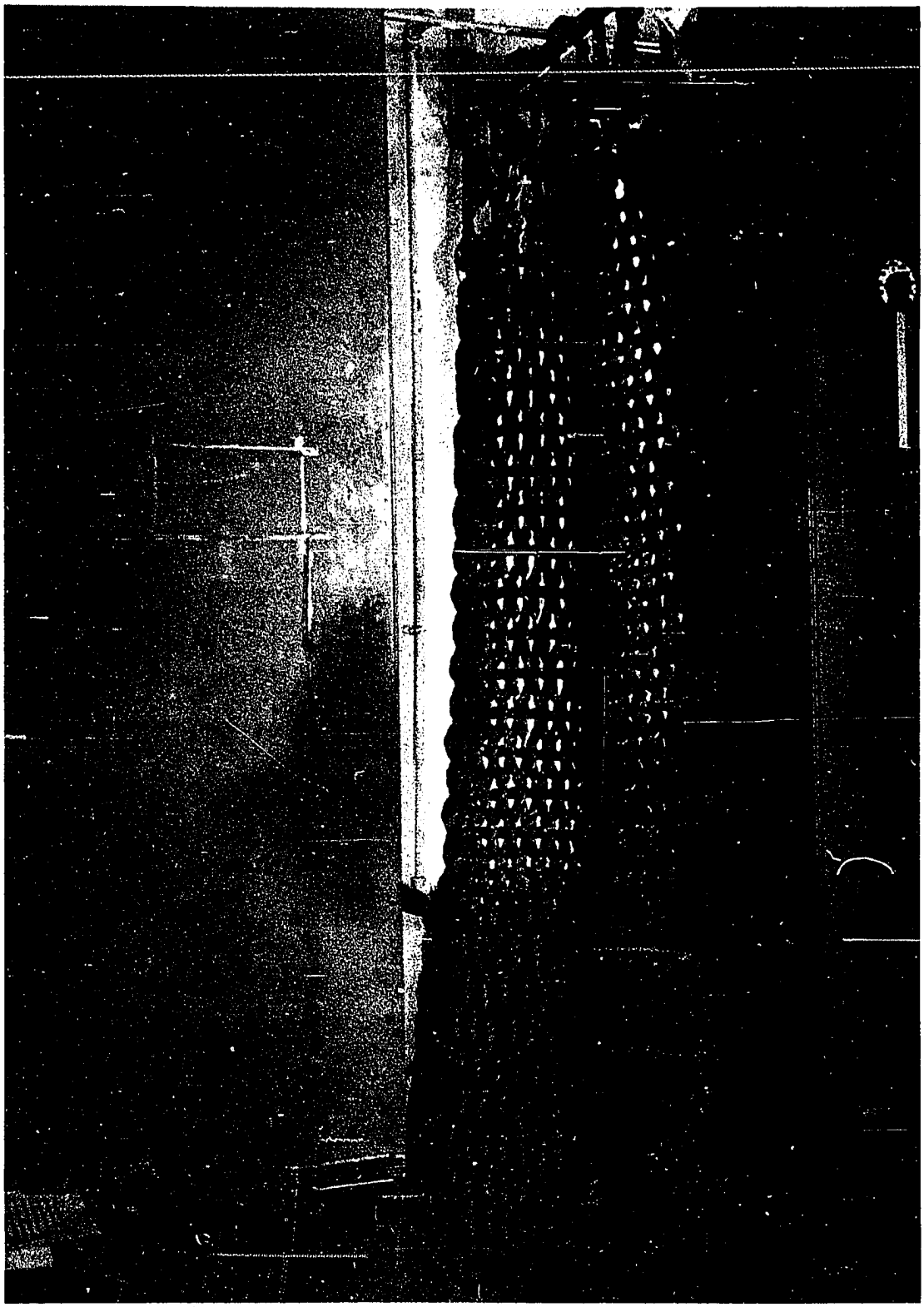

Figure 4 - Blast Mat Door

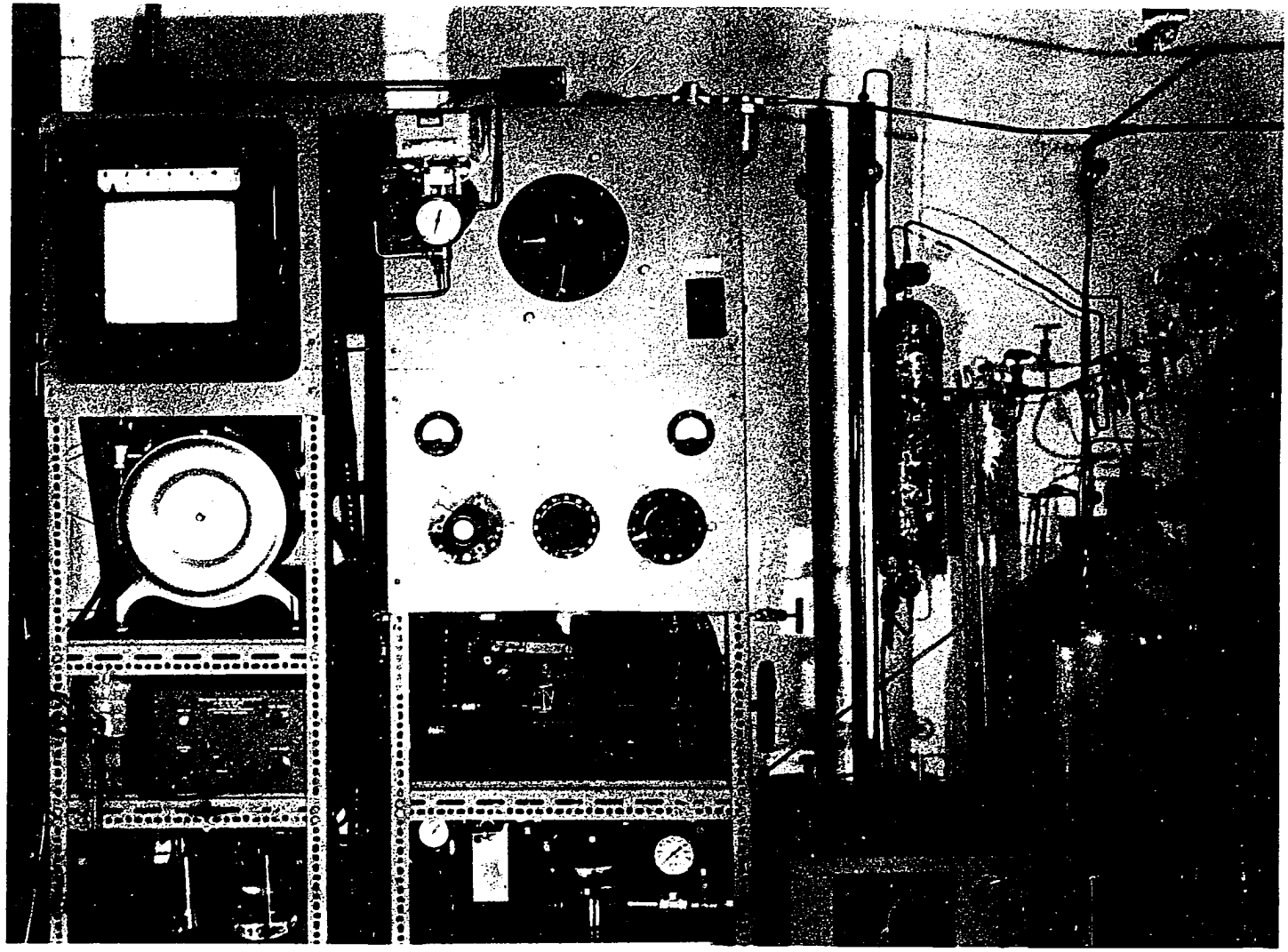

Figure 5 - Associated Equipment Located Outside of Barricaded Area

but it can not be seen in the picture. Located below the panel board are the Hills-McCanna liquid pump and the Sprague air-driven liquid pump. To the right of the panel board is the liquid butadiene reservoir. The large glass carboy at the right is the oxygen free distilled water reservoir. At the far right is the nitrogen cylinder with the connections required for blanketing the distilled water and for pressurizing the liquid butadiene feed. Figure 6 is a complete view of the area outside of the barricade showing the location of the associated equipment with respect to the barricade and blast mat.

A view of the equipment located behind the barrier is shown in Figure 7. The insulated liquid salt pot is mounted on the steel table in the middle of the photograph. The mixer shaft, resistance thermometer lead, immersion heater lead, feed tube and thermocouple lead can be seen extending from the top of the reactor. The air-driven mixer along with its pressure regulator and lubricator are mounted on the steel beam which extends across above the salt pot. The hot oil bath is mounted on the left beam support. On the right side of the picture is located the high pressure ethylene reservoir. All of the remaining tubing, fittings and associated equipment are shown mounted on the wooden side of the duplex barricade.

A 4,000 CFM exhaust fan with an explosion proof motor was mounted in the window behind the steel table. A

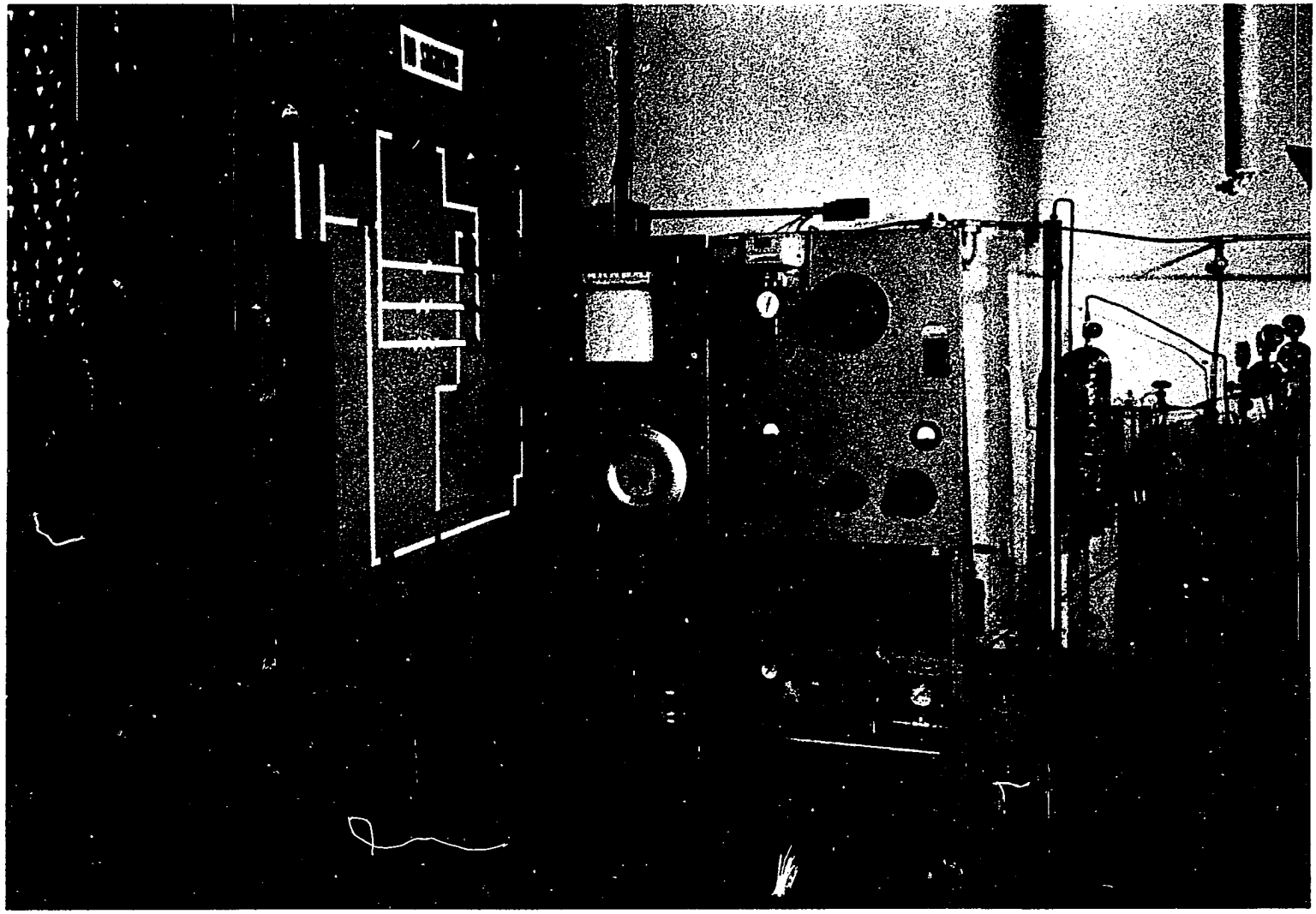

Figure 6 - Over-all View in Front of Barricade

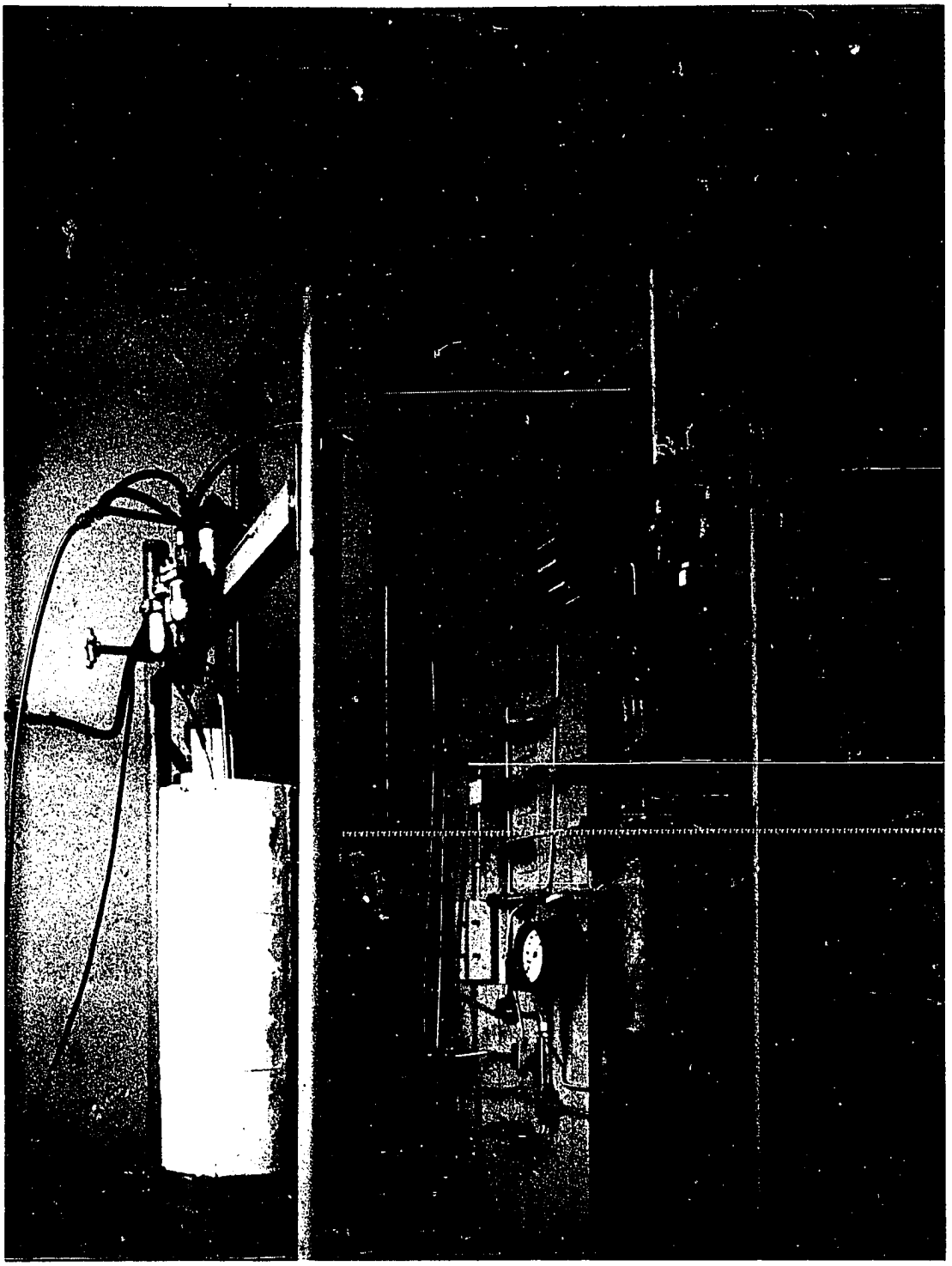

Figure 7 - View Behind Barricade

water fog nozzle mounted above the liquid salt could be activated in case of emergency by means of an electric solonoid located at a considerable distance from the equipment.

# CHAPTER III

## DESIGN CALCULATIONS AND CONSTRUCTION

The design and construction of any equipment for high temperature, high pressure service involves certain basic factors not usually encountered in most design procedures. Since the ultimate objective in the construction of any piece of equipment is that it operate satisfactorily under the specified conditions, the final design will depend on certain basic methods which have already proved satisfactory in similar service. In the case of high pressure, high temperature service where extreme care must be exercised, the design is inclined to be rather conservative and to adhere to well-established methods. The design of the equipment necessary for this investigation was very conservative as the temperature and pressure requirements were not severe for the materials used. The maximum design conditions established were 900°F. at 5,000 lb./sq.in.

### Basic Design Formula

Several formulas are available for determining the elastic stress distribution in a uniformly thick cylinder but those of Lame' are the most common. The Lame'

equations (2) are as follows*:

$$\sigma_t = \frac{P_1 - P_2K^2 + (r_2/r)^2(P_1 - P_2)}{K^2 - 1} \qquad 1$$

$$\sigma_r = \frac{P_2K^2 - P_1 + (r_2^2/r^2)(P_1 - P_2)}{K^2 - 1} \qquad 2$$

where $\sigma_t$ = tangential stress

$\sigma_r$ = radial stress

$r_1$ = internal radius

$r_2$ = external radius

$r$ = any radius within the tube wall

$P_1$ = internal pressure

$P_2$ = external pressure

$K = r_2/r_1$.

The Lame' equations can be used to calculate the stress distribution in a simple cylinder when the walls deform elastically and are not stressed beyond the range of elastic behavior.

The maximum-shear-stress theory (2) is one of the most generally accepted theories for determining the limit of elastic behavior of a ductile metal. This theory states that the breakdown of elastic action occurs when the shearing stress at any point, due to any combination of

---

*A third equation for the longitudinal stress, $\sigma_Z$, is neglected in this design since in the critical stress regions its absolute value is the smallest of the three principal stresses.

stresses, exceeds the shearing proportional limit of the material. The shear stress at any point is equal to one-half the algebraic difference between the maximum and minimum principal stresses. For a thick-walled cylinder the shearing stress is one-half the difference between the tensile and compressive stresses. Therefore:

$$\tau = \frac{1}{2} (\sigma_t - \sigma_r) \qquad 3$$

where $\tau$ = shear stress.

The shear stress at any point in a thick-walled cylinder is found by substituting the Lame' equations into the shear stress equation. Therefore:

$$\tau = \frac{K^2(P_1-P_2)r_1^2}{r^2(K^2-1)} \qquad 4$$

The shear stress will be maximum at the inner radius; therefore the maximum shear stress will be:

$$\tau_m = \frac{K^2(P_1-P_2)}{K^2-1} \qquad 5$$

where $\tau_m$ = maximum shear stress.

The shear proportional limit of the material is determined from the yield properties of the steel. Equation 3 indicates that the proportional limit in shear is equal to one-half the yield stress in pure tension. Therefore:

$$\tau_y = \frac{1}{2} \sigma_y \qquad 6$$

where $\tau_y$ = shear proportional limit

$\sigma_y$ = yield stress in pure tension.

The maximum allowable operating pressure, $P_m$ (within elastic limits) of a thick-walled cylinder is determined by setting the maximum shear stress equal to the shear proportional limit. Therefore:

$$P_m = \frac{1}{2} \frac{\sigma_y (K^2-1)}{K^2} \qquad 7$$

## Tubing and Fittings

Tubing and fittings used in this equipment were obtained from Autoclave Engineers, Inc. Speedline valves and fittings with a pressure rating of 10,000 lb./sq.in. proved to be very satisfactory for this service when used with annealed stainless steel tubing. Standard 1/4-inch O.D. by 1/8-inch I.D. and 1/8-inch O.D. by 1/16-inch I.D. annealed, 304 stainless steel tubing was used. A maximum pressure rating of 13,000 lb./sq.in. was determined for this tubing from Equation 7 using a yield stress of 35,000 lb./sq.in. for the stainless steel as compared to the maximum operating pressure of 5,000 lb./sq.in. required for this study.

## Reactors

The large reactor, constructed from standard 1/4-inch O.D. by 1/8-inch I.D. annealed, 304 stainless steel tubing, was 39.5-feet long. The small reactor,

constructed from standard 1/8-inch O.D. by 1/16 I.D. annealed, 304 stainless steel tubing was 56.5-feet long. The length required could only be obtained by joining lengths of tubing together. The large reactor was formed from two lengths of tubing while three lengths were used for the small reactor. The joint was made by slipping the two ends of the tubes to be joined into a short piece of stainless steel, 1/2-inch O.D. by 1/4-inch I.D. for the large reactor and 1/4-inch O.D. by 1/8-inch I.D. for the small reactor, and then welding. The tubes then were coiled together around a 4-inch mandrel to form the final coil which was approximately 6-inches in diameter.

The reactors were immersed in a liquid salt bath and had to operate satisfactorily at a maximum temperature of 900°F and the maximum pressure of 5,000 lb./sq.in. At ordinary temperatures the design of equipment is based on the standard yield strength of the various metals. At high temperatures, however, continuous plastic deformation or creep at constant stress is encountered in addition to the reduced strength at the higher temperature. Freeman and Voorhies (3) reported that the stress required to cause a creep rate of one per cent per 10,000 hours in 304 stainless steel at 900°F was 28,000 lb./sq.in. Using this value as the allowable stress Equation 7 gave a maximum pressure rating of 10,500 lb./sq.in. for the reactor compared to the maximum operating pressure of 5,000 lb./sq.in.

## Ethylene Storage Vessel and Dryer

The ethylene high pressure storage vessel, obtained from Autoclave Engineers, Inc., was 12-inches O.D. by 8-inches I.D. by 52-inches inside depth. This vessel was manufactured from 4340 alloy steel with a self-sealing closure at one end. The vessel had three openings in the cover and two at the bottom. One of the openings in the top was connected to a pressure gauge, one to the ethylene input-output line and the third connected to a rupture disk, safety head assembly. The working pressure of this high pressure vessel was 15,000 lb./sq.in. at 72°F and it was hydrostatically pressure tested at 22,500 lb./sq.in. at 72°F. The rupture disk was rated at 20,000 lb./sq.in. at 72°F.

An Autoclave modified KB-15 Kuentzel Bomb, 2-inches O.D. by 1-inch I.D. by 15-inches inside depth, was used for the ethylene dryer. This vessel was manufactured from 316 stainless steel having a specified yield stress of 60,000 lb./sq.in. Each end of double-ended vessel had a confined stainless steel, compression gasket-type closure which was provided with a 3/8-inch high pressure connection. The working pressure of this vessel was stated to be 10,000 lb./sq.in. at 650°F with a hydrostatic pressure test of 16,500 lb./sq.in. at 72°F. Drierite was used as the desiccant in the dryer.

## Ethylene Flow Device

The ethylene flow rate was determined by measuring the pressure drop across a coiled capillary tube. A Barton Model 200 Indicator having a differential pressure range of 10-inches of water was used to measure the pressure drop. Three coils were used to cover the range of flow from 2 to 60 SCFM. Coil 1, 6 feet of 1/8-inch O.D. by 0.030 I.D. stainless steel tubing coiled in a 1-inch coil, covered the range from 2 to 11 SCFM. Coil 2, similar to coil 1, but only 2.5 feet long, covered the range from 5 to 30 SCFM. Coil 3, similar to coil 1 except being 1/16 I.D., covered the range above 30 SCFM. Figure 8 indicates the flow diagram of the ethylene flow device. The valving was designed with the handles extending through the wall so that the desired coil could be selected from in front of the barricade, Figure 3. The second valve shown in conjunction with Coil 3 was installed so that if needed Coil 3 could be replaced with any other desired coil without depressurizing the system. Figure 9 shows the ethylene flow device as seen from behind the barricade.

## Liquid Salt Pot

The liquid salt pot was constructed from a piece of 8-inch, schedule 40, steel pipe 22-inches long. A 3/8-inch thick steel plate was welded to one end to form the bottom. This bottom plate was then drilled and fitted with two

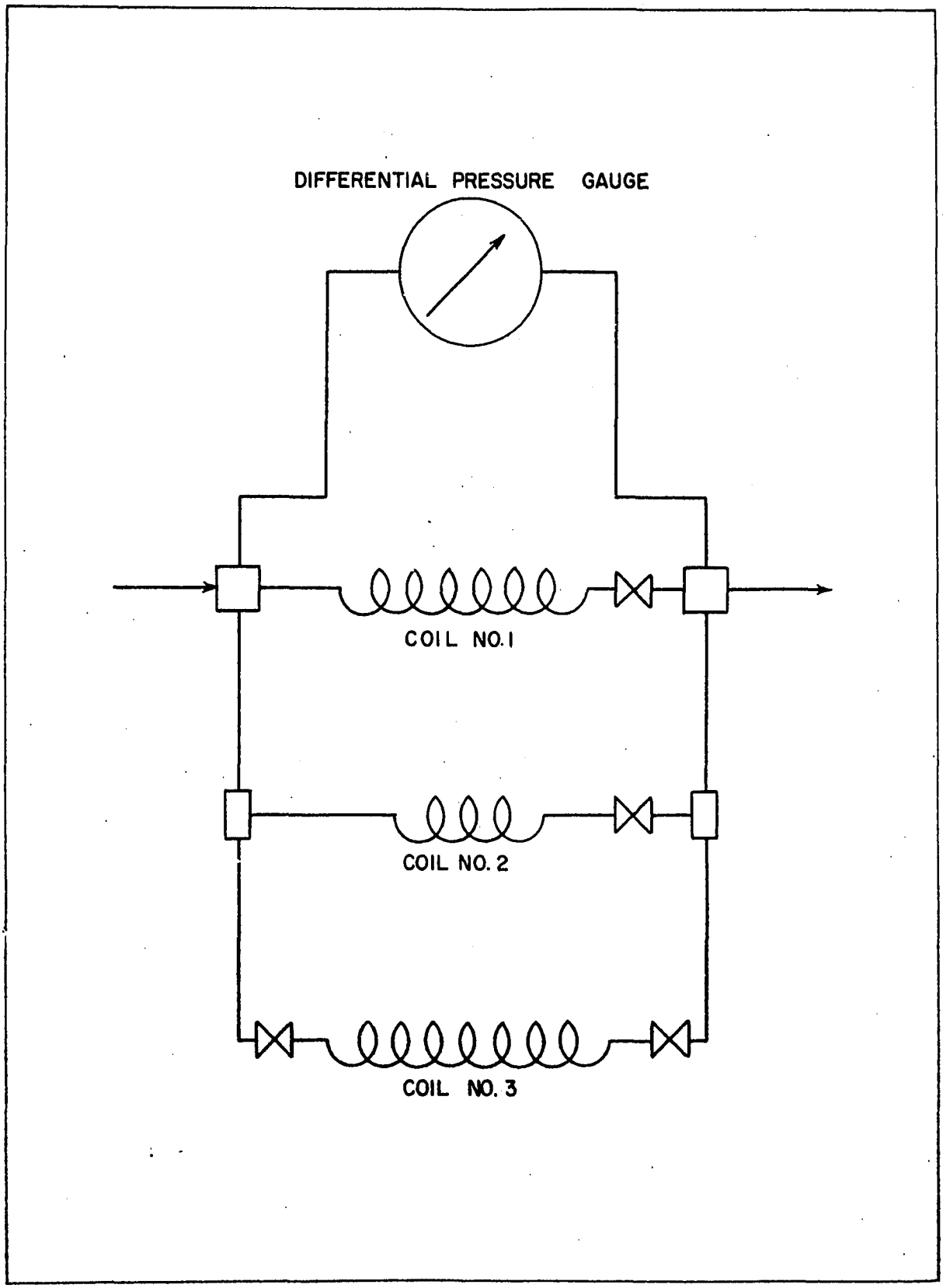


Figure 8 - Flow Diagram of Ethylene Flow Device

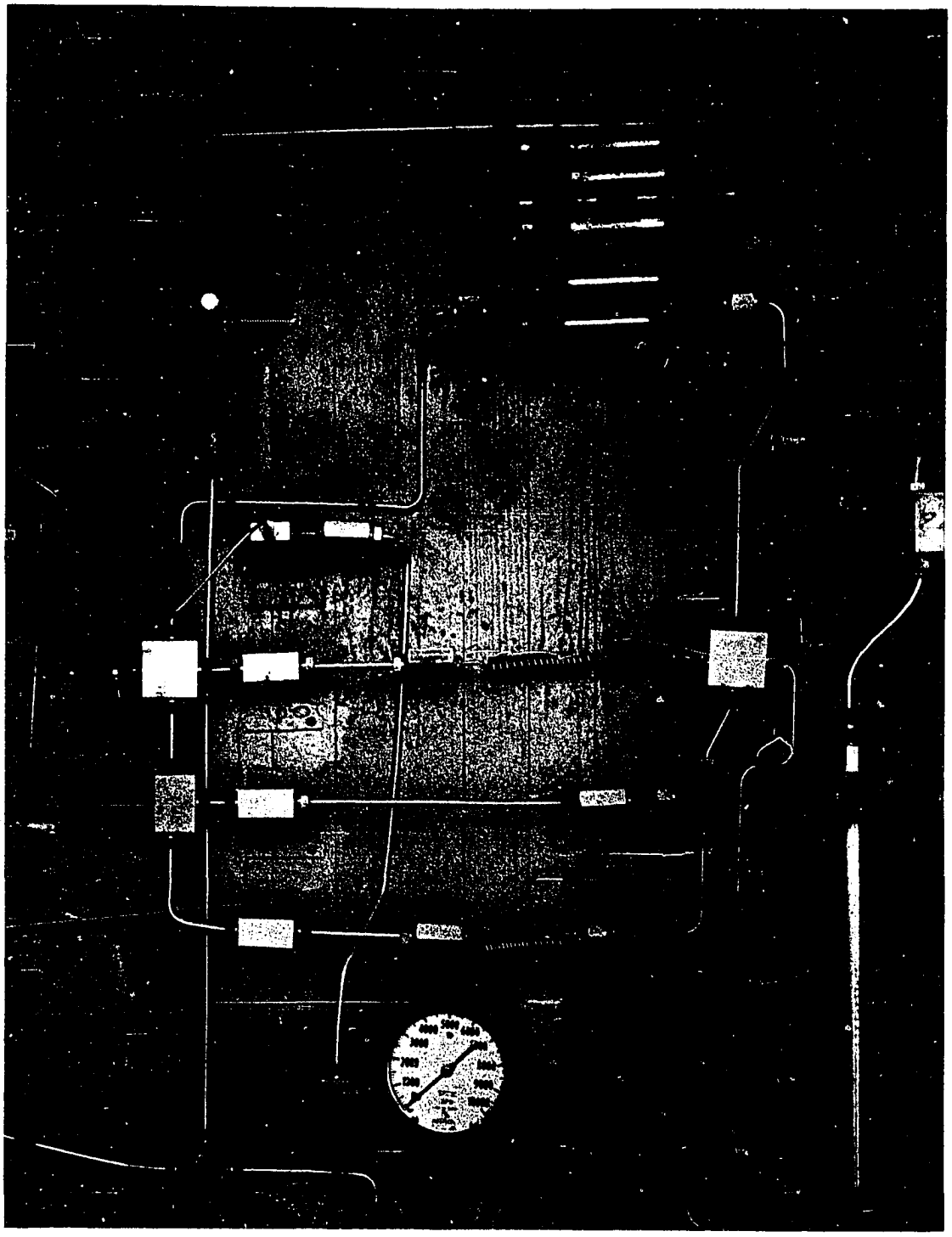

Figure 9 - Ethylene Flow Device

Speedline fittings, one 1/4-inch and the other 1/8-inch, which were welded in place. The fittings were drilled out so that the ends of both coiled reactors could pass through the bottom of the salt pot. Standard Speedline nuts and sleeves were used to seal between the reactor tube and the salt pot. Four legs were welded to the bottom of the pot so that it could be mounted approximately 4-inches above the steel table. Four, 500-watt Chromolox strip heater elements were mounted vertically around the outside of the salt pot. Thermon was used to increase the effective area of contact between the strip heaters and the salt pot. The areas between and above the heaters were filled flush with the outer periphery of the heaters with asbestos paste as a precautionary measure to protect the heaters in case any of the liquid salt was splashed out of the salt pot. Kaylo high temperature pipe insulation, two-inches thick, was then used to insulate the outside of the salt pot.

The cover for the salt pot consisted of a 3/16-inch thick steel plate, resting on the outer edge of the salt pot. It was held in place by three lugs welded to the outside of the salt pot. A stainless steel thermocouple well and a round copper tube, both sealed at the bottom, extended into the salt and were welded to the cover. The copper tube contained a 170-watt Chromalox cartridge element which was connected in series with the Bayley Precesion Temperature Controller. The salt pot cover also

had a center hole for the mixer shaft and a small hole where the resistence thermometer extended into the salt bath. The 1/8-inch O.D. preheater and reactor tubes entered at the edge of the salt pot through a slot in the top. The cover of the salt pot was insulated with 4-inches of block Kaylo. Figure 6 shows the salt pot with the insulation in place; Figure 10, the salt pot and cover with the insulation removed; and Figure 11, the cover with attachments.

## Hot Oil Bath

The hot oil bath was a small 6-inch I.D. by 6-inch deep vessel filled with Wesson oil and insulated on the outside. A 500-watt Chromalox cartridge element inserted inside a copper sheath and immersed in the oil was the heat source. The temperature was controlled at approximately 400°F by means of a Fenwal Thermoswitch temperature controller.

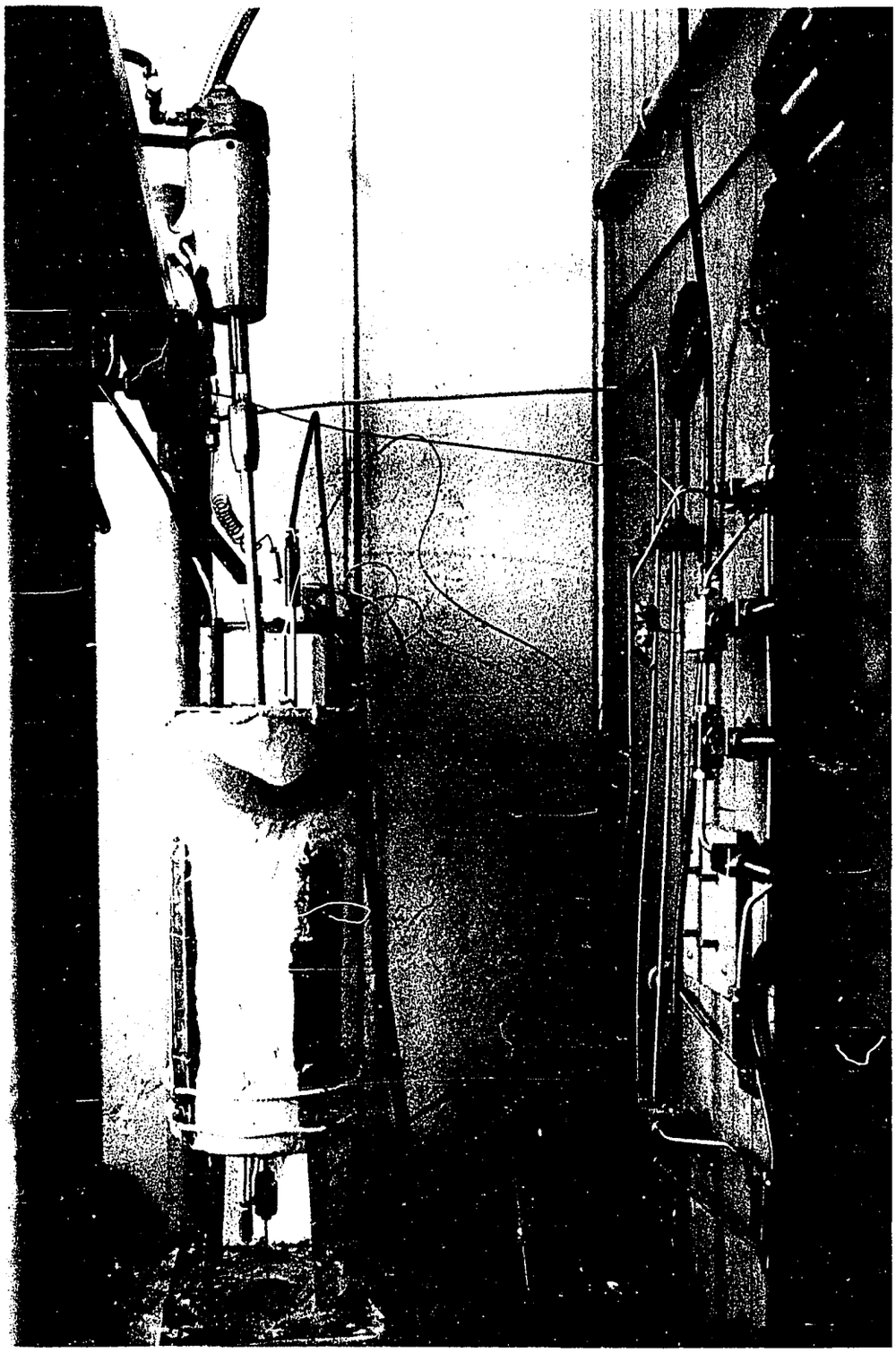

Figure 10 - Salt Pot with Insulation Removed

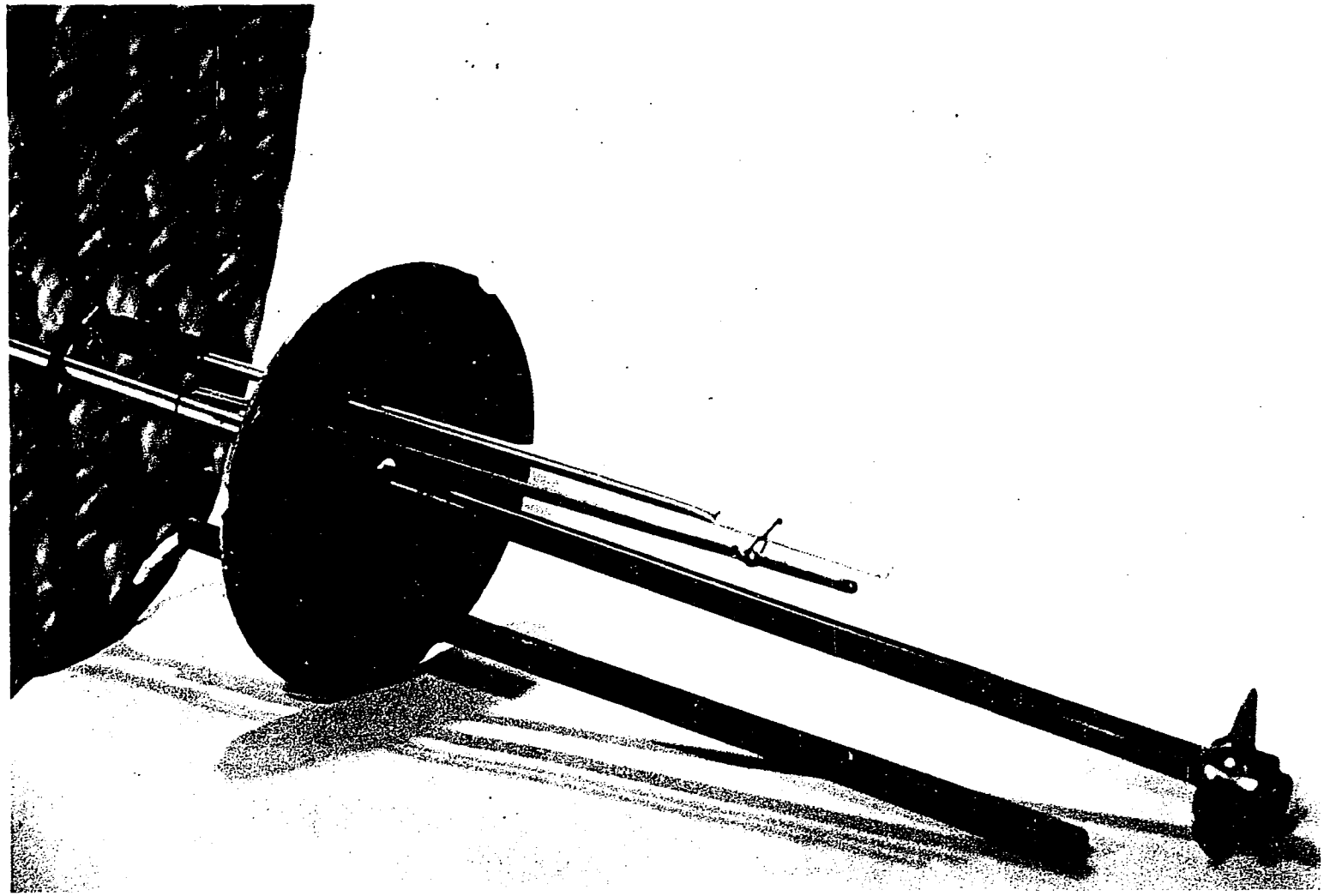

Figure 11 - Salt Pot Cover with Attachments

# CHAPTER IV

# PRESSURE GENERATION AND FLOW REGULATION

## Ethylene Pressurization

In most applications where a gas is required at high pressure a multi-stage gas compressor is used, but when one is not available substitute procedures are necessary. In this design a gas intensifier was used to increase the pressure of the ethylene from that available in standard 1A gas cylinders to the 5,000 lb./sq.in. required for the high pressure ethylene feed vessel.

The gas intensifier unit consisted of two, low-pressure reservoirs connected through a Seco high pressure, hydraulic, radial piston pump to two high pressure reservoirs. Ethylene from the standard ethylene cylinders was fed to the empty high pressure reservoirs. The Seco pump then pumped the hydraulic oil from the low pressure reservoirs into the bottom of the high pressure reservoirs and hence intensified the pressure on the ethylene. The cycle was completed when the oil was moved back to the low pressure reservoirs. The maximum pressure rating of the intensifier was 10,000 lb./sq.in. Difficulty in the

operation of the intensifier was due to the solubility of the ethylene in the hydraulic oil, which caused extreme foaming when the oil from the high pressure reservoir, in contact with the ethylene, was returned to the low pressure reservoir. Although the addition of Dow Corning Antifoam A to the hydraulic oil reduced the stability of the foam, it still remained the limiting factor in the operation of the intensifier. Due to the low pressure source of ethylene and the foaming of the hydraulic oil the charging of the ethylene high pressure storage vessel was a very, time-consuming undertaking and a source of consternation. The problem of a low pressure source of ethylene was partially alleviated by injecting distilled water into the ethylene cylinders with the Sprague liquid pump to increase the ethylene pressure.

## Butadiene Pumping

The pumping of liquid butadiene at a constant flow rate proved to be the most difficult problem to solve in this investigation. A duel feed, Hills-McCanna "U" type metering pump, fitted with a variable stroke, 5/16-inch ceramic plunger and double cone type check valves, was recommended by the manufacture as satisfactory for this service. This pump had a rated maximum capacity of 1.2 gph. and minimum capacity of 0.06 gph. The pump was tested by pumping against a gas pressure of 1,000 lb./sq.in. The cone

checks leaked so much that an appreciable stroke had to be used just to overcome the leak. The four check valves in series are shown in Figure 12 (A). As these checks did not prove satisfactory they were replaced by a set of ball checks which was even more unsatisfactory. It, therefore, became necessary to embark on the development of a new design for the check valves.

Figures 12 (B, C) show the original cone type check valve and the first modification. The original check was a cone type with a line contact. The first modification consisted of pressing the cone into the seat so that an area contact rather than a line contact was formed. Admittedly the area contact was more susceptible to fouling, but it formed a better seal. Although the operation of the cone check was improved, it still was not satisfactory. The next modification consisted of machining a new seat, containing a small hole, as shown in Figure 12 (D) for use with the same cones. Further improvement of the operation of the check was noted, but there was still a small leak which affected the flow rate at very small flow rates. This check was further modified, Figure 12 (E), by pressing the check into the seat to form an area seat. Then the cone was lapped to the seat with a very fine grinding compound. On the initial test this modification proved to be satisfactory, but after long periods of time, during a run, the flow rate would start decreasing without

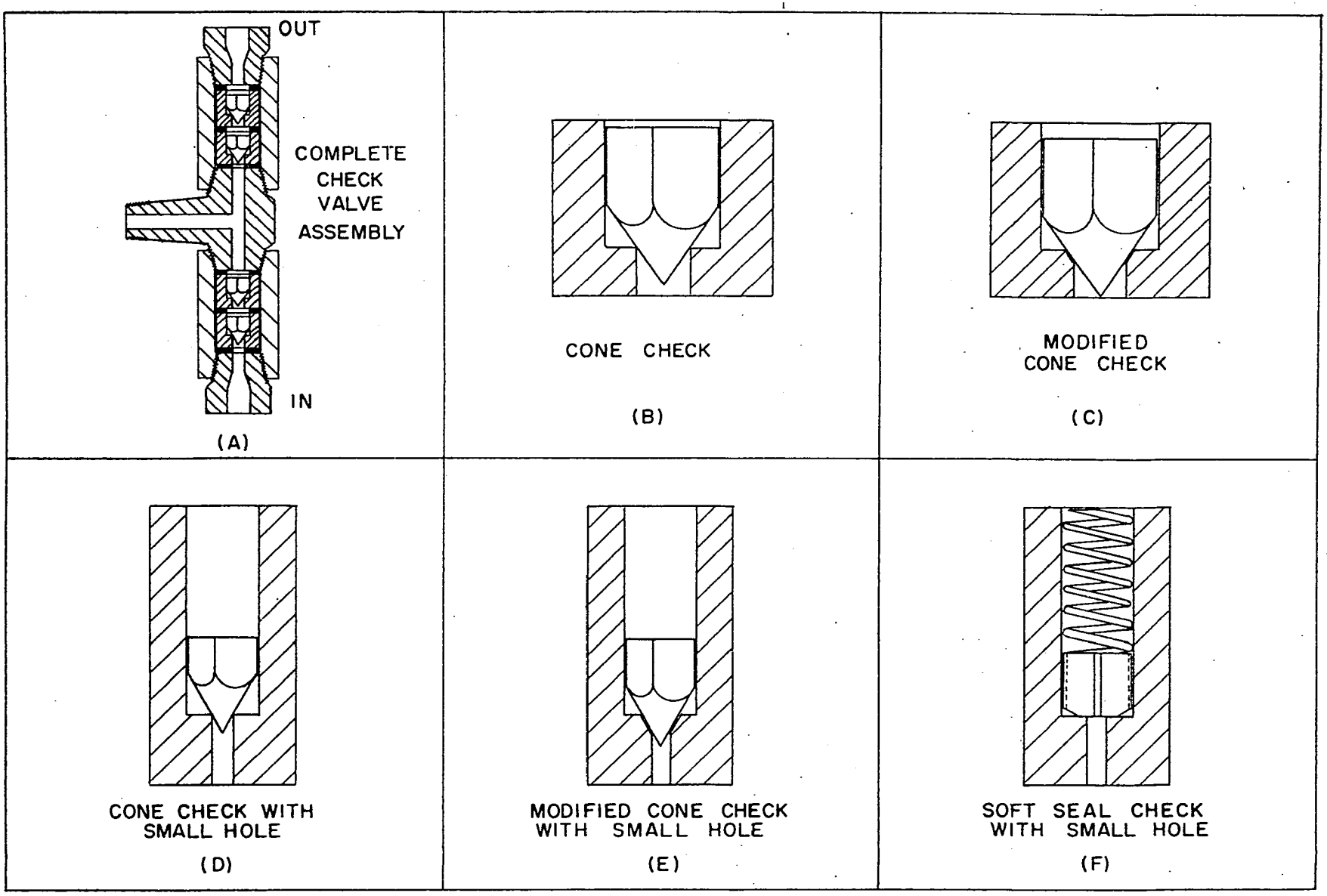


Figure 12 - Check Valve Configurations

the stroke adjustment being changed. Inspection of the check and pump cylinder showed that part of the packing was flaking off inside the pump chamber and after a period of time would cause the check to start leaking. Since previous tests of the check valves had been made without the pump operating for any extended period, the flaking of the packing represented another potential source of difficulty. Therefore, a completely new design for a check valve was devised and tested. The seat and check were machined so that there was a small flat area of contact as shown in Figure 12 (F). The check was made from a hard plastic and was spring loaded so that it took approximately 500 lb./sq.in. pressure to unseat the check. This check has been in continuous use since it was installed and has proven very satisfactory under all operating conditions.

As mentioned above, inspection of the check valve body at the end of some of the first runs showed that the packing was flaking off into the pump chamber. The suggested packing assembly for this service consisted of oil and graphite-lubricated, babbit foil. In order to eliminate this contamination of the system several other types of packing were tried. In most cases the coefficient of friction was so large that when the packing nut was tightened to prevent the packing from leaking, considerable force was required to move the plunger through the packing. The babbit foil packing was replaced by a teflon assembly

shown in Figure 13 (A). It has operated satisfactorily since it was installed with essentially no leakage and with only a minimum amount of force required to move the plunger through the packing. Since no lubrication was required, there was no possibility of contaminating the butadiene. Another packing design which also worked quite satisfactorily is shown in Figure 13 (B).

The pump has operated satisfactorily at all flow rates and pressures since modifying the packing and check valves. Tests have shown that there was less than two per cent error with flow rates as low as 0.03 gph. At higher flow rates the pump was even more consistent.

## Ethylene Flow Regulation

The flow rate of ethylene was controlled by means of a metering valve as shown in Figure 1. The ethylene in the high pressure storage vessel was maintained at 5,000 lb./sq.in.; therefore the pressure in the metering capillary and on the upstream side of the metering valve was maintained at 5,000 lb./sq.in. irrespective of the operating pressure within the reactor. As the operating pressure in the reactor varied from 250 to 4,500 lb./sq.in. the pressure drop across the metering valve varied from 4,750 to 500 lb./sq.in. With the higher pressure drops across the valve the metering of the lower flow rates was very difficult.

A standard Autoclave 1/4-inch Speedline metering

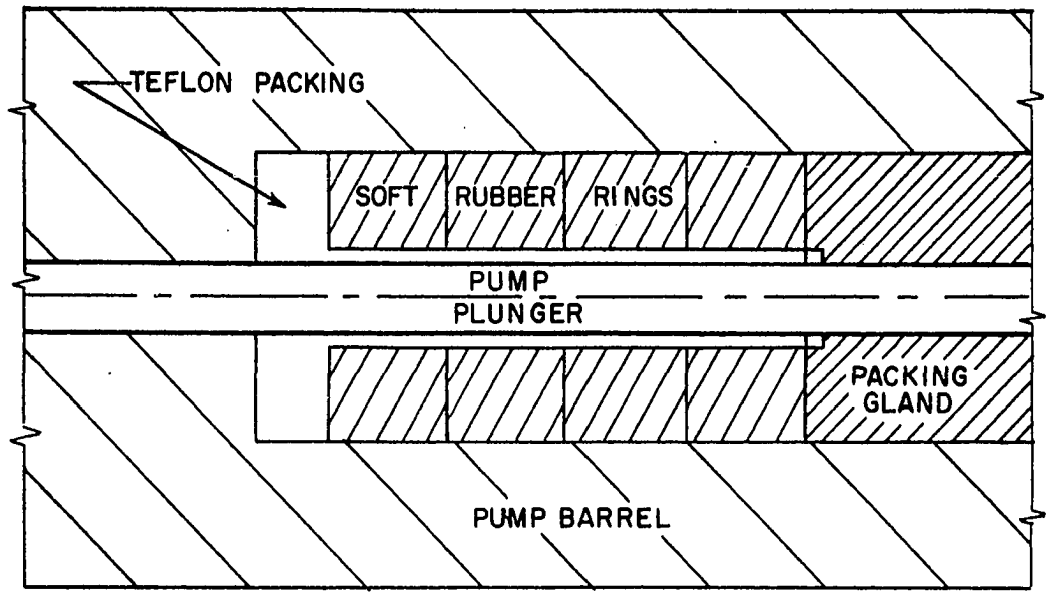


(A) TEFLON PACKING ASSEMBLY

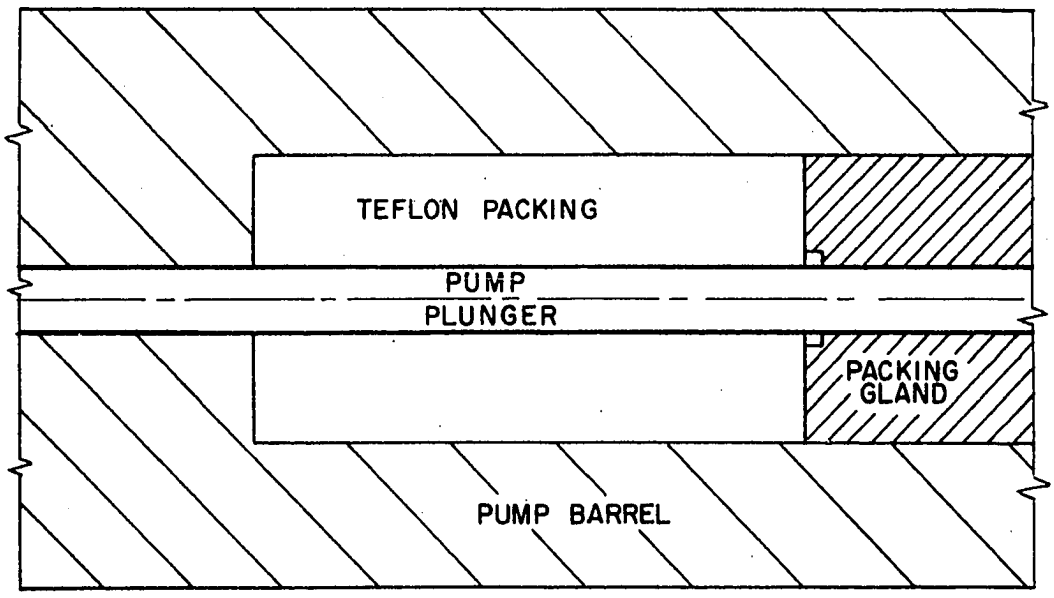


(B) SOLID TEFLON PACKING

Figure 13 - Packing Configurations for High Pressure Liquid Butadiene Pump

valve was first purchased, but it was not sensitive enough for this service. Another metering valve which did not prove to be satisfactory was the Veegroo, tapered-orifice, micro-flow valve purchased from the General-American Valve Company. The valve had a long narrow tapered slot in its tip. The tip moving in or out of the O-ring had the effect of a variable orifice to the flow of gas through the valve. At the tip of the tapered grove it was 0.02 inches deep with a $45^{\circ}$ angle. This orifice area decreased to zero as the valve moved through its 3/4-inch travel. Of the metering valves tested this one was the best for flow regulation because a preset ethylene flow rate was easy to obtain and a fairly large movement of the handle resulted in only a small change in the flow rate. The objection to this metering valve was that it would not maintain a constant flow over a long period of time with a large pressure drop across the valve. However this decrease in flow was easily corrected manually by constant monitoring and adjustment during a run. The decrease in flow was probably due to the cold flow of the O-ring into the orifice grove at the large pressure drops. With a low pressure drop across the valve the same problem was not encountered.

The metering valve which was the most satisfactory was the Autoclave, 1/8-inch, fine metering valve. This valve was equipped with a tapered stem which had a 2-degree angle on the tip. The stem travel was controlled by a

fine micrometer thread (1/4-inch-40) which permits fine control of the stem travel. This valve was much more difficult to adjust, particularly at flow rates under 10 SCFH, than the Veegroo tapered orifice valve, but when once set, the ethylene flow rate held constant.

# CHAPTER V

## REVIEW OF PREVIOUS WORK

The occurrence of the Diels-Alder reaction between ethylene and butadiene was first demonstrated by Wheeler and Woods (4, 5). They found in their studies on the mechanism of thermal decomposition of the normal olefins that some cyclohexene was formed when a mixture of 13 per cent butadiene and 87 per cent ethylene was heated to 600°C. Previously it had been thought that some type of activated group was necessary to render the double bond capable of entering into the Diels-Alder synthesis. This contention was proven to be false as ethylene, the simplest olefin, was found to react with 1,3-diene.

Joshel and Butz (6) found that ethylene reacts readily with butadiene at 200°C and 200 to 400 atm. pressure. Forty grams of 1,3-butadiene were added to a 300 ml. rocking-type autoclave and pressurized to 900 lb./sq.in. at room temperature with ethylene. The autoclave was then heated to approximately 200°C whereupon the pressure rose to 4,500 lb./sq.in. While shaking at this temperature for 15 hours the pressure dropped to 2,875 lb./sq.in. and held

constant. The products showed an 18 per cent conversion to cyclohexene.

Joshel (7, 8) indicates a process for manufacturing organic compounds of the alicyclic class. The process comprises reacting ethylene with a 1,3-diene under the action of heat and pressure. The reaction proceeds by the 1,4-addition of the ethylene to the diene, whereby the alicyclic compound produced has, in each case, a six-membered ring. Examples were given for the formation of cyclohexene and 1,2-dimethyl-cyclohexene by reacting ethylene respectively with 1,3-butadiene and 2,3-dimethyl-1,3-butadiene.

Gorin and Oblad (9) describe a continuous process for the production of cyclohexene from pentenes. The process consists of the pyrolysis of straight chain pentenes to form approximate stoichiometric quantities of ethylene and 1,3-butadiene which are then condensed to form cyclohexene. The reaction is stated to take place at about 150 atm. pressure with a temperature range of 300 to 350°C. An initial ratio of ethylene to butadiene of between 5 to 1 to 30 to 1 should be maintained in the reactor.

Whitman (10) relates a process of preparing cyclohexene from ethylene in rather large yields. He states that the yield of cyclohexene is increased by using a large mole ratio of ethylene to butadiene. The effect of increasing the mole ratio of ethylene is to favor the

production of cyclohexene at the expense of the competing reaction which leads to the formation of 4-vinylcyclohexene. Based on 100 per cent butadiene recovery, yields greater than 60 per cent were obtained with a mole ratio of 10 to 1 and greater than 75 per cent with a mole ratio of 20 to 1. The reaction was carried out at a temperature of about 100 to 300°C and a pressure of at least 100 atm. Whitman states that ethylene containing less than 200 parts per million of oxygen should be used.

The above references indicate that ethylene will react with butadiene to give cyclohexene at elevated pressures and fairly low temperatures, but they give no information as to the rate or mechanism of the reaction.

Evans and Warhurst (11) have applied the semi-empirical method for calculating the activation energy of simple chemical reactions, first developed by Eyring and Polanyi (12), to diene association reactions. As the prototype of the reaction they considered the addition of ethylene to butadiene using a planar transition state. They predicted, from the theoretical study, that the activation energies of diene association reactions between molecules containing no specially polar substituents were the same and of the order of 18 k. cals. Data available on the activation energies of diene association reactions show that the activation energies are approximately constant with a mean value of 26.3 k. cals.

Rowley and Steiner (13) in their study of the kinetics of diene reactions at high temperatures measured the rates of the reaction of butadiene with ethylene to form cyclohexene in the temperature range of 400 to 600°C at low pressures with low conversions. The products of the reaction were cyclohexene and vinylcyclohexene, the latter arising from the simultaneous dimerization of butadiene. The reaction was determined to be a homogeneous, bimolecular association having a rate constant as a function of temperature equal to

$$k_c = 3.0 \times 10^{10} \exp(-27{,}500/RT) \text{moles}^{-1} \text{cm.}^3 \text{sec.}^{-1} .$$

The equilibrium constant between cyclohexene, butadiene and ethylene based on thermal and spectroscopic data was calculated to be

$$K_c = \frac{(C_6H_{10})}{(C_2H_4) \times (C_4H_6)} = 0.33 \times 10^{-2} \exp(36{,}280/RT) \text{moles}^{-1} \text{cm.}^3 .$$

The activated or transition state, based on statistical rate calculations, was determined to be a cyclic complex similar to the final reaction product rather than a straight chain complex.

These experiments were carried out in a flow system using metal reactor tubes. Some of the reactor tubes were manufactured from mild steel, others from phosphor bronze. The results were identical in both types of reactors; furthermore, the rate was not affected by an increase in the surface to volume ratio, which was increased by a

factor of ten in one experiment, and therefore indicates that the reaction is homogeneous and not surface catalyzed.

In the study of Diels-Alder reactions in the gas phase (14) the diene addition has been observed as a homogeneous reaction of the second order while the division of the diene-adduct has been observed as a homogeneous reaction of the first order. The Arrhenius frequency factors for the gas reactions are of an order about $10^5$ times smaller than the collision rate for a gas reaction; they are small enough to show that a highly special orientation of diene and dienophile is required for conversion into the transition state of reaction.

A review of the reaction of ethylene with butadiene would not be complete without a review of the dimerization of butadiene. The dimerization of butadiene has been studied by several authors under various conditions. The general conclusion derived is that it is a homogeneous bimolecular reaction, not catalyzed by oxygen, and unaffected by anti-oxidants. The primary product was identified as vinylcyclohexene although in some investigations cyclooctadiene was also found in small amounts.

Kistiakowsky and Ranson (15) studied the dimerization of gaseous butadiene in the temperature range from 446 to 660°K at low pressure. The reaction was of second order with a rate constant expressed by the equation,

$$k_c = 9.20 \times 10^9 \exp(-23{,}690/RT) \text{moles}^{-1}\text{cm.}^3\text{sec.}^{-1} .$$

They postulated the linear transition state or activated complex based on statistical calculations. However the activation energy obtained was considerably lower than that of other investigations.

Wasserman (16) revised the calculations of Kistiakowsky and Ranson and carried them through for the activated complex which is stereochemically similar to vinylcyclohexene. In both cases (15, 16) the agreement with experiment was comparable so that no positive conclusions regarding the identity of the activated complex could be drawn. However if attention is directed to the fact that the kinetic course of the association of butadiene and of other bimolecular diene synthesis is not altered by oxygen or peroxides, then it can be concluded that free radicals do not play a role as intermediates. It appears more probable, therefore, that the slowest stage of these processes involves activated complexes of the same stereochemical type as the stable product molecules.

Robey, Wiese and Morrell (17) studied the reactions which butadiene undergoes in the liquid phase during storage and plant processing. The two reactions observed were the dimerization by the Diels-Alder type condensation, and the polymerization to plastic materials of high molecular weight. The reaction rate constants for the first reaction, which was bimolecular and homogeneous, agreed with those obtained

by Kistiakowsky. The formation of higher-molecular-weight polymers was found to be peroxide-catalyzed.

Rowley and Steiner (13) studied the dimerization of butadiene to form vinylcyclohexene at temperatures of 400 to 600°C at low pressures with low conversions. The dimerization was found to be a simple, homogeneous, bimolecular reaction leading essentially to the product indicated. The reaction rate constant for the reaction was calculated to be

$$k_c = 1.38 \times 10^{11} \exp(-26{,}800/RT) \text{moles}^{-1} \text{cm.}^3 \text{sec.}^{-1} .$$

Combination of this rate data with that obtained by Kistiakowsky and Ransom (15) at lower temperatures shows that the activation energy is temperature dependent. They showed, by statistical rate calculations, that a cyclic transition complex accounts best for all available rate data, which supports Wasserman's assumption.

Duncan and Janz (18) determined, based on previous investigations and thermodynamic equilibrium calculations, the expression for the equilibrium constant between butadiene-vinylcyclohexene to be

$$K_c = 2.76 \times 10^{-5} \exp(35{,}000/RT) \text{moles}^{-1} \text{cm.}^3 .$$

In a few investigations an eight-membered ring compound was found in the reaction products of the dimerization reaction. Foster and Schreiber (19) found that the dimerization of 1,3-butadiene at 100 to 130°C proceeded to

give a preponderence of vinylcyclohexene although the presence of 1-5 per cent of an eight-membered ring dimer was demonstrated. The structure of this eight-membered ring compound was not determined, but cyclooctane was formed when it was hydrogenated.

Hillger and Smith (20) studied the conditions under which the eight-membered ring formation is most favored in the butadiene dimerization reaction. No cyclooctadiene was found in the products when the reaction was carried out at atmospheric pressure, but at pressures between 40 to 100 lbs./sq.in. gauge with a temperature of 660 to 800°F, as much as 8 per cent of the product was determined to be cyclooctadiene. At higher pressures the amount of cyclooctodiene dimer formed was markedly reduced.

The investigations presented have been concerned with the reactions taking place at low pressure. No data are available for these reactions at more than a few lbs./sq.in. In fact the only data available for a bimolecular homogeneous reaction in the gas phase at elevated pressures are Kistiakowsky's (1). Kistiakowsky determined the behavior of the rate constant with pressure for the decomposition of hydrogen iodide at 300°C at pressures ranging from 1 to 300 atm. At moderate pressures (concentrations of HI from 0.02 to 1 mol./l.), the rate constant increased very slowly with increased pressure; however, at higher pressures (concentrations from 1 to 7

mol./l.) the increase in the rate constant was quite rapid with increased pressure.

# CHAPTER VI

# THEORETICAL CONSIDERATIONS

## Effect of Pressure on the Rate of Reaction

The effect of pressure on the rate of chemical reactions has been observed in the gas and liquid phases for both homogeneous and catalyzed reactions. In general, the effect of pressure on the rate of reaction is much more pronounced in gas phase reactions than in liquid or solid phase reactions although even in these reactions the effect can be considerable. Over the last thirty years considerable effort has been given to the study of the effect of pressure on reaction rates in homogeneous and catalyzed liquid reactions and in catalyzed gaseous reactions. However, essentially no work has been done on the effect of pressure on the reaction rate for a homogeneous gas phase reaction. For this investigation the theoretical considerations will be limited to the discussion of the effect of pressure on a bimolecular, homogeneous gas phase reaction.

In considering the effect of pressure on a homogeneous gas reaction it is important to relate the effect of pressure to the various characteristics of the reaction

system, such as: (1) concentration of reactants, (2) condition of equilibrium, (3) deviation from perfect and ideal solution behavior, (4) reaction rate constants.

The concentration of reactants and the condition of equilibrium are the two factors which are normally considered as being affected by pressure in a gaseous reaction. The increase in pressure not only increases the reaction rate by increasing the concentration of reactants but also reduces the reaction volume required. Increased pressure can also have a pronounced effect on the equilibrium concentration depending upon the mole ratio of the products to the reactants. The deviation from perfect gas and ideal solution behavior with increased pressure are not independent characteristics. The effect of this non-ideal behavior is felt through its effect on the above discussed considerations.

The reaction rate constant is also effected by pressure, and this effect is of primary interest in this investigation. It will be explained in terms of the two principal rate theories: (1) the collision theory, (2) the absolute reaction rate theory.

In a sense the two theories are equivalent, but their methods of approaching the problem of kinetics are quite different. It seems that the transition state model is better suited for the present purpose.

## The Collision Theory and Pressure

The collision theory (21) is based on the assumption that two conditions are necessary for a chemical reaction. The reacting molecules must collide before they can react and only those molecules possessing energies in excess of a critical amount, called energy of activation, react upon impact. The collision theory is expressed by the Arrhenius equation

$$k = Ae^{-E_a/RT} \qquad 8$$

where k = reaction rate constant

A = frequency factor representing the total number of collisions per unit time among the reacting molecules in a unit volume

$E_a$ = energy of activation

R = gas constant

T = absolute temperature.

Unfortunately, the agreement of the collision theory with direct experiment is limited only to a few very simple bimolecular reactions. For a more general application of the Arrhenius equation, a corrective factor known as the probability or steric factor q must be introduced. This factor includes all the errors of simplification involved in the collision theory, but it is mainly considered to represent the fraction of collisions that have the proper orientation for the colliding molecules. The modified equation is

$$k = Aqe^{-E_a/RT} \qquad 9$$

Although the Arrhenius equation does not contain a pressure term, the variation of the rate constant with pressure is manifested by the variation of the A, q, and $E_a$ terms in the equation.

Experimental evidence (based on liquid systems) indicates that the energy of activation is practically independent of pressure. The probability or steric factor appears to be only slightly effected. Consequently it is logical to assume that increased pressure accelerates the rate of collisions as can be expected from the increase in concentrations which shortens the free paths for molecular motions and increases the effect of van der Waal's forces, etc.

The Absolute Reaction Rate Theory and Pressure

The theory of absolute reaction rates (the Eyring Theory) is founded on statistical mechanics and the semi-empirical calculation of the energy of activation. It assumes a formation of an activated complex, in equilibrium with the reactants, as an intermediate step in the simple reaction. The rate of reaction is determined by the concentration of this complex present in the reaction system. The theory of absolute reaction rates provides a means of deriving an equation to determine the effect of pressure on the rate constant at constant temperature. The

derivation, based on the works of Evans and Polanyi (22), involves the following steps.

The rate constant in terms of the absolute rate theory is expressed as

$$k = \frac{K' k' T}{h} K^* \qquad 10$$

where $K'$ = transmission coefficient expressing the probability of conversion of the activated complex into products

$k'$ = Boltzmann constant

$h$ = Planck constant

$K^*$ = equilibrium constant in terms of the activated complex and initial reactants.

The equilibrium constant for a chemical reaction, $K_a$, is related thermodynomically to the standard free energy, $\Delta G^o$, by the equation

$$-RT\ln K_a = \Delta G^o. \qquad 11$$

Applying this equation to the formation of the activated complex,

$$-RT\ln K^* = \Delta G^* \qquad 12$$

where $\Delta G^*$ is the standard free energy of formation of the activated complex. Combining Equations 10 and 12

$$-RT\ln K^* = -RT\ln\left(k \frac{h}{K' k' T}\right) = \Delta G^* \qquad 13$$

Differentation of Equation 13 with respect to pressure at constant temperature yields

$$-RT\left(\frac{d\ln K^*}{dP}\right)_T = -RT\left(\frac{d\ln k}{dP}\right)_T = \frac{d(\Delta G^*)}{dP} \qquad 14$$

But at constant temperature, by definition,

$$\left(\frac{dG^*}{dP}\right)_T = V^* \qquad 15$$

then

$$\frac{d(\Delta G^*)}{dP}_T = \Delta V^* \qquad 16$$

where $\Delta V^*$ is the difference in volume between the activated complex and the original reactants. Combining Equations 14 and 16 gives the desired relation between the reaction rate constant and pressure.

$$\left(\frac{d\ln k}{dP}\right)_T = -\frac{\Delta V^*}{RT} \qquad 17$$

A simple analysis of this equation indicates that the rate constant increases with pressure if $\Delta V^*$ is negative, is independent of pressure when $\Delta V^*$ is zero, and decreases with pressure if $\Delta V^*$ is positive.

The constancy of the reaction rate constant in the gas phase at moderate pressures indicates that $\Delta V^*$ is zero or that the volume of the activated complex is the same as that of the initial reactants.

## Reaction Kinetics

The reaction rate of a chemical reaction is usually defined as the rate of change of mass of some participant that is formed or transformed per unit of

volume of the system. Expressed mathematically,

$$r = -\frac{-1}{V}\frac{dN}{dt}, \qquad 18$$

where r = reaction rate, moles formed or consumed per unit volume per unit time

N = moles of reactant or product present at time t

V = volume of the system

t = time of reaction.

The law of mass action states that the rate of a chemical reaction is proportional to the active masses of the participants. This law was first obtained on experimental grounds and was subsequently derived from the molecular theory in gases and liquids. In the original development, "active mass" meant concentration but other interpretations have been ventured from time to time. The rate equation may be written as

$$r = -\frac{1}{V}\frac{dN}{dt} = kf(N_a,N_b....) \qquad 19$$

where k = rate constant

$f(N_a,N_b...)$ = function established by the law of mass action.

From a study of reversible processes it appears that thermodynamic activity should be regarded as the "active mass." Take the general reaction

$$aA+bB+....\underset{k_2}{\overset{k_1}{\rightleftharpoons}} rR+sS+.... \qquad 20$$

The net rate of decomposition of substance A which participates in both the forward and reverse reaction can be expressed by the law of mass action as follows:

$$-\frac{1}{V}\frac{dN_a}{dt} = -\frac{1}{V}\left(\frac{dN_a}{dt}\right)_1 + \frac{1}{V}\left(\frac{dN_a}{dt}\right)_2 = k_1 C_A^a C_B^b \ldots\ldots - k_2 C_R^r C_S^s \ldots \quad 21$$

where $C_A$, $C_B$, .... = concentrations of components A, B, etc. At equilibrium the net rate of decomposition is zero, so that

$$k_1 (C_A^a)_e (C_B^b)_e \ldots\ldots - k_2 (C_S^s)_e (C_R^r)_e \ldots\ldots = 0 \quad 22$$

or

$$\frac{k_1}{k_2} = \frac{(C_S^s)_e (C_R^r)_e \ldots\ldots}{(C_A^a)_e (C_B^b)_e \ldots\ldots} = K_c \quad 23$$

where $K_c$ = equilibrium constant expressed in terms of concentrations.

In nonideal systems the equilibrium constant should be expressed in terms of activities rather than the concentration. Thus it appears that the thermodynamic activity should be used as the active mass term in the law of mass action. Therefore Equation 21 should be written as

$$-\frac{1}{V}\frac{dN_a}{dt} = k_1 (a_A^a)(a_B^b) \ldots\ldots - k_2 (a_R^r)(a_S^s) \ldots\ldots \quad 24$$

where $a_A$, $a_B$, $a_R$, and $a_S$ = activities of components A, B, R, and S respectively.

Theoretical considerations based on the activated complex theory also suggest that activities should be used in

expressing reaction rates (23).

Most kinetic data available in the literature are based on concentrations or partial pressures. In ideal systems, such as gas phase reactions at low pressures, no error is involved in using concentrations and partial pressures rather than activities. At high pressures, however, gas mixtures tend to become non-ideal and the use of partial pressures or concentration can lead to severe errors. Therefore, activities should be used in the formulation of the rate equation at elevated pressures.

## Determination of Activities in Gas Mixtures

The activities of the reactants will have to be determined for the gaseous mixtures used in this investigation so that the rate constants can be properly evaluated. No data are available for determining the activities, but three methods are presented for predicting the activity of a component in a gas mixture.

G. N. Lewis in 1901 (24, 25) introduced the concept of fugacity and activity in order to simplify the treatment of cases in which the ideal-gas and ideal solution concepts do not apply. The fugacity of a real gas is defined by the following two equations:

$$d\underline{G}_T = RTd\ln f = \underline{V}dP \qquad 25$$

and

$$\lim_{P \to 0} f/P = 1 \qquad 26$$

where f = fugacity of the gas

$\underline{G}$ = free energy of the gas

$\underline{V}$ = molal volume of the gas

P = pressure on the gas

Equation 25 can be integrated to give

$$\ln \frac{f}{P} = \ln \phi = \int_0^P \frac{Z-1}{P} dP \qquad 27$$

where f = fugacity at pressure P

$\phi$ = fugacity coefficient

Z = compressibility factor.

The value of the fugacity or fugacity coefficient can be determined by evaluating the integral on the right either by substituting an equation of state for Z or from experimental data by graphical integration.

The rigorous determination of the fugacity for a component in a mixture is possible when sufficient PVT-composition data are available for the system. The procedure is similar to that for a pure compound (shown above) except that the partial molal quantities are substituted for the molal quantities in Equation 25. At constant temperature

$$(d\overline{G}_j)_T = RTd\ln\overline{f}_j = \overline{V}_j dP \qquad 28$$

where $\overline{G}_j$ = partial molal free energy of component j in the mixture

$\overline{V}_j$ = partial molal volume of component j in the

mixture

$\bar{f}_j$ = fugacity of component j in the mixture

P = total pressure exerted on the mixture.

Equation 28 can be integrated to give

$$\ln\bar{f}_j = \ln y_j + \ln P + \int_0^P \frac{\bar{Z}_j - 1}{P}\, dP \qquad 29$$

where $\bar{Z}_j$ = partial molal compressibility factor of component j in the mixture

$y_j$ = mole fraction of component j in the mixture.

The fugacity of component j in the mixture may be calculated from this equation by using PVT-composition data to evaluate the integral on the right. For the special case in which there is no volume change on mixing at constant temperature, combining Equation 27 with Equation 29 gives

$$\ln\bar{f}_j = \ln y_j + \ln f_j \qquad 30$$

or

$$\bar{f}_j = y_j f_j \ . \qquad 31$$

This Equation is known as Lewis and Randall fugacity rule, and it applies to ideal solutions. It is applicable to gases over a considerably wider range than the perfect-gas law or Dalton's law of partial pressures.

Equation 29 may be expressed more simply by designating the integral on the right as $\ln\bar{\Phi}_j$, where $\bar{\Phi}_j$ is called the fugacity coefficient for component j in the mixture. Then

$$\ln \bar{\phi}_j = \int_0^P \frac{\bar{Z}_j - 1}{P} \, dP \qquad 32$$

where $\bar{f}_j = y_j \bar{\phi}_j P$ . 33

The fugacity coefficient, $\bar{\phi}_j$, may be evaluated when sufficient information is available to carry out the integration in Equation 32. The most accurate evaluation of $\bar{\phi}_j$ is likely to be obtained from an equation of state with several constants. However the equations are limited to substances for which the constants are available; they apply only over the region where the equations are applicable. Two procedures will be briefly described which can be applied to any substance and which require a minimum of data. The first uses the two-constant equation of state of Redlich and Kwong and the second employs the generalized charts based on the theorem of corresponding states.

The Redlich and Kwong equation of state is advantageous in that it requires only a minimum amount of data and has been constructed to be in accord with the behavior of real gases at high pressure. It has been adapted for use in calculating the fugacity coefficient for a component in a mixture (26). The constants for the equation of state for the mixture are obtained from the constants for the pure components which are determined from the critical temperature and critical pressure of each component and the temperature of the mixture. The equation

for $\bar{\phi}_j$ was obtained as

$$\log \bar{\phi}_j = 0.4343(Z_m-1)-\log(Z_m-BP)-\frac{A}{B}^2\left[\frac{2A_j}{A}-\frac{B_j}{B}\right]\log(1+\frac{BP}{Z_m}) \quad 34$$

where $A_j$, $B_j$ = constants for the pure components

$A$, $B$ = constants for the mixture

$Z_m$ = compressibility factor for the mixture.

The fugacity coefficient for a component in a mixture can also be determined from the generalized charts using the theorom of corresponding states. The following equation was proposed by Joffe (27).

$$\ln\bar{\phi}_j = \ln\phi+\frac{H^*-H}{RTT'_c}(T'_c-T_{cj})+\frac{(Z-1)(P'_c-P_{cj})}{P'_c} \quad 35$$

where $(H^*- H)$ represents the difference in molal enthalpy of the mixture at a low pressure and at the pressure where $\bar{\phi}_j$ is to be evaluated.

$T'_c$, $P'_c$ = pseudocritical temperature and pressure of the mixture.

$T_{cj}$, $P_{cj}$ = critical temperature and pressure of the pure component.

# CHAPTER VII

## EXPERIMENTAL PROCEDURE

The homogeneous reaction of ethylene with butadiene to form cyclohexene was first reported by Wheeler and Woods (4) in 1929. Although many investigators have studied this reaction since then, none of the investigations have been carried out at pressures of more than a few pounds per square inch. The present work was undertaken to investigate the effect of pressure on the homogeneous, gaseous (fluid), bimolecular reaction of ethylene with butadiene in the pressure range of 250 to 4,500 lbs./sq.in. gauge and in the temperature range of 500 to 700°F in a tubular reactor.

### Materials

Pure grade ethylene was supplied by the Phillips Petroleum Company. This ethylene had a minimum purity of 99 mol. per cent with an oxygen content of approximately 5 ppm. A sample analyzed on the chromatograph indicated that the actual purity was considerably better than the 99 per cent guaranteed.

Pure grade butadiene, containing an inhibitor, was supplied by Esso Research Laboratories. As dimerization of

butadiene to vinylcyclohexene takes place slowly at room temperature, even in the presence of an inhibitor, it is impossible to keep butadiene pure over an appreciable length of time. Pure butadiene for the reaction was obtained by single stage distillation immediately before each experimental run. Butadiene obtained in this manner was determined by chromatographic analysis to be essentially pure with only a trace of impurities.

## Calibrations

It was necessary to calibrate the coiled capillary ethylene flow device and the butadiene reservoir before any data could be taken. The ethylene flow device was calibrated as follows. After charging the high pressure reservoir with ethylene to approximately 5,000 lb./sq.in. gauge, the air pressure to the Sprague, air-driven, high-pressure pump was adjusted so the ethylene pressure was maintained at 5,000 lb./sq.in. gauge by injecting water into the bottom of the pressure vessel. The outlet of the metering valve was connected directly to the water saturator and hence to the "Precision" wet-test meter. The metering valve was adjusted to give the desired reading on the Barton gauge. The ethylene flow rate was determined by measuring the time required for a predetermined amount of ethylene to flow through the wet-test meter. These values were then converted to standard conditions by correcting

for pressure, temperature, water content and compressibility factor. Data were obtained for the complete range of pressure drop for each coil. A plot was made of flow rate versus pressure drop for each coil (see Appendix B).

The butadiene reservoir was calibrated by filling the reservoir with water and then reading the liquid height before and after a calibrated amount of water was removed from the system. This procedure was continued from top to bottom for only the sight glass as it was used for all butadiene flow rate determinations. As the cross-sectional area varied slightly from top to bottom, a plot of reservoir volume versus liquid height was obtained by integrating the volume over the height of the liquid for the sight glass (see Appendix B).

## Preliminary Procedure

The equipment for this investigation was designed in such a way that considerable preparation was required before an actual run could be made. The high pressure ethylene storage vessel had to be filled as previously discussed. Freshly distilled butadiene was obtained by one step distillation from the main butadiene supply cylinder to a small butadiene feed tank mounted in a cold water bath. This freshly-distilled butadiene was then used to fill the butadiene feed reservoir. A water reservoir for the Sprague, high pressure water pump was filled with oxygen-free,

distilled water. Then the salt in the salt bath was melted and heated to the desired temperature. The power input to the salt pot was adjusted and the temperature controller set so that the controller would control at the desired temperature. The hot oil bath was activated and allowed to heat. Then the refrigeration unit was activated so that cold water would be supplied to the condenser. The pressure transmitter was set at the desired operating range. The chromatograph was activated and allowed to come to the desired temperature. After the above operations were completed the equipment was ready for operation.

## Operating Procedure

After all the preliminary operations had been completed the system was activated by opening the metering valve. The pressure in the system increased until the system pressure was equal to the preset operating pressure, at which time the back pressure control system activated and maintained a constant pressure. If needed the set point on the controller could be changed to give the desired operating pressure. The air pressure to the Sprague, air-operated, liquid pump was then adjusted so that the ethylene pressure would be maintained at 5,000 lb./sq.in. After the metering valve had been adjusted to give the desired ethylene flow rate, the valve from the butadiene supply was opened and the butadiene pump was activated. The butadiene flow rate, determined by measuring the decrease

in liquid butadiene height in the sight glass per unit time, was set to the desired value by adjusting the stroke length. This adjustment could be made with the pump in operation. The system was then allowed to reach steady state conditions, which required from ten to forty-five minutes depending upon the flow rate and pressure. In most cases it was not necessary to adjust either the ethylene flow or the butadiene flow during a run.

Upon reaching steady state operations the data recording process was started. A set of readings were taken at regular intervals of five to twenty minutes, depending upon the pressure and flow rate, until a sufficient number of sets had been obtained. A normal data set consisted of the following:

(1) Time (hour and minute)

(2) Ethylene storage vessel pressure (lb./sq.in. gauge)

(3) Pressure drop as obtained from the differential pressure gauge

(4) Reactor temperature ($^{o}$F)

(5) Reactor pressure (lb./sq.in. gauge)

(6) Wet-test meter reading (zero at start of run)

(7) Butadiene sight glass reading (centimeters)

(8) Liquid product sample reading (cc., 50 at start)

(9) Temperature of gas in wet-test meter ($^{o}$F).

The date, run number, coil number and barometric pressure

were recorded only at the beginning of each run. Immediately after recording each set of data a gas sample was taken, and a chromatographic analysis made which was identified with the time and run number. Normally three to five sets of data were taken per run. A liquid sample was taken at the end of each run for analysis at a later time.

After each run was completed the butadiene pump was stopped and a new run started by repeating the above procedure, provided that the pressure and temperature remained constant. If the operating pressure were changed, the back pressure control system had to be set to the new operating pressure before a run could be started. In most cases this setting could be accomplished without depressurizing the system. If the operating temperature were changed, the system had to be depressurized, the liquid salt had to be heated and the temperature controller had to be set for the new temperature before a new run could be started.

After completing a set of runs, chromatographic analyses were made of the liquid samples obtained during the runs.

## Method of Analysis

Several methods were available for the analysis of the gases and liquids in the product streams. Vapor phase, partition chromatography was selected because it was the

cheapest, simplest and most convenient for obtaining an accurate analysis.

A chromatograph, built in conjunction with a previous research project (28), was suitable for use only after major modifications in the method of controlling the temperature of both the thermoconductivity cell detector and the column. Figure 14 is a picture of the chromatograph including the strip chart recorder.

Several different column packings were tried before one was found which was satisfactory. Most of the packings had too great an affinity for the unsaturated compounds and the desired separation could not be obtained within a reasonable length of time. Apiezon-L on celite and Resoflex 446 on 42-60 tyler support were two of the packings tried which did not give the desired separation. Silicone oil 550 on fire brick and LAC-728 (diethylene glycol succinate) on fire brick both proved to be satisfactory packing material.

An eight foot 1/4-inch copper tube, packed with silicone oil 550 on fire brick, constituted the column used for the gas analysis. The column temperature was maintained at 225 F with a helium flow rate of 150 cc. per minute. The analysis was determined by comparing the elution curves obtained for the gas samples to those obtained from the standard gas sample. Two standards of different compositions were used.

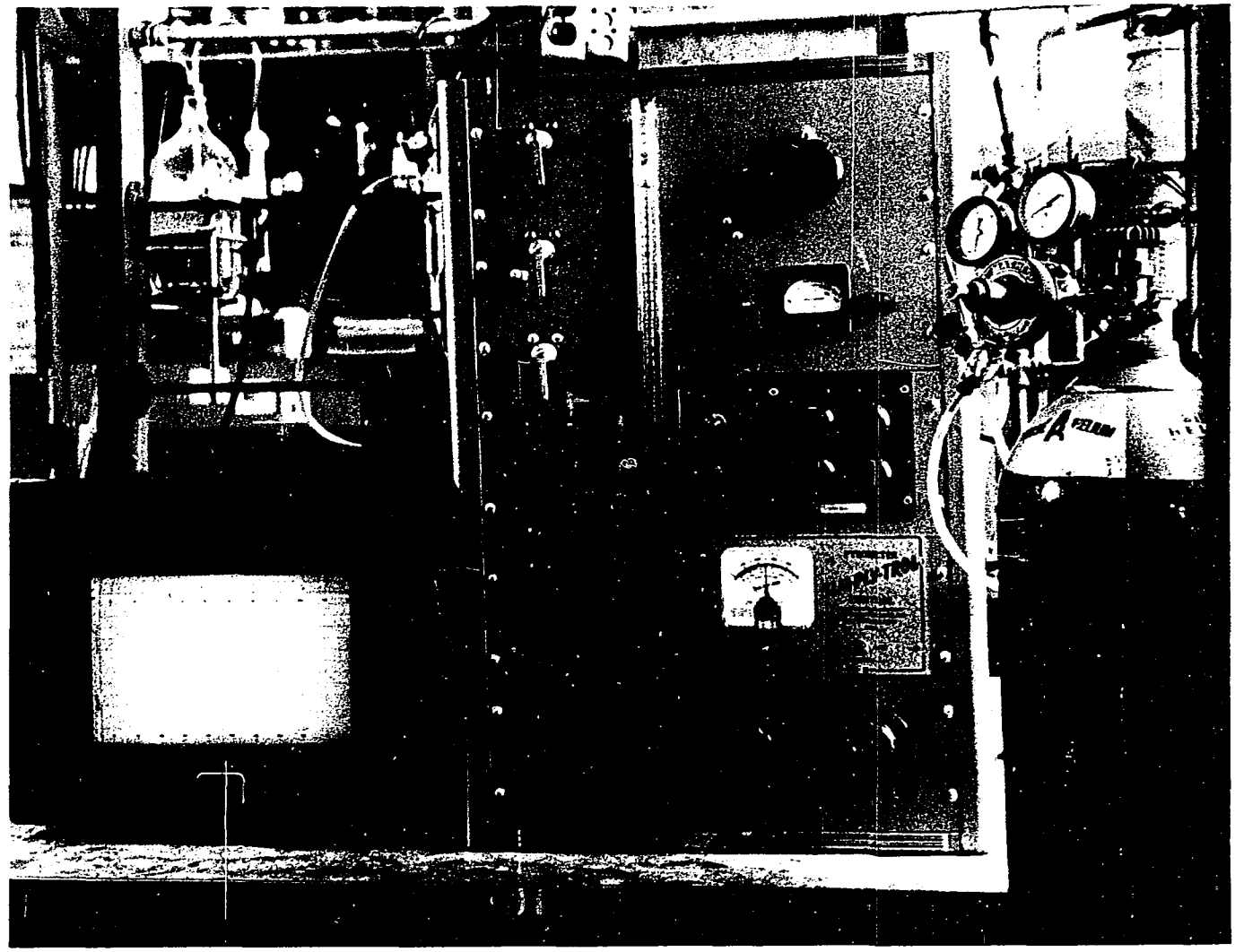

Figure 14 - Chromatograph

The procedure for obtaining the standard gas samples was conducted in the following manner. A 500 cubic inch stainless steel cylinder was evacuated and a weighed amount of cyclohexene added with a syringe through a rubber septum in the system. Butadiene and ethylene were then added in succession to the cylinder, and the amounts were determined from absolute pressure measurements taken before and after each gas addition. The absolute pressure measurements were obtained from a mercury manometer connected to the cylinder.

A one cubic centimeter gas sample was used for the gas analysis. The complete gas analysis was completed in approximately thirteen minutes. If the vinylcyclohexene content of the gas could be neglected (as was true many times), the analysis was completed in only five minutes.

For the liquid analysis two different column packings were used. The same column used for the gas analysis was used for the first set of liquid samples. The temperature was increased to 320°F but all other conditions remained the same. A six-feet long, 1/4-inch copper tube, packed with LAC-728 on fire brick, was used as the column packing for all subsequent liquid analysis. The temperature was maintained at 320°F for this column, but the helium flow rate was decreased to 80 cubic centimeters per minute. As with the gas analysis, the liquid analysis was obtained by the comparison of the elution curve of the liquid sample

with the elution curve of the standard liquid sample. This procedure gave the relative amounts of all the liquid products through $C_8H_{12}$ but did not indicate the amount of the heavier polymerization products in the liquid phase. The amount of the heavier polymerization products was determined by injecting a known amount of liquid sample into the chromotograph and then calculating the total amount of the lighter components from the elution curves. The difference represents the amount of the heavier components in the liquid phase. A liquid sample of 4 micro-liters was used for the analysis.

## Preliminary Runs

A series of preliminary runs were conducted to determine the best experimental procedure for operating the equipment and also to determine the maximum conditions at which the polymerization of ethylene could be neglected in the reaction. At the time the preliminary runs were made, the maximum pressure available with the back pressure regulator in use was 3,000 lb./sq.in. Based on these runs at a pressure of 3,000 lb./sq.in., with a flow rate of approximately 4 SCFH, the polymerization of pure ethylene can be neglected at temperatures below 700°F. Above 700°F ethylene polymerization products start to appear in the product stream.

## Problems Encountered

As expected the primary problem encountered in the actual operation of the experimental equipment was the polymerization of butadiene. Robey, Wise, and Morrel (17) showed that the polymerization of butadiene was small compared to the dimerization reaction in the absence of a catalyst. Their studies were made in the liquid phase at considerably lower temperatures than are encountered in this investigation, but it was assumed that these statements would apply to the present investigation. This assumption has been proved to be correct. Butadiene is very readily catalyzed by oxygen; therefore special precautions were taken to keep the system as oxygen-free as possible. Even with these precautions the polymerization of butadiene was a problem as discussed below.

In the initial design only one pressure gauge was used to measure the pressure in the reaction section, and it was connected to the exit end of the reactor. Therefore, the only indication of incipient plugging due to a presence of polymers was a decrease in ethylene flow rate. By the time this change in flow was noticeable the system would become completely plugged. By locating a second pressure gauge immediately upstream from the reactor, the two gauges would indicate a slightly different reading when the system first started to plug, and corrective action could be taken before the plug had formed.

The normal procedure observed when the system first started to plug was to open the valve to the vent line and allow the system pressure to blow-out the polymer if possible. The system was then heated to at least 600°F and air fed to the reactor to oxidize the polymer present. The polymer oxidizes in air at 600°F (29). This procedure worked in most cases, but a few times the system became completely plugged.

The high temperature preheater appeared to be more susceptible to plugging than the reactor itself, and as such, it probably prevented the more serious problem of polymer deposits within the reactor. The first time the system plugged, the preheater was removed and the reactor was inspected. The preheater was completely plugged with polymer but the reactor appeared to be clean. No appreciable polymer deposit was present, and a volume check showed no detectable change.

The second time a plug occurred, the reactor was heated to approximately 1,000°F and the plug was blown out by pressurizing with a hydraulic hand pump. All subsequent plugs except one were removed by this method. This one exception occurred when a run was started at 700°F and 4,500 lb./sq.in. The plug occurred before the system could be vented. All methods were tried, but the plug could not be removed. Finally the reactor had to be removed and replaced. This reactor was cut into several

pieces, and the plug was found to be approximately two feet long and located near the preheater. From this and the other runs it appears that polymer formation is more prevalent at the higher temperatures. Most of the difficulties were encountered at the higher temperatures and at the higher pressures.

# CHAPTER VIII

## RESULTS

The experimental runs made during the course of this investigation for the reaction of ethylene with butadiene were limited almost entirely to three temperatures, 500, 550, and 600°F. At each of those temperatures the runs were carried out at pressures of 500, 1,000, 2,000 and 4,500 lbs./sq.in. gauge. Approximately four runs, having different flow rates and compositions, were made at each combination of pressure and temperature. A few experimental runs were made at 700°F but the reaction was so fast above 500 lb./sq.in. at that temperature that most of the butadiene reacted and an accurate kinetics study could not be conducted. In addition, the polymerization of butadiene became quite a problem at the higher temperatures. At temperatures below 500°F, the reaction was so slow that accurate analysis could be made only at the highest pressures, therefore, 500°F was the lowest temperature investigated.

Most of the runs were made using the larger (1/8-in. I.D.) reactor with the preheater. The last six runs were made using the smaller (1/16-in. I.D.) reactor

without a preheater. The small reactor was used to demonstrate the absence of wall effects in this reaction.

## Data

Because of the considerable amount of data taken, the actual, raw experimental data will not be presented. However, a sample of the actual experimental data for a typical run is given in Table 1. In calculating the computed data from the experimental data, values averaged over the duration of the run, were used. Sample calculations and a complete list of the computed data are presented in Appendices C and D respectively. An IBM 650 computer was utilized for the actual calculations.

The data reported in this study were obtained using rather large mole ratios of ethylene to butadiene (mole ratio varied from 3 to 16). This large mole ratio was required to reduce the side reaction of the dimerization of butadiene to vinylcyclohexene and polymerization to longer chains. The data represent a wide variation with respect to the amount of reaction which had occured, in that at the low pressures and temperatures only a small amount of the butadiene had reacted where as at the highest pressures and temperatures the butadiene had almost completely reacted. The results of the material balance calculations presented in Appendix D indicated that the data were consistent in that in only eight of sixty four

TABLE I

RAW EXPERIMENTAL DATA FOR THE REACTION OF ETHYLENE WITH BUTADIENE

| | Run #111 | Date 10-17-61 | | |
|---|---|---|---|---|
| | Baro. Press. in Hg. 28.90 | Ethylene Flow Coil #1 | | |
| 1. | Time | 9:15 | 9:20 | 9:25 |
| 2. | Differential pressure across ethylene flow coil | 9.90 | 9.95 | 9.90 |
| 3. | Reactor pressure (lb./sq. in. gauge) | 4,500 | 4,500 | 4,500 |
| 4. | Reactor temperature ($^{o}$F) | 500 | 500 | 500 |
| 5. | Butadiene flow (cm.) | 114.7 | 79.3 | 43.7 |
| 6. | Gas product ($ft.^3$) | 0 | 1.06 | 2.115 |
| 7. | Liquid product ($cm.^3$) | 50 | 41.2 | 32.6 |
| 8. | Main Ethylene Reservoir pressure (lb./sq.in. gauge) | 5,000 | 5,000 | 5,000 |
| 9. | Wet test meter temperature ($^{o}$F) | 75 | 75 | 75 |

Note: (1) Gas analysis was determined at every data point.

(2) Liquid sample was taken at the completion of the run for analysis at a later time.

runs was the butadiene mass balance off greater than 5 per cent and in only three runs greater than 10 per cent. However, an earlier set of runs were discarded because of the inconsistency of the material balance calculations.

## Kinetic Analysis

The kinetic analysis of the reaction of ethylene with butadiene involves the study of two reactions: the reaction of ethylene with butadiene to form cyclohexene and the dimerization of butadiene to form vinylcyclohexene. Both reactions are similar Diels-Alder reactions and, based on data obtained at low pressure, are simple bimolecular homogeneous second-order reactions. Actually the dimerization of butadiene yielded a small amount of cyclooctadiene in addition to the vinylcyclohexene, as shown in Appendix D, but it was included with the vinylcyclohexene for the purpose of studying the butadiene dimerization reaction. Thermodynamic calculations on the reverse reactions, that is the formation of ethylene and butadiene from cyclohexene and butadiene from vinylcyclohexene, indicate that these reactions can be neglected at these temperatures and pressures. Only at much higher temperatures and at very low pressures would these reactions become appreciable.

Under steady state conditions in a tubular flow reactor a material balance over a differential volume of the reactor yields

$$Fdx = rdV_r \qquad 36$$

where F = reactor feed rate, moles per unit time

x = moles of a component converted per mole of feed

$r$ = rate of reaction, moles of a component converted per unit volume per unit time

$V_r$ = reactor volume occupied by reacting system.

The rate of reaction r, as previously discussed, can be expressed in terms of activities for a bimolecular, homogeneous, second-order reaction by the equation

$$r = k(a_A)(a_B) \qquad 37$$

Therefore the differential rate equation for a tubular flow reactor, determined by combining Equations 36 and 37, is expressed as

$$\frac{F dx}{dV_r} = k(a_A)(a_B) \; . \qquad 38$$

Since this equation is to be used to interpret experimental kinetic data it can be rearranged to give

$$k = \frac{F dx}{dV_r (a_A)(a_B)} \; . \qquad 39$$

The integral rate equation can be expressed as

$$k = \frac{F}{V_r} \int_{x_i}^{x_o} \frac{dx}{(a_A)(a_B)} \qquad 40$$

Equations 39 and 40 are the basic rate equations for a tubular flow reactor, assuming a homogeneous second-order reaction, and are used to determine the reaction rate constant from experimental data.

In obtaining experimental kinetic data the tubular flow reactor can be classified either as a differential reactor or an integral reactor. In a differential reactor

the change in composition must be small, and consequently the reaction rate will be constant throughout the reactor. When the conditions of approximately constant reaction rate cannot be met, the reactor will be considered an integral reactor. The advantage of the differential reactor is that the reaction rate constant can be obtained directly from the differential rate equation (Equation 39) by assuming average values for the activities throughout the reactor, whereas for the integral reactor the activities have to be expressed in terms of composition as indicated by the integral rate equation (Equation 40).

The kinetic data obtained in this investigation was such that at the low pressures and temperatures, where only a small amount of reaction occured, the reactor operated as a differential reactor and essentially no error was introduced by determining the reaction rate constant from the differential rate equation. At the higher pressures and temperatures, with the increased reaction rate the conditions required for the differential reactor were no longer satisfied. The reactor then operated as an integral reactor requiring the use of the integral rate equation.

The rate of reaction r, as previously discussed, is a function of the active masses of the reactants and is usually expressed as activities or concentrations. Activities are generally agreed to be more correct, but

concentrations are more common. The rate constants for these reactions are calculated using concentrations in addition to activities so that the rate constants based on concentrations can be compared to those based on activities.

## Rate Constants Based on Activities

The two competing reactions involved in the reaction of ethylene with butadiene can be written as follows:

$$C_2H_4 + C_4H_6 \xrightarrow{k_1} C_6H_{10}$$

$$C_4H_6 + C_4H_6 \xrightarrow{k_2} C_8H_{12}$$

where $k_1$ and $k_2$ are the rate constants for the formation of cyclohexene and vinylcyclohexene respectively. The kinetic rate equations for the above reactions, based on activities and assuming homogeneous bimolecular reactions, can be written as

$$\frac{dx_c}{dV_r} = \frac{(k_1)(a_a)(a_b)}{F} \qquad 41$$

$$\frac{dx_d}{dV_r} = \frac{(k_2)(a_b)^2}{F} \quad . \qquad 42$$

where $x_c$, $x_d$ = moles of cyclohexene and vinylcyclohexene respectively per mole of feed

$a_a$, $a_b$ = activities of ethylene and butadiene respectively.

The above equations can be solved provided the activities can be expressed in terms of composition.

Several methods were previously discussed for calculating the activity of a component in a mixture. All of the methods except the Lewis fugacity rule are too complicated to be included in the rate equation; therefore, the Lewis fugacity rule is used. The activities of the reactants in the mixture, based on the Lewis fugacity rule and assuming unit fugacity as the standard state, can be written as

$$a_a = \bar{f}_a = X_a f_a \qquad 43$$

$$a_b = \bar{f}_b = X_b f_b \qquad 44$$

where $\bar{f}_a$, $\bar{f}_b$ = fugacity of ethylene and butadiene respectively in the mixture

$X_a$, $X_b$ = mole fraction of ethylene and butadiene respectively in the mixture

$f_a$, $f_b$ = fugacity of pure ethylene and butadiene respectively at the pressure and temperature in question.

The mole fractions of the various components of the mixture in terms of $x_a$, $x_b$, $x_c$ and $x_d$ are determined as follows, where $A_o$ and $B_o$ are the mole fractions of ethylene and butadiene respectively in the feed.

Mol. $C_2H_4$/mol. feed = $x_a = A_o - x_c$ 45

Mol. $C_4H_6$/mol. feed = $x_b = B_o - x_c - 2x_d$ 46

Mol. $C_6H_{10}$/mol. feed = $x_c = x_c$ 47

Mol. $C_8H_{12}$/mol. feed = $x_d = x_d$ 48

Total mol/mol. feed = $A_o + B_o - x_c - x_d = 1 - x_c - x_d$ 49

The mole fraction of each component is therefore

$$X_a = (A_o - x_c)/(1 - x_c - x_d) \qquad 50$$

$$X_b = (B_o - x_c - 2x_d)/(1 - x_c - x_d) \qquad 51$$

$$X_c = x_c/(1 - x_c - x_d) \qquad 52$$

$$X_d = x_d/(1 - x_c - x_d) \qquad 53$$

Making the appropriate substitutions, the differential Equations 41 and 42 can be rewritten as

$$\frac{dx_c}{dV_r} = \frac{(k_1)(f_a)(f_b)(A_o - x_c)(B_o - x_c - 2x_d)}{(F)(1 - x_c - x_d)^2} \qquad 54$$

$$\frac{dx_d}{dV_r} = \frac{(k_2)(f_b)^2(B_o - x_c - 2x_d)^2}{(F)(1 - x_c - x_d)^2} \qquad 55$$

Equations 54 and 55 are two differential equations having two dependent variables and one independent variable; therefore, knowing the exit composition from the reactor, the two equations can be solved simultaneously to give the two rate constants. The actual solutions of the above equations were obtained by two methods.

The first set of solutions were obtained by programing and solving the two differential equations on the Donner 3100 analog computer available at the University of Oklahoma. Appendix E contains the calculations and analog program used for solving the equations on the analog computer. The analog computer handles simultaneous differential equations of this type quite readily and the

analog program is fairly simple; however, due to minor malfunctions of the computer at the time the solutions were made, the results were not as accurate as anticipated. Comparison of the analog results with those obtained assuming a differential reactor at the low conversion runs showed a deviation as large as 10 per cent.

The second set of solutions were obtained from a analytical solution of the two differential equations. The analytical solution which is rather tedious is presented in Appendix F. The resulting equations are as follows:

$$k_1 = \frac{(C)(F)}{(V_r)(f_a)(f_b)} \qquad 56$$

and

$$k_2 = \frac{(N)(C)(F)}{(V_r)(f_b)^2(2)} \qquad 57$$

where

$$C = \int_1^S \frac{-(N-1)\left[1+S^N\left(B_o+\frac{A_o}{N-1}\right)+\frac{A_oS(N-2)}{N-1}\right]^2}{(4)(S)\left[S^N\left[B_o(N-1)+A_o\right]-(A_o)(S)\right]}\,dS \qquad 58$$

and

$$S = \frac{A_o-x_c}{A_o} \qquad 59$$

The factor N in Equations 57 and 58 has been previously determined as shown in Appendix F. The actual numerical solutions were obtained on the IBM 650 computer. Appendix G contains a complete list of the rate constants calculated from the experimental data obtained during this investigation. The results obtained by assuming a differential reactor for some of the low conversion runs are in very

close agreement with the results obtained by solving the above equations.

The natural logarithm of the rate constant based on fugacity, for the formation of cyclohexene from ethylene and butadiene, are plotted versus pressure in Figure 15 for the temperatures investigated. The isothermal curves in Figure 15 were obtained by fitting a quadratic equation to the data by the method of least squares using the IBM 650 computer. The equations obtained for the least square fit are

$$\ln k_1 = -16.35 + 8.20 \times 10^{-4}P - 8.92 \times 10^{-8}P^2$$

$$\ln k_1 = -15.15 + 6.63 \times 10^{-4}P - 8.02 \times 10^{-8}P^2$$

and $$\ln k_1 = -13.94 + 2.12 \times 10^{-4}P - 1.70 \times 10^{-8}P^2$$

respectively for the temperatures 500, 550 and 600°F. Figure 15 also contains the rate constant obtained from the rate equation developed by Rowley and Steiner in their work at low pressures. The present data appears to agree with their work.

The absolute reaction rate theory states that the relationship between the rate constant and pressure is given by Equation 17, where

$$\left(\frac{d\ln k}{dp}\right)_T = -\frac{\Delta V^*}{RT} \quad . \qquad 17$$

Figure 16 shows a plot of $\Delta V^*$ versus P for the three principal temperatures investigated. The values of $\Delta V^*$

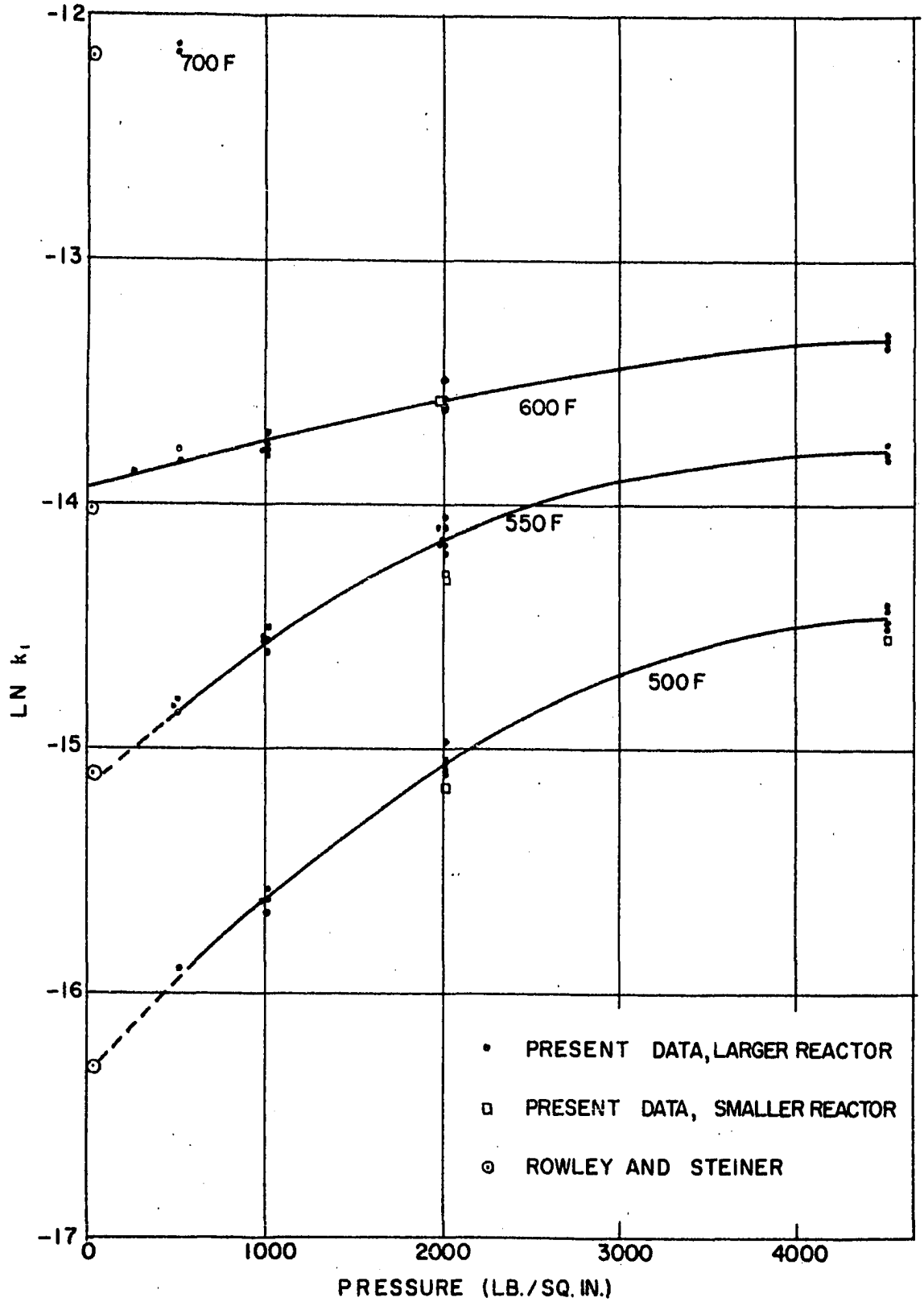


Figure 15 - Reaction Rate Constant Versus Pressure for the Ethylene-Butadiene Reaction Based on Activities

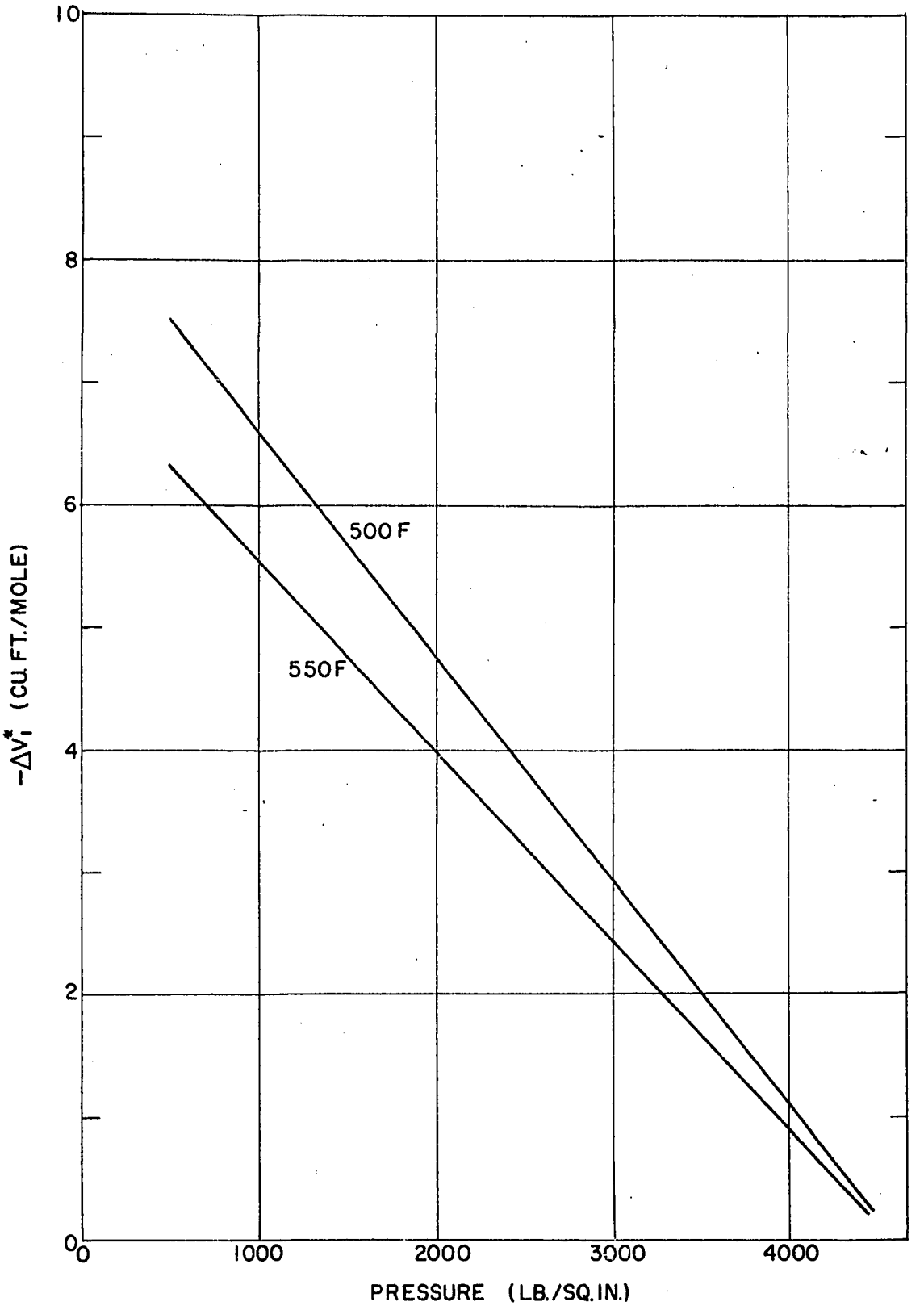


Figure 16 - $\Delta V_1^*$ Versus Pressure for the Ethylene-Butadiene Reaction

were obtained by differentiating the equations of the curves in Figure 15 with respect to P.

Figure 17 contains similarly for the butadiene dimerization reaction, a plot of ln $k_2$ versus pressure for the temperatures investigated. Also included in Figure 17 are the corrected curves, obtained by fitting a quadratic equation to the data obtained in this work at 2,000 and 4,500 lb./sq.in. in conjunction with the data of Rowley and Steiner (13) at low pressures, all at temperatures 500 and 550°F. The equations obtained for the corrected curves are

$$\ln k_2 = -14.16 + 6.80 \times 10^{-4}P - 6.28 \times 10^{-8}P^2$$

and $$\ln k_2 = -12.93 + 4.61 \times 10^{-4}P - 4.75 \times 10^{-8}P^2$$

respectively for the temperatures 500 and 550°F. Figure 18 contains a plot of $\Delta V_2^*$ versus pressure for the corrected curves at 500 and 550°F.

Rate Constants Based on Concentrations

The kinetic rate equations based on concentrations are similar to Equations 41 and 42 except that concentrations are used instead of activities. Therefore

$$\frac{dx_c}{dV_r} = \frac{(k_{1c})(C_a)(C_b)}{F} \qquad 60$$

$$\frac{dx_d}{dV_r} = \frac{(k_{2c})(C_b)^2}{F} \qquad 61$$

where $k_{1c}$, $k_{2c}$ = reaction rate constants for the

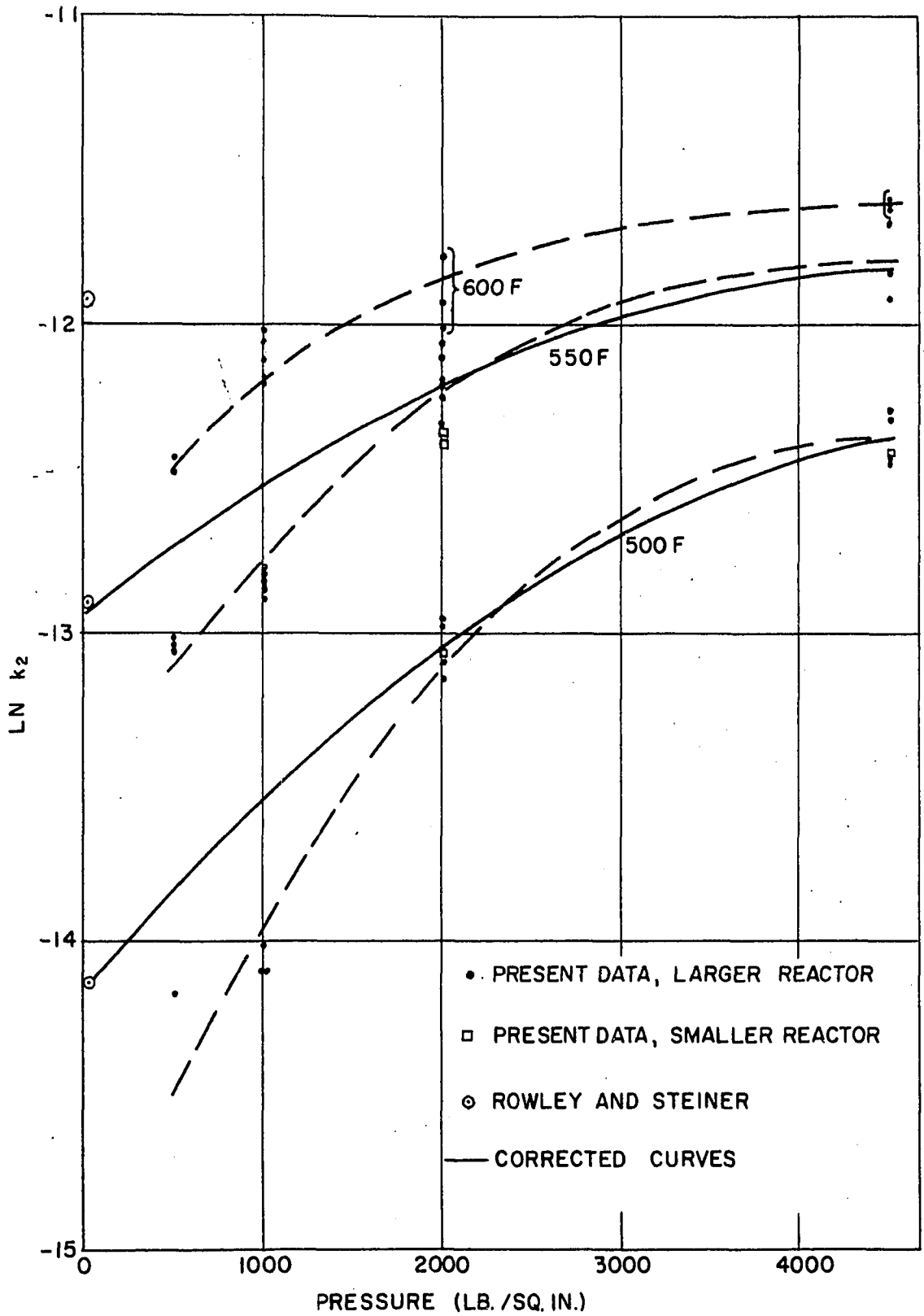


Figure 17 - Reaction Rate Constant Versus Pressure for the Butadiene Dimerization Reaction Based on Activities

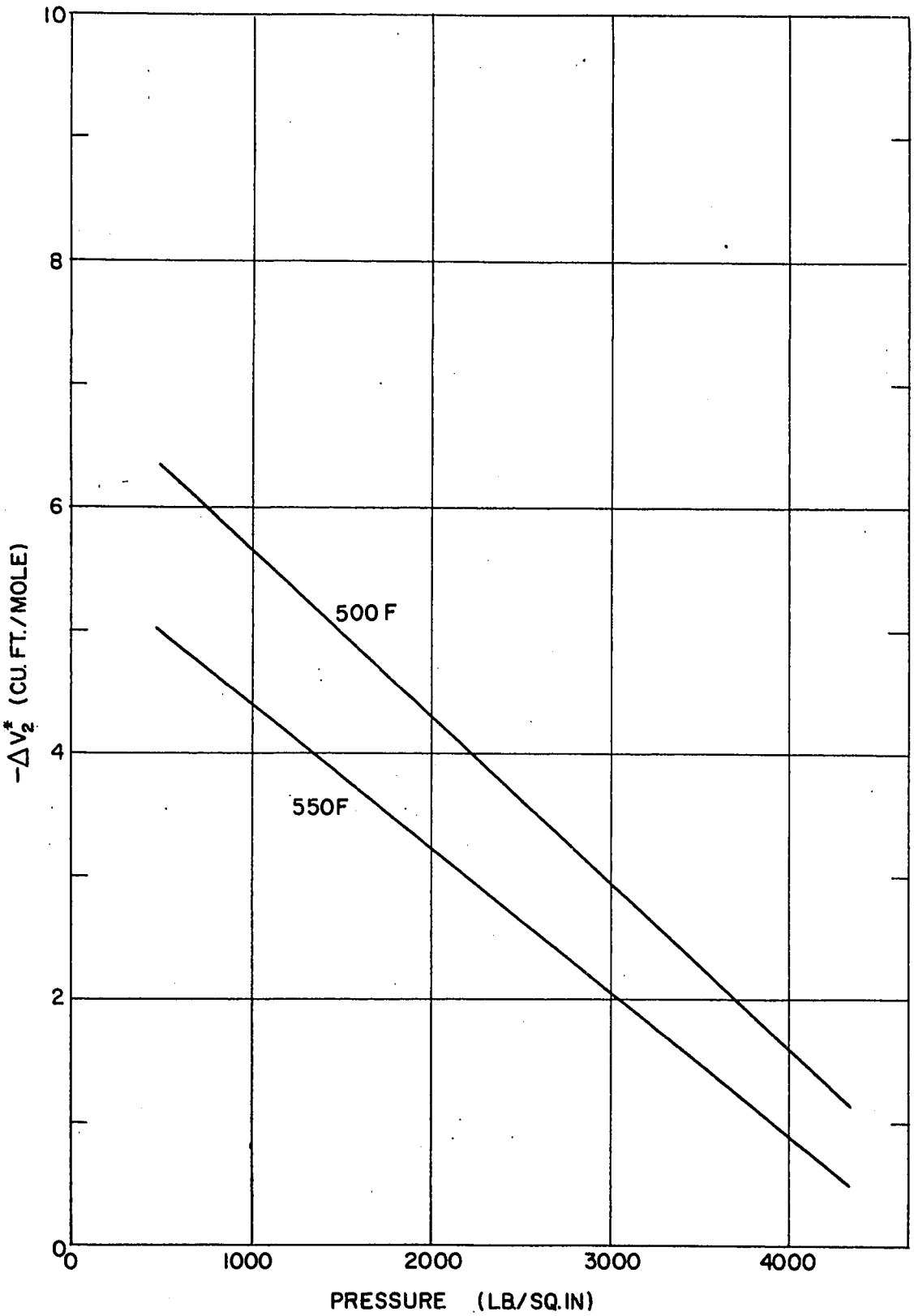


Figure 18 - $\Delta V_2^*$ Versus Pressure for the Butadiene Dimerization Reaction (Corrected Data)

formation of cyclohexene and vinylcyclohexene based on concentrations.

$C_a$, $C_b$ = concentrations of ethylene and butadiene respectively, mol/ft$^3$.

The concentrations are expressed as

$$C_a = (X_a)\left(\frac{P}{Z_m RT}\right) \qquad 62$$

$$C_b = (X_b)\,\frac{P}{Z_m RT} \qquad 63$$

where $Z_m$ = compressibility factor for the mixture.

Substituting Equations 62, 63, 50 and 51 into Equations 60 and 61 gives

$$\frac{dx_c}{dV_r} = \frac{(k_{1c})(P)^2(A_o-x_c)(B_o-x_c-2x_d)}{(F)(Z_m RT)^2(1-x_c-x_d)^2} \qquad 64$$

$$\frac{dx_d}{dV_r} = \frac{(k_{2c})(P)^2(B_o-x_c-2x_d)}{(F)(Z_m RT)^2(1-x_c-x_d)^2} \qquad 65$$

The solutions of Equations 64 and 65 are presented in Appendix F.

The resulting equations are

$$k_{1c} = \frac{(C)(F)(RT)^2}{(V_r)(P)^2} \qquad 66$$

$$k_{2c} = \frac{(C)(F)(RT)^2(N)}{(V_r)(P)^2(2)} \qquad 67$$

where C = complex function of the exit conditions as presented in Appendix F

N = previously determined factor as shown in Appendix F.

Figures 19 and 20 contain a plot of the natural logarithm of the rate constants versus pressure as obtained in the solution of the above equations. Also included in Figures 19 and 20 are the rate constants determined from the rate equations obtained by Rowley and Steiner in their work at low pressure.

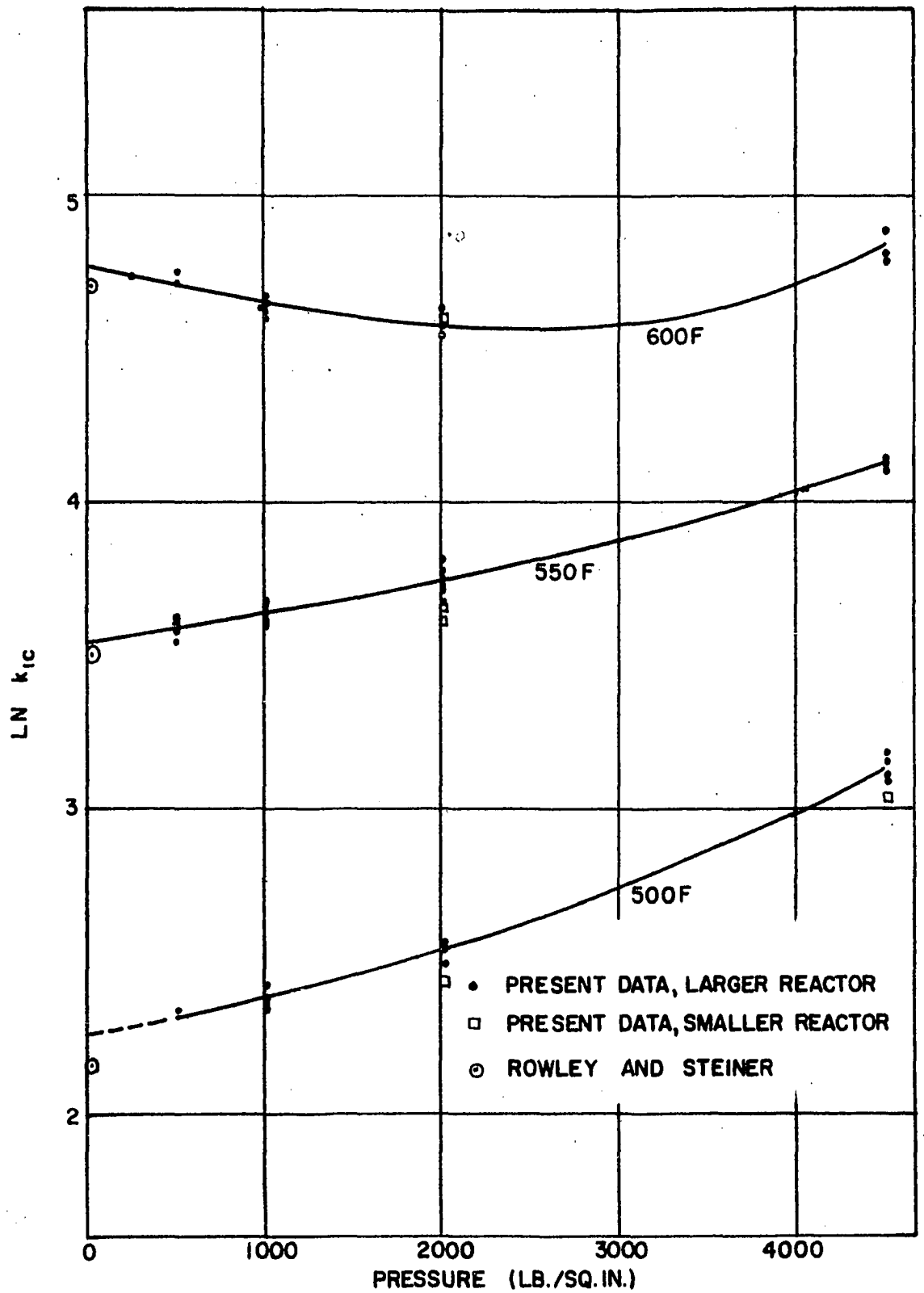


Figure 19 - Reaction Rate Constant Versus Pressure for the Ethylene-Butadiene Reaction Based on Concentrations

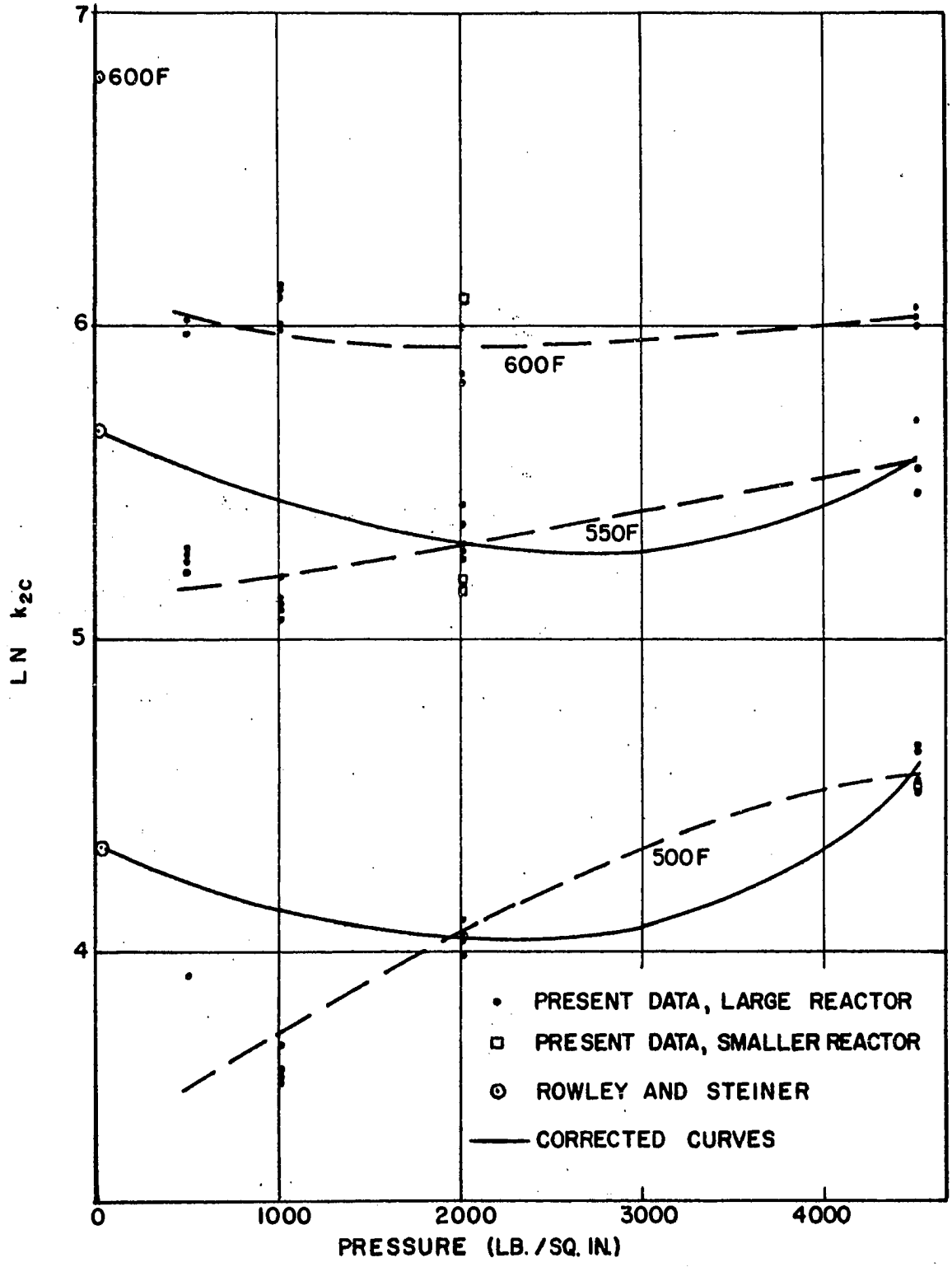


Figure 20 - Reaction Rate Constant Versus Pressure for the Butadiene Dimerization Reaction Based on Concentrations

# CHAPTER IX

## DISCUSSION OF RESULTS

The rate constants based on activities obtained from the experimental data for the Diels-Alder reaction of the formation of cyclohexene from ethylene and butadiene at pressures up to 4,500 lb./sq.in. gauge for the temperatures investigated are presented in Figure 15. The assumption of a second order reaction, as was the case for this reaction at low pressure, appears to be in agreement with the data obtained in this investigation at the elevated pressures. That is, the increase in pressure from atmospheric to 4,500 lb./sq.in. gauge does not appear to effect the order of the reaction.

When the rate constants obtained in this investigation are extrapotated to atmospheric pressure they agree quite readily as shown in Figure 15 with those obtained from the rate equation developed by Rowley and Steiner (13) in their work at low pressure but at substantially higher temperatures than in this study. This result indicates a somewhat surprising agreement for kinetic data taken over two sets of temperature ranges which are separated about

300°F.

The absolute reaction rate theory predicts, according to Equation 17, that if $\Delta V^*$ (the difference in volume between the activated state and the reactants) is negative the reaction rate constant should increase with increased pressure. In this reaction there is a considerable volume decrease between the reactants and products--one mole of ethylene reacts with one mole of butadiene to give one mole of cyclohexene. Therefore it would not be unreasonable to assume that there will be a decrease in volume in going from the reactants to the activated state. Also, based on statistical rate calculations, Rowley and Steiner (13) determined the activated state to be a cyclic complex similar to the final reaction product. Therefore, the assumption of a decrease in volume between activated state and the reactants for this reaction appears to be justified. Figure 15 shows that as predicted the rate constants are appreciably affected by an increase in pressure. In fact at 500°F, the rate constant at 4,500 lb./sq.in. gauge is approximately 4 times as large as it is at 500 lb./sq.in. gauge. A plot of $\Delta V^*$ versus P as obtained from the isothermal curves in Figure 15, according to Equation 17, is contained in Figure 16. This plot shows that as the pressure increases, $\Delta V^*$ decreases, as would be expected due to the compressibility of gases.

In general, the shape of the isothermal curves in

Figure 15 should be similar since they are functions of $\Delta V^*$ which should vary only slightly with temperature. The curves at 500°F and 550°F appear to be quite similar; however, the curve at 600°F appears to deviate from the other two. This difference can be explained by the fact that at the higher temperatures, especially at the higher pressures, considerably more reaction took place, and butadiene polymerization was much more of a problem.

The rate constants determined from the experimental runs in the small I.D. reactor as plotted in Figure 15, are consistently smaller than those determined from the larger reactor. Since the small reactor did not utilize a preheater, resulting in a slightly decreased effective reaction volume, this result was as expected. If the reaction had been wall catalyzed, the reaction rate would have increased due to the increased area to volume ratio of the small reactor over the large one. As the rate constants were not increased, it is concluded that the wall effects were negligible for this reaction.

The rate constants based on concentrations for the reaction of ethylene with butadiene to form cyclohexene at pressures up to 4,500 lb./sq.in. gauge are presented in Figure 19. These rate constants increase with increasing pressure but they are not effected nearly as much by pressure as the rate constants based on activities. The isothermal curves in Figure 19 are nearly straight, but

they tend to curve up at the highest pressure. These curves do not agree with the absolute reaction rate as previously presented in that the slope of the isothermal curves increase at the higher pressure rather than decrease. This result would indicate that the $\Delta V^*$ was increasing with increasing pressure, which does not appear to be possible.

The nonsimilarity of the isothermal curve at 600°F compared to the other curves is probably due, as previously explained, to the butadiene polymerization at the higher temperature.

The reaction of primary interest in this investigation is the reaction of ethylene with butadiene to form cyclohexene. However this reaction, can not be isolated due to the dimerization reaction of butadiene. Therefore any kinetic investigation of the reaction of ethylene with butadiene would necessarily have to include the study of the formation of vinylcyclohexene in addition to the formation of cyclohexene.

The dimerization reaction of butadiene is quite similar to the reaction of ethylene with butadiene. Both are bimolecular, homogeneous, second-order, Diels-Alder type reactions yielding an unsaturated cyclic product. The only difference is the vinyl group on the cyclohexene ring in the dimerization reaction. It would seem probable, due to the similarity of the reactions, that they would behave

in a similar manner. This assumption is verified by Rowley and Steiner (13) in that the activation energies and the temperature-independent factors determined for the two reactions are quite similar. It would also be reasonable to expect that for the two reactions $\Delta V^*$ would be approximately equal.

The experimental rate constants based on activities obtained in this investigation for the butadiene dimerization reaction are plotted versus pressure in Figure 17. However, the extrapolated values of the rate constants do not agree very closely with those obtained by Rowley and Steiner; also the isothermal curves obtained by a least square fit of a quadratic equation to the data are not similar in shape to the corresponding curves in Figure 16. This observation would tend to discredit the assumption that $\Delta V^*$ would be approximately equal for the two reactions. These discrepancies are probably due to the inaccuracy involved in determining the vinylcyclohexene concentration in the gas phase.

The chromatograph, which was used for the gas analysis, was set for the optimum conditions for analyzing for ethylene, butadiene and cyclohexene in the gas phase. As the chromatograph has a limited range as to molecular size of the components which can be analyzed in a reasonable length of time, it was almost impossible to analyze accurately for both ethylene and vinylcyclohexene. Therefore,

there was a considerable time delay between the sample injection and the sample traces for the vinylcyclohexene. As the initial composition of vinylcyclohexene in the gas phase was small in the beginning, it was almost impossible to determine the area under the curve. In the runs where there was an appreciable amount of liquid formed the small error in the analysis of the gas phase could be negligible, but in the runs where there was low conversion, and thus essentially no liquid formed, the error could be appreciable. A probable case in point were of the runs at 500 to 1,000 lb./sq.in. gauge at both 500 and 550°F. Consequently the validity of these points obtained at low conversion are very doubtful.

If these points at the lower pressure are neglected and a new isothermal curve drawn between the higher pressure data and the data of Rowley and Steiner, as shown in Figure 17, the resulting curves are similar to the corresponding curves in Figure 15, and consequently the assumption that $\Delta V^*$ is approximately equal for the two reactions is justified as shown in Figures 16 and 18.

The non-similarity of the curve at 600°F is probably a result of two factors. One, as previously mentioned, is butadiene polymerization, and the other is that in this particular set of runs the vinylcyclohexene in the gas phase was neglected. This latter factor probably effects only the runs at 500 lb./sq.in. gauge,

appreciably.

The experimental rate constants based on concentrations for the dimerization reaction are plotted in Figure 20. The isothermal curves plotted in Figure 20 correspond to the corrected curves in Figure 17. The data at 600°F are not considered because of the reasons previously given. These curves do not agree with the absolute reaction rate theory in that they predict an increase in $\Delta V^*$ (from a negative value to a positive value) as the pressure increases.

# CHAPTER X

## CONCLUSIONS

The reaction rate constants obtained for the reaction of ethylene with butadiene showed an appreciable increase with increasing pressures up to the maximum pressure investigated of 4,500 lb./sq.in. gauge at constant temperature. The variation of rate constants with pressure at constant temperature was easily explained by the absolute reaction rate theory.

The rate constants obtained for the reaction of ethylene with butadiene agreed, when extrapolated to low pressures, quite well with those obtained by a previous investigator at low pressures. The results also agreed with the previous investigations at low pressure in that the reaction was found to be a homogeneous, bimolecular, second order reaction leading essentially to the expected products, except for the increased polymerization of butadiene at the higher temperatures.

The reaction rate constants obtained for the dimerization of butadiene were not in good agreement, when extrapolated to low pressures, with those obtained by

previous investigators at low pressures. Also the variation of the rate constants with pressure at constant temperature was not similar to the previous reaction as would be expected by the similarity of the reactions. When corrected curves were drawn, the results not only agreed with those obtained by previous investigators, but also the variation of the rate constants with pressure was similar to the variation obtained from the previous reaction, (ethylene with butadiene) as would be expected.

## REFERENCES


1. Kistiakowsky, G. B., J. Am. Chem. Soc. 50, 2315 (1928).
2. Comings, E. W., High Pressure Technology, New York: McGraw-Hill Book Co., Inc. (1956).
3. Freeman, J. W. and Voorhies, H. R., Ind. Eng. Chem. 48, 861 (1956).
4. Wheeler, R. C. and Woods, W. L., J. Chem. Soc. 1819 (1930).
5. Wheeler, R. C., J. Chem. Soc. 378 (1929).
6. Joshel, L. M. and Butz, L. W., J. Am. Chem. Soc. 63, 3350 (1941).
7. Joshel, L. M., U. S. Patent 2,349,173 (May 16, 1944).
8. Joshel, L. M., U. S. Patent 2,349,232 (May 16, 1944).
9. Gorin, E. and Oblad, A. G., U. S. Patent 2,473,472 (June 14, 1949).
10. Whitman, G. M., U. S. Patent, 2,662,102 (Dec. 8, 1953).
11. Evans, M. G. and Warhurst, E., Trans. Faraday Soc. 34, 614 (1938).
12. Eyring, H. and Polanyi, M., Z. Physik. Chem. B12, 279 (1931).
13. Rowley, D. and Steiner, H., Discussions of the Faraday Soc. 10, 198 (1951).
14. Ingold, C. K., Structure and Mechanism in Organic Chemistry, New York: Cornell University Press, (1953).
15. Kistiakowsky, G. B. and Ranson, W. W., J. Chem. Phys. 7,725 (1939).

16. Wassermann, A., J. Chem. Soc. 612 (1942).

17. Robey, R. F., Wiese, H. K. and Morrel, C. E., Ind. Eng. Chem. 36, 3 (1944).

18. Duncan, N. E. and Janz, G. J., J. Chem. Phys. 20, 1644 (1952).

19. Foster, R. E. and Schreiber, R. S., J. Am. Chem. Soc. 70, 2303 (1948).

20. Hillyer, J. C. and Smith, Jr., J. V., Ind. Eng. Chem. 45, 1133 (1953).

21. Frost, A. A. and Pearson, R. G., Kinetics and Mechanism, New York: John Wiley & Sons, Inc. (1961).

22. Evans, G. M. and Polanyi, M., Trans. Faraday Soc. 31, 873 (1935).

23. Prausnitz, J. M., A. I. Ch. E. Journal, 5, No. 1, (1959).

24. Lewis, G. N., Proc. Am. Acad. Art. Sci., 37, 49 (1901).

25. Lewis, G. N. and Randall, M., Thermodynamics, New York: McGraw-Hill Book Co., Inc. (1923).

26. Redlich, Otto and Kwong, N. S., Chem. Revs. 44, 237 (1949).

27. Joffe, J., Ind. Eng. Chem. 40, 1738 (1948).

28. Norris, T. G., M.S. Thesis, University of Oklahoma (1957).

29. Lobo, P. A. Continental Oil Company, Ponca City, Oklahoma; Personal Communications.

# APPENDIX A

# NOMENCLATURE

## NOMENCLATURE

$a$ = Subscript designating ethylene

$a_j$ = Activity of component j

$A$ = Frequency factor representing the total number of collisions per unit time among the reacting molecules per unit volume

$A_o$ = Mole fraction ethylene in feed

$b$ = Subscript designating butadiene

$B_o$ = Mole fraction butadiene in feed

$c$ = Subscript designating cyclohexene

$C_j$ = Concentration of component j

$d$ = Subscript designating vinylcyclohexene

$E_a$ = Energy of activation

$f_j$ = Fugacity of pure component j

$\overline{f}_j$ = Fagacity of component j in a mixture

$F$ = Reactor feed rate, moles per unit time

$\underline{G}$ = Free energy

$\overline{G}_j$ = Partial molal free energy of component j

$\Delta G^o$ = Standard free energy change

$\Delta G^*$ = Standard free energy of formation of the activated complex

$h$ = Planck constant

$k$ = Reaction rate constant

$k_1$ = Reaction rate constant for the reaction of ethylene with butadiene based on activities

$k_2$ = Reaction rate constant for the dimerization reaction of butadiene based on activities

$k_{1c}$ = Reaction rate constant for the reaction of ethylene with butadiene based on concentrations

$k_{2c}$ = Reaction rate constant for the dimerization reaction of butadiene based on concentrations

$k'$ = Boltzmann constant

$K$ = $r_2/r_1$

$K'$ = Transmission coefficient expressing the probability of conversion of the activated complex into products

$K_a$ = Equilibrium constant expressed in terms of activities

$K_c$ = Equilibrium constant expressed in terms of concentrations

$K^*$ = Equilibrium constant in terms of the activated complex and initial reactants

$N$ = Moles of reactant or product present at time t

$P$ = Pressure

$P_1$ = Internal pressure

$P_2$ = External pressure

$P_m$ = Maximum allowable operating pressure

$q$ = Probability or steric factor

$r$ = Reaction rate, moles formed or consumed per unit volume per unit time

$r$ = Radius within the tube wall

$r_1$ = Internal radius

$r_2$ = External radius

$R$ = Gas constant

$t$ = Time

$T$ = Absolute temperature

$V$ = Volume

$\underline{V}$ = Molal volume

$\overline{V}_j$ = Partial molal volume of component j

$V_r$ = Reactor volume occupied by reacting system

$\Delta V^*$ = Difference in volume between the activated complex and the original reactants

$x$ = Moles of a component converted per mole of feed

$x_j$ = Moles of component j converted per mole of feed

$X_j$ = Mole fraction of component j

$y_j$ = Mole fraction component j in a mixture

$Z$ = Compressibility factor

$Z_m$ = Compressibility factor for a mixture

$\overline{Z}_j$ = Partial molal compressibility factor of component j

$\sigma_r$ = Radial stress

$\sigma_t$ = Tangential stress

$\sigma_Z$ = Longitudinal stress

$\tau$ = Shear stress

$\tau_m$ = Maximum shear stress

$\tau_y$ = Shear proportional limit

$\phi$ = Fugacity coefficient

$\overline{\phi}_j$ = Fugacity coefficient for component j in a mixture

# APPENDIX B

# CALIBRATION CURVES

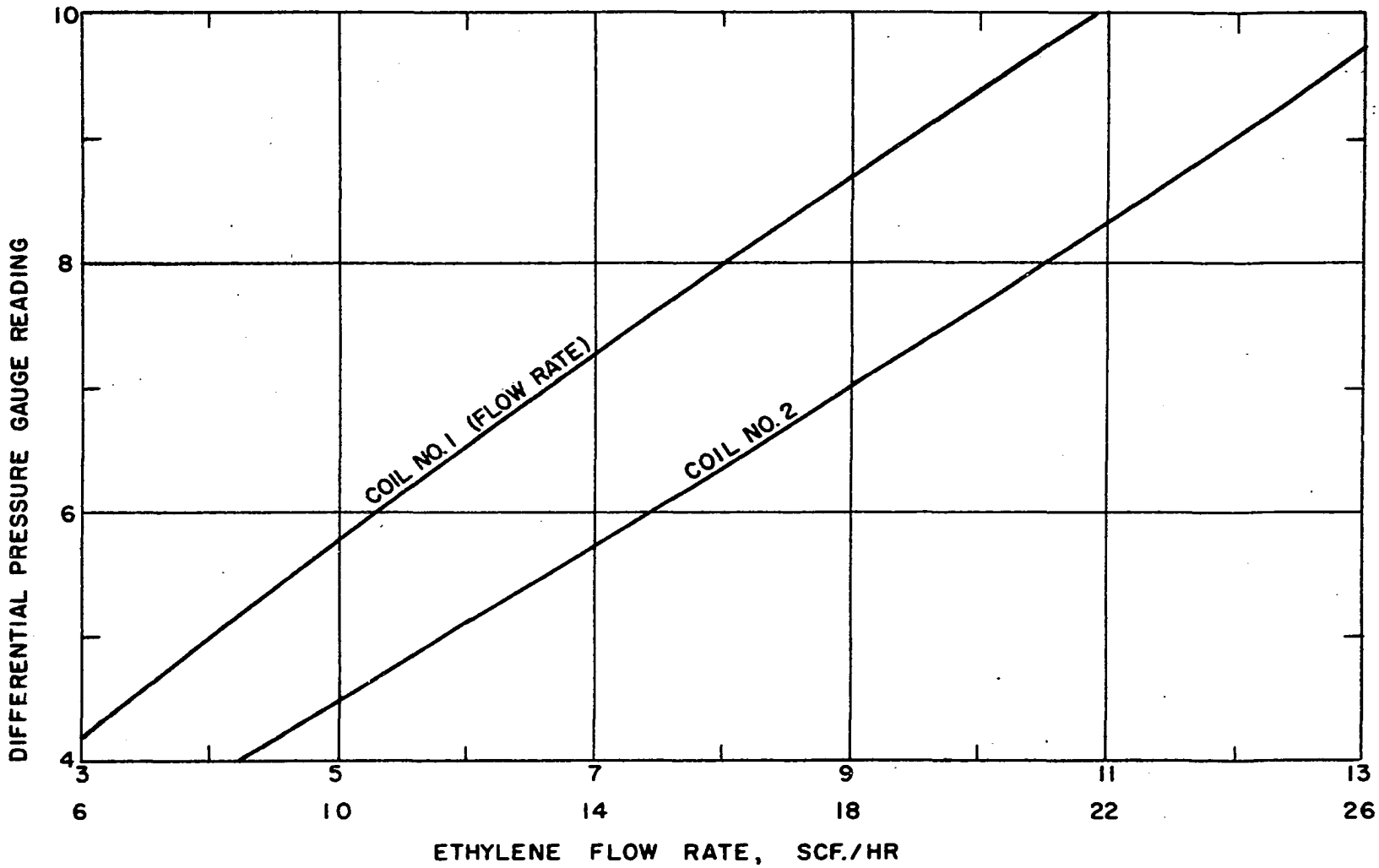


Figure 21 - Ethylene Flow Device Calibration Curve

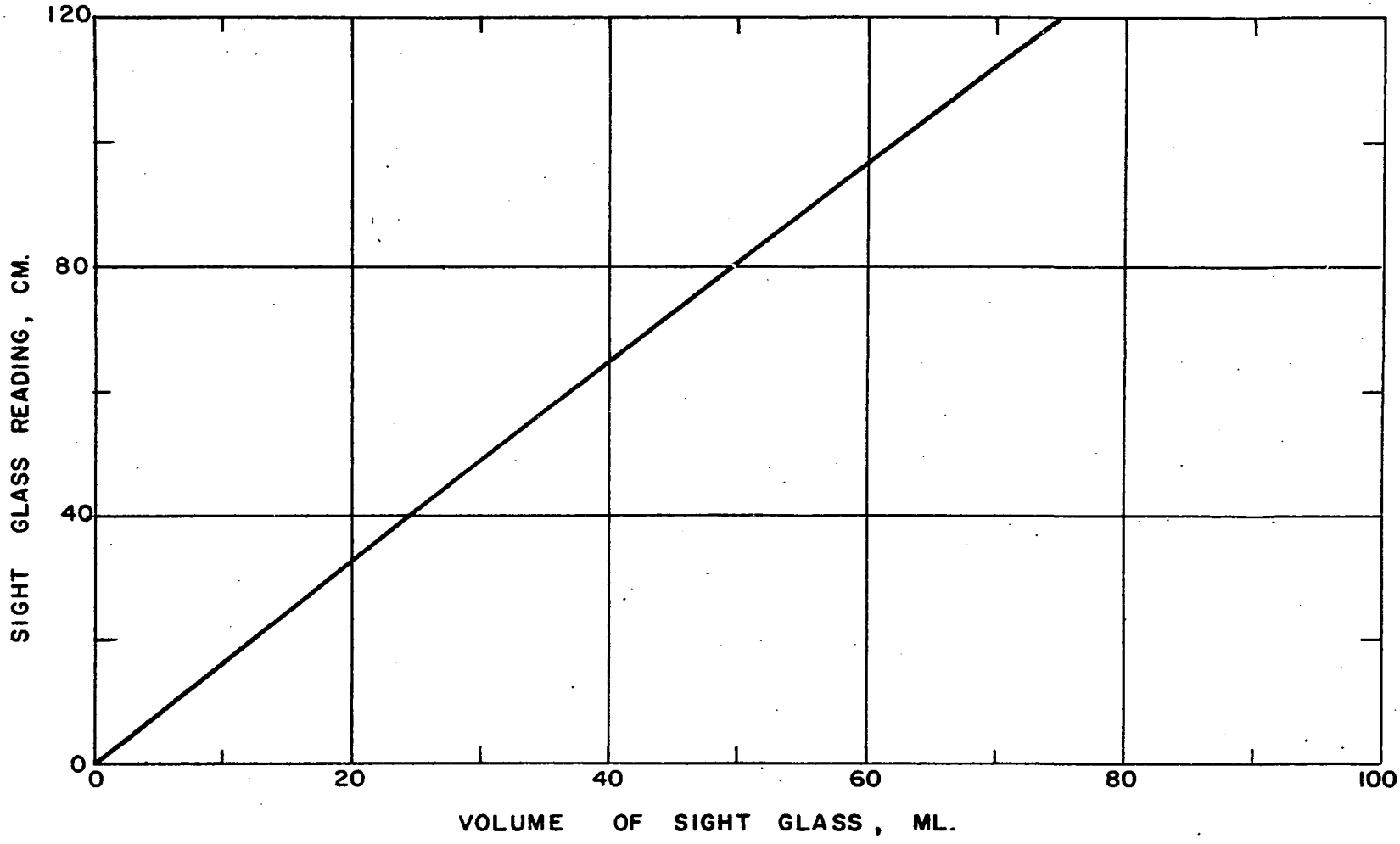


Figure 22 - Butadiene Reservoir Calibration Curve

# APPENDIX C

# SAMPLE MATERIAL BALANCE CALCULATIONS

## Sample Material Balance Calculations for Run #111.

1. Input Data (Based on 10 minute duration of run)

Ethylene (SCF) 10.77 SCF/hr. or 1.795 SCF

Butadiene (SCF) 45.2 ml. or 27.9 gm. ($\rho$ = 0.618)

$$\frac{27.9(\text{gm.})(\text{SCF})}{64.7(\text{gm.})} = 0.432 \text{ SCF}$$

$$\text{Mol. Fr. Ethylene} = \frac{1.795}{1.795 + 0.432} = 0.806$$

$$\text{Mol. Fr. Butadiene} = \frac{0.432}{1.795 + 0.432} = 0.194$$

2. Exit Gas Product

Data:

| Composition | Mol. Fr. | Amount | 2.115 CF |
|---|---|---|---|
| Ethylene | = 0.8746 | Atmospheric Press. | 28.9 |
| Butadiene | = 0.1036 | in. Hg. | |
| Cyclohexene | = 0.0201 | Room Temp. | 75°F |
| Vinylcyclohexene | = 0.0017 | Water Content | 0.0285 mol. Fr. |

The gas product has to be corrected to standard conditions and for water content. Therefore:

$$\text{Exit Gas (SCF)} = \frac{(2.115)(520)(28.90)(0.9715)}{(29.92)(535)} = 1.93 \text{ SCF}$$

The amount of each component found in the gas product is determined from the amount of gas product and the gas product composition. Therefore:

$$\text{Gas (gm.)} = \frac{(\text{SCF})(\text{Mol.Fr.})(\text{gm.})}{(\text{SCF})} = (\text{gm.})$$

Ethylene = (1.93)(0.8746)(33.57) - 57.12 gm.

Butadiene = (1.93)(0.1036)(64.73) = 13.05 gm.

Cyclohexene = (1.93)(0.0201)(98.31) = 3.85 gm.

Vinylcyclohexene = (1.93)(0.0017)(129.5) = 0.44 gm.

3. Exit Liquid Product

Data:

| Composition | Vol. Fr. | Amount 17.4 cc. |
|---|---|---|
| Butadiene | = 0.0424 | |
| Cyclohexene | = 0.3803 | 1% polymer |
| Vinylcyclohexene | = 0.5162 | |
| Cyclooctadiene | = 0.0611 | |

The amount of each component found in the liquid product is determined from the amount of liquid product, per cent liquid product polymer and liquid product composition. Therefore:

| | | |
|---|---|---|
| Liquid (gm.) | = (cc)(Vol. Fr.)(density)(% product) | = gm. |
| Butadiene | = (17.4)(0.0424)(0.628)(0.99) | = 0.46 gm. |
| Cyclohexene | = (17.4)(0.3803)(0.820)(0.99) | = 5.39 gm. |
| Vinylcyclohexene | = (17.4)(0.5161)(0.840)(0.99) | = 7.495 gm. |
| Cyclooctadiene | = (17.4)(0.0611)(0.883)(0.99) | = 0.933 gm. |
| Polymer | = (17.4)(0.01) (1.0) | = 0.170 gm. |

4. Total Exit Product Stream

The over all exit composition is determined by adding the amount of each component from both the gas and liquid product streams. The mole fraction os each component in the exit stream is found by dividing the amount in moles of that component by the total moles of product. Therefore:

| Component | grams | mole fraction |
|---|---|---|
| Ethylene | 57.11 | 0.821 |
| Butadiene | 13.51 | 0.101 |
| Cyclohexene | 9.24 | 0.0454 |
| Vinylcyclohexene | 7.94 | 0.0296 |
| Cyclooctadiene | 0.93 | 0.0035 |
| Polymer | 0.17 | -- |
| Total | 88.86 | |

5. Ethylene Material Balance

Ethylene in feed = (1.795)(33.57) = 60.3 gm.

Ethylene in exit product = 57.1 gm.

Equivalent ethylene in cyclohexene product = 3.2 gm.

Total equivalent ethylene in product = 60.3 gm.

Material balance $\frac{\text{Grams Ethylene out}}{\text{Grams Ethylene in}} = \frac{60.3}{60.3} = 1$

6. Butadiene Material Balance

Butadiene in feed = 27.9 gm.

Total equivalent butadiene in product = 28.6 gm.

Material balance $\frac{\text{Grams Butadiene out}}{\text{Grams Butadiene in}} = \frac{28.6}{27.9} = 1.02$

# APPENDIX D

# COMPUTED DATA FOR THE REACTION OF ETHYLENE WITH BUTADIENE

TABLE 2

COMPUTED DATA FOR THE REACTION OF ETHYLENE WITH BUTADIENE

| Run Number | 77 | 78 | 79 | 80 | 81 | 82 | 83 |
|---|---|---|---|---|---|---|---|
| Reactor Pressure (lb./sq.in.gauge) | 500 | 500 | 500 | 500 | 1000 | 1000 | 1000 |
| Reactor Temp. ($^{o}$F) | 701 | 701 | 701 | 701 | 700 | 700 | 700 |
| Reactor Volume (cu. in.) | 5.80 | 5.80 | 5.80 | 5.80 | 5.80 | 5.80 | 5.80 |
| Input Flow Rate (SCFH) | 9.39 | 9.40 | 7.73 | 6.95 | 7.81 | 16.06 | 16.06 |
| Mol. % $C_2$ In | 83.0 | 82.4 | 78.9 | 87.7 | 87.6 | 86.5 | 86.5 |
| Mol. % $C_4$ In | 17.0 | 17.6 | 21.1 | 12.3 | 12.4 | 13.5 | 13.5 |
| Duration of Run (min.) | 30 | 15 | 15 | 20 | 20 | 20 | 15 |
| Product Out (gm.) | 181.2 | 90.3 | 77.0 | 84.2 | 96.2 | 195.0 | 142.0 |
| Mol. % $C_2$ Out* | 84.7 | 84.1 | 82.0 | 90.4 | 90.1 | 88.8 | 89.5 |
| Mol. % $C_4$ Out | 11.6 | 12.0 | 11.8 | 7.01 | 3.31 | 6.26 | 5.99 |
| Mol. % $C_6$ Out | 2.23 | 2.30 | 3.13 | 1.85 | 4.82 | 3.43 | 3.19 |
| Mol. % $C_8$ Out | 1.21 | 1.34 | 2.64 | 0.67 | 1.57 | 1.26 | 1.12 |
| Mol. % $C_8$' Out | 0.21 | 0.25 | 0.42 | 0.11 | 0.19 | 0.21 | 0.19 |
| Weight % Polymer | 0.3 | 0.2 | 0.8 | 1.1 | 2.1 | 0.2 | 1.3 |
| $C_2$ Mass Balance** | 1.01 | 1.00 | 1.01 | 1.00 | 0.99 | 0.99 | 0.96 |
| $C_4$ Mass Balance | 0.96 | 0.95 | 0.96 | 0.87 | 0.96 | 0.88 | 0.87 |

TABLE 2--Continued

| Run Number | 84 | 85 | 86 | 87 | 88 | 89 | 90 |
|---|---|---|---|---|---|---|---|
| Reactor Pressure (lb./sq.in. gauge) | 500 | 500 | 1000 | 1000 | 1000 | 1000 | 1000 |
| Reactor Temp. ($^{o}$F) | 600 | 601 | 600 | 600 | 600 | 600 | 600 |
| Reactor Volume (cu. in.) | 5.80 | 5.80 | 5.80 | 5.80 | 5.80 | 5.80 | 5.80 |
| Input Flow Rate (SCFH) | 6.31 | 3.61 | 6.74 | 9.19 | 8.06 | 5.36 | 10.43 |
| Mol. % $C_2$ In | 75.7 | 81.1 | 76.5 | 78.3 | 89.0 | 84.3 | 92.1 |
| Mol. % $C_4$ In | 24.3 | 18.9 | 23.5 | 21.7 | 11.0 | 15.7 | 7.9 |
| Duration of Run (min.) | 20 | 20 | 10 | 20 | 20 | 20 | 20 |
| Product Out (gm.) | 86.0 | 48.9 | 45.3 | 124.3 | 99.5 | 69.6 | 127.7 |
| Mol. % $C_2$ Out | 77.0 | 82.4 | 78.8 | 79.8 | 89.6 | 85.2 | 92.3 |
| Mol. % $C_4$ Out | 21.1 | 15.5 | 14.5 | 16.2 | 9.02 | 10.9 | 6.79 |
| Mol. % $C_6$ Out | 0.93 | 1.19 | 2.93 | 1.92 | 1.18 | 2.38 | 0.69 |
| Mol. % $C_8$ Out | 0.87 | 0.81 | 3.22 | 1.85 | 0.23 | 1.34 | 0.23 |
| Mol. % $C_8$' Out | 0.11 | 0.09 | 0.49 | 0.22 | -- | 0.18 | -- |
| Weight % Polymer | -- | 0.2 | -- | 0.1 | -- | 0.1 | -- |
| $C_2$ Mass Balance | 1.01 | 1.04 | 0.99 | 1.01 | 1.01 | 1.01 | 1.02 |
| $C_4$ Mass Balance | 0.97 | 1.00 | 0.98 | 1.00 | 0.96 | 1.01 | 1.02 |

TABLE 2--Continued

| Run Number | 91 | 92 | 93 | 94 | 95 | 96 | 97 |
|---|---|---|---|---|---|---|---|
| Reactor Pressure (lb./sq.in. gauge) | 1000 | 250 | 2000 | 2000 | 2000 | 2000 | 4500 |
| Reactor Temp. ($^{o}$F) | 600 | 600 | 600 | 600 | 600 | 600 | 600 |
| Reactor Volume (cu. in.) | 5.80 | 5.80 | 5.80 | 5.80 | 5.80 | 5.80 | 5.80 |
| Input Flow Rate (SCFH) | 11.45 | 3.65 | 10.24 | 11.09 | 17.77 | 19.40 | 15.87 |
| Mol. % $C_2$ In | 83.9 | 78.5 | 83.9 | 77.4 | 91.7 | 84.0 | 87.7 |
| Mol. % $C_4$ In | 16.1 | 21.5 | 16.1 | 22.6 | 8.3 | 16.0 | 12.3 |
| Duration of Run (min.) | 20 | 30 | 20 | 15 | 20 | 10 | 15 |
| Product Out (gm.) | 150.0 | 75.1 | 130.8 | 110.7 | 225.5 | 127.4 | 149.1 |
| Mol. % $C_2$ Out | 84.4 | 80.1 | 86.1 | 81.2 | 92.3 | 86.5 | 89.3 |
| Mol. % $C_4$ Out | 13.0 | 19.3 | 6.58 | 7.83 | 5.62 | 9.25 | 1.13 |
| Mol. % $C_6$ Out | 1.37 | 0.37 | 4.78 | 5.97 | 1.64 | 2.69 | 7.62 |
| Mol. % $C_8$ Out | 1.01 | 0.27 | 2.19 | 4.39 | 0.42 | 1.40 | 1.71 |
| Mol. % $C_8$' Out | 0.15 | -- | 0.35 | 0.66 | 0.02 | 0.19 | 0.26 |
| Weight % Polymer | 0.2 | -- | 0.4 | 0.5 | 0.3 | 0.4 | 0.8 |
| $C_2$ Mass Balance | 1.02 | 1.04 | 1.00 | 1.00 | 1.07 | 1.02 | 1.01 |
| $C_4$ Mass Balance | 1.03 | 0.96 | 0.97 | 0.96 | 1.05 | 0.96 | 0.98 |

TABLE 2--Continued

| Run Number | 98 | 99 | 100 | 101 | 102 | 103 | 104 |
|---|---|---|---|---|---|---|---|
| Reactor Pressure (lb./sq.in. gauge) | 4500 | 4500 | 1000 | 1000 | 1000 | 1000 | 1000 |
| Reactor Temp. ($^{o}$F) | 600 | 600 | 500 | 500 | 500 | 500 | 500 |
| Reactor Volume (cu. in.) | 5.80 | 5.80 | 5.12 | 5.12 | 5.12 | 5.12 | 5.12 |
| Input Flow Rate (SCFH) | 28.29 | 30.68 | 10.90 | 12.25 | 6.94 | 6.59 | 9.78 |
| Mol. % $C_2$ In | 93.8 | 86.5 | 91.3 | 81.3 | 80.9 | 85.3 | 84.9 |
| Mol. % $C_4$ In | 6.2 | 13.5 | 8.7 | 18.7 | 19.1 | 14.7 | 15.1 |
| Duration of Run (min.) | 15 | 10 | 20 | 20 | 20 | 20 | 20 |
| Product Out (gm.) | 256.3 | 192.8 | 131.4 | 160.3 | 88.8 | 79.7 | 123.9 |
| Mol. % $C_2$ Out | 94.2 | 88.9 | 91.3 | 81.3 | 79.1 | 85.2 | 85.6 |
| Mol. % $C_4$ Out | 2.00 | 3.12 | 8.6 | 18.4 | 20.4 | 14.2 | 13.0 |
| Mol. % $C_6$ Out | 3.33 | 5.94 | 0.09 | 0.17 | 0.31 | 0.29 | 0.83 |
| Mol. % $C_8$ Out | 0.41 | 1.79 | -- | 0.13 | 0.24 | 0.24 | 0.48 |
| Mol. % $C_8'$ Out | 0.04 | 0.26 | -- | 0.01 | -- | -- | 0.05 |
| Weight % Polymer | 0.4 | 0.6 | -- | 0.8 | 1.6 | -- | 1.1 |
| $C_2$ Mass Balance | 1.02 | 1.03 | 1.00 | 0.99 | 0.95 | 0.96 | 0.99 |
| $C_4$ Mass Balance | 1.02 | 0.97 | 0.99 | 1.02 | 1.07 | 0.97 | 1.00 |

TABLE 2--Continued

| Run Number | 105 | 106 | 107 | 108 | 109 | 110 | 111 |
|---|---|---|---|---|---|---|---|
| Reactor Pressure (lb./sq.in. gauge) | 2000 | 2000 | 2000 | 2000 | 4500 | 4500 | 4500 |
| Reactor Temp. ($^{o}$F) | 500 | 500 | 500 | 500 | 500 | 500 | 500 |
| Reactor Volume (cu. in.) | 5.12 | 5.12 | 5.12 | 5.12 | 5.12 | 5.12 | 5.12 |
| Input Flow Rate (SCFH) | 11.27 | 10.68 | 14.17 | 13.00 | 9.11 | 12.01 | 13.36 |
| Mol. % $C_2$ In | 75.0 | 67.2 | 75.5 | 85.6 | 83.4 | 88.4 | 80.6 |
| Mol. % $C_4$ In | 25.0 | 32.8 | 24.5 | 14.4 | 16.6 | 11.6 | 19.4 |
| Duration of Run (min.) | 20 | 15 | 15 | 20 | 10 | 15 | 10 |
| Product Out (gm.) | 154.9 | 104.6 | 146.3 | 167.2 | 58.1 | 112.4 | 88.9 |
| Mol. % $C_2$ Out | 76.9 | 68.5 | 76.4 | 85.6 | 84.4 | 88.7 | 82.1 |
| Mol. % $C_4$ Out | 20.2 | 26.2 | 21.3 | 13.4 | 6.85 | 6.79 | 10.1 |
| Mol. % C6 Out | 1.19 | 1.81 | 0.99 | 0.62 | 5.54 | 3.21 | 4.54 |
| Mol. % C8 Out | 1.53 | 3.16 | 1.23 | 0.40 | 2.90 | 1.22 | 2.96 |
| Mol. % C8' Out | 0.16 | 0.38 | 0.12 | 0.02 | 0.34 | 0.14 | 0.35 |
| Weight % Polymer | 0.7 | -- | 0.4 | 0.9 | -- | 0.3 | 0.1 |
| $C_2$ Mass Balance | 1.01 | 0.90 | 1.00 | 1.00 | 0.98 | 0.99 | 1.00 |
| $C_4$ Mass Balance | 0.98 | 0.91 | 1.00 | 1.05 | 1.01 | 1.05 | 1.02 |

TABLE 2--Continued

| Run Number | 112 | 113 | 114 | 115 | 116 | 117 | 118 |
|---|---|---|---|---|---|---|---|
| Reactor Pressure (lb./sq.in. gauge) | 1000 | 1000 | 500 | 500 | 500 | 500 | 1000 |
| Reactor Temp. ($^{o}$F) | 550 | 550 | 550 | 550 | 550 | 550 | 550 |
| Reactor Volume (cu. in.) | 5.12 | 5.12 | 5.12 | 5.12 | 5.12 | 5.12 | 5.12 |
| Input Fow Rate (SCFH) | 9.30 | 10.12 | 8.14 | 10.58 | 5.95 | 5.07 | 9.75 |
| Mol. % $C_2$ In | 89.2 | 82.0 | 74.9 | 80.5 | 78.1 | 91.6 | 79.5 |
| Mol. % $C_4$ In | 10.8 | 18.0 | 25.1 | 19.5 | 21.9 | 8.4 | 20.5 |
| Duration of Run (min.) | 20 | 10 | 20 | 20 | 20 | 20 | 20 |
| Product Out (gm.) | 115.1 | 65.5 | 109.9 | 138.6 | 79.5 | 60.2 | 129.5 |
| Mol. % $C_2$ Out | 89.0 | 82.1 | 75.8 | 81.1 | 78.3 | 90.8 | 79.9 |
| Mol. % $C_4$ Out | 10.3 | 16.8 | 23.6 | 18.5 | 21.1 | 8.91 | 18.6 |
| Mol. % $C_6$ Out | 0.42 | 0.60 | 0.23 | 0.16 | 0.25 | 0.16 | 0.72 |
| Mol. % $C_8$ Out | 0.26 | 0.45 | 0.43 | 0.20 | 0.31 | 0.11 | 0.66 |
| Mol. % $C_8$' Out | -- | 0.05 | -- | -- | -- | -- | 0.07 |
| Weight % Polymer | -- | 0.6 | -- | -- | 1.9 | -- | 1.3 |
| $C_2$ Mass Balance | 1.00 | 0.98 | 0.99 | 1.00 | 0.97 | 0.97 | 0.98 |
| $C_4$ Mass Balance | 1.02 | 1.02 | 0.96 | .97 | 1.02 | 1.05 | 1.02 |

TABLE 2--Continued

| Run Number | 119 | 120 | 121 | 122 | 123 | 124 | 125 |
|---|---|---|---|---|---|---|---|
| Reactor Pressure (lb./sq.in. gauge) | 1000 | 1000 | 1000 | 2000 | 2000 | 2000 | 2000 |
| Reactor Temp. ($^{o}$F) | 550 | 550 | 550 | 550 | 550 | 550 | 550 |
| Reactor Volume (cu. in.) | 5.12 | 5.12 | 5.12 | 5.12 | 5.12 | 5.12 | 5.12 |
| Input Flow Rate (SCFH) | 18.07 | 19.94 | 8.57 | 9.02 | 8.98 | 12.47 | 13.99 |
| Mol. % $C_2$ In | 89.3 | 83.0 | 74.3 | 80.4 | 80.0 | 83.4 | 74.3 |
| Mol. % $C_4$ In | 10.7 | 17.0 | 25.7 | 19.6 | 20.0 | 16.6 | 25.7 |
| Duration of Run (min.) | 20 | 15 | 20 | 20 | 15 | 20 | 10 |
| Product Out (gm.) | 231.6 | 194.0 | 115.0 | 117.1 | 88.0 | 160.8 | 96.2 |
| Mol. % $C_2$ Out | 89.2 | 83.2 | 75.2 | 81.5 | 81.5 | 84.3 | 76.2 |
| Mol. % $C_4$ Out | 10.5 | 16.2 | 22.2 | 12.4 | 12.1 | 12.3 | 17.8 |
| Mol. % $C_6$ Out | 0.17 | 0.30 | 0.91 | 3.10 | 3.28 | 2.00 | 2.62 |
| Mol. % $C_8$ Out | 0.11 | 0.25 | 1.52 | 2.59 | 2.82 | 1.27 | 3.05 |
| Mol. % $C_8$' Out | -- | 0.01 | 0.22 | 0.34 | 0.37 | 0.18 | 0.41 |
| Weight % Polymer | 0.9 | 0.8 | 0.1 | -- | 0.1 | 0.6 | 0.8 |
| $C_2$ Mass Balance | 0.99 | 1.00 | 0.97 | 0.97 | 0.98 | 0.99 | 0.98 |
| $C_4$ Mass Balance | 1.04 | 1.02 | 0.98 | 1.01 | 1.00 | 1.01 | 1.00 |

TABLE 2--Continued

| Run Number | 126 | 127 | 128 | 129 | 130 | 131 | 132 |
|---|---|---|---|---|---|---|---|
| Reactor Pressure (lb./sq.in. gauge) | 2000 | 4500 | 4500 | 4500 | 4500 | 2000 | 4500 |
| Reactor Temp. ($^{o}F$) | 550 | 550 | 550 | 550 | 550 | 550 | 500 |
| Reactor Volume (cu. in.) | 5.12 | 5.12 | 5.12 | 5.12 | 5.12 | 5.12 | 5.12 |
| Input Flow Rate (SCFH) | 29.27 | 23.58 | 30.76 | 29.13 | 26.62 | 31.14 | 22.04 |
| Mol. % $C_2$ In | 84.8 | 86.5 | 87.3 | 92.5 | 89.6 | 79.8 | 87.1 |
| Mol. % $C_4$ In | 15.2 | 13.5 | 12.7 | 7.5 | 10.4 | 10.2 | 12.9 |
| Duration of Run (min.) | 10 | 10 | 10 | 15 | 10 | 5 | 10 |
| Product Out (gm.) | 188.8 | 150.3 | 196.3 | 269.5 | 168.0 | 103.1 | 144.1 |
| Mol. % $C_2$ Out | 85.7 | 87.1 | 88.3 | 93.0 | 90.0 | 80.8 | 85.3 |
| Mol. % $C_4$ Out | 12.9 | 6.06 | 6.83 | 4.40 | 5.65 | 17.2 | 10.8 |
| Mol. % $C_6$ Out | 0.77 | 4.58 | 3.38 | 2.08 | 3.23 | 0.94 | 2.41 |
| Mol. % $C_8$ Out | 0.63 | 1.98 | 1.33 | 0.48 | 1.04 | 1.01 | 1.35 |
| Mol. % $C_8'$ Out | 0.03 | 0.24 | 0.16 | 0.05 | 0.12 | 0.09 | 0.14 |
| Weight % Polymer | 0.5 | 0.2 | 0.7 | 0.9 | 1.0 | 0.7 | 0.5 |
| $C_2$ Mass Balance | 1.01 | 1.00 | 1.01 | 1.03 | 1.02 | 1.00 | 0.99 |
| $C_4$ Mass Balance | 1.00 | 1.05 | 1.02 | 1.08 | 1.08 | 1.00 | 1.01 |

TABLE 2--Continued

| Run Number | 133 | 134 | 135 | 136 | 137 | 138 | 139 |
|---|---|---|---|---|---|---|---|
| Reactor Pressure (lb./sq.in. gauge) | 4500 | 500 | 2000 | 4500 | 2000 | 2000 | 2000 |
| Reactor Temp. ($^{o}$F) | 500 | 500 | 500 | 500 | 550 | 550 | 600 |
| Reactor Volume (cu. in.) | 5.12 | 5.12 | 2.08# | 2.08 | 2.08 | 2.08 | 2.08 |
| Input Flow Rate (SCFH) | 28.93 | 6.33 | 8.12 | 12.82 | 12.50 | 20.68 | 22.48 |
| Mol. % $C_2$ In | 87.8 | 74.3 | 80.9 | 81.1 | 82.7 | 89.7 | 90.1 |
| Mol. % $C_4$ In | 12.2 | 25.7 | 19.1 | 18.9 | 17.3 | 10.3 | 9.9 |
| Duration of Run (min.) | 10 | 20 | 20 | 5 | 15 | 5 | 15 |
| Product Out (gm.) | 182.2 | 88.1 | 108.3 | 43.0 | 125.7 | 64.0 | 211.2 |
| Mol. % $C_2$ Out | 88.6 | 74.2 | 81.1 | 81.4 | 83.4 | 89.8 | 90.3 |
| Mol. % $C_4$ Out | 9.32 | 25.5 | 17.9 | 14.7 | 15.1 | 9.78 | 8.71 |
| Mol. % $C_6$ Out | 1.38 | 0.09 | 0.48 | 2.02 | 0.77 | 0.31 | 0.60 |
| Mol. % $C_8$ Out | 0.62 | 0.18 | 0.48 | 1.68 | 0.68 | 0.16 | 0.32 |
| Mol. % $C_8$' Out | 0.05 | -- | 0.04 | 0.17 | 0.07 | -- | 0.02 |
| Weight % Polymer | 0.8 | -- | 1.1 | 0.5 | 1.0 | -- | 0.6 |
| $C_2$ Mass Balance | 1.01 | 1.00 | 1.00 | 1.00 | 1.03 | 1.01 | 1.02 |
| $C_4$ Mass Balance | 1.01 | 1.01 | 1.04 | 1.06 | 1.04 | 1.00 | 1.05 |

Note:

# Runs number 135-140 were made by use of 1/8-in. I.D. reactor

TABLE 2--Continued

| | |
|---|---|
| Run Number | 140 |
| Reactor Pressure (lb./sq.in. gauge) | 2000 |
| Reactor Temp. ($^{o}F$) | 600 |
| Reactor Volume (cu. in.) | 2.08 |
| Input Flow Rate (SCFH) | 24.65 |
| Mol. % $C_2$ In | 85.2 |
| Mol. % $C_4$ In | 14.8 |
| Duration of Run (min.) | 10 |
| Product Out (gm.) | 158.7 |
| Mol. % $C_2$ Out | 85.8 |
| Mol. % $C_4$ Out | 12.6 |
| Mol. % $C_6$ Out | 0.86 |
| Mol. % $C_8$ Out | 0.65 |
| Mol. % $C_8$' Out | 0.04 |
| Weight % Polymer | 0.7 |
| $C_2$ Mass Balance | 1.01 |
| $C_4$ Mass Balance | 1.01 |

Note:

*$C_2$ = Ethylene, $C_4$ = Butadiene, $C_6$ = Cyclohexene, $C_8$ = Vinylcyclohexene
$C_8$' = Cyclooctadiene

**Mass Balance = Mass out/ Mass in

# APPENDIX E

# ANALOG SOLUTION OF DIFFERENTIAL RATE EQUATIONS

Analog Solution of Differential Rate Equations for Determining the Rate Constants Based on Fugacities.

The differential rate equations to be solved for the reaction rate constants are

$$\frac{dx_c}{dV} = \frac{(k_1)(f_a)(f_b)(A_o-x_c)(B_o-x_c-2x_d)}{(F)(1-x_c-x_d)^2} \qquad \text{E-1}$$

$$\frac{dx_d}{dV_r} = \frac{(k_2)(f_b)^2(B_o-x_c-2x_d)^2}{(F)(1-x_c-x_d)^2} \qquad \text{E-2}$$

Before the above equations can be solved on the analog computer they must be properly scaled. The variables available on the analog are voltage and time. Therefore, let the dependent variables, $x_c$ and $x_d$, correspond to the voltages and the independent variable, $V_r$, correspond to time. Since the maximum mole fraction is one and the maximum working voltage is 100 volts, the scale factor for the dependent variables is 100. The scale factor for the independent variable is found by evaluating w from the following equation.

$$V_r = w\theta, \quad dV_r = wd\theta \qquad \text{E-3}$$

where $V_r$ = reactor volume

$\theta$ = solution time (sec)

w = scale factor.

Substituting the scale factors into Equations E-1 and E-2 yields

$$\frac{d(100x_c)}{d\theta} = \frac{(k_1)(f_a)(f_b)(w)(100)^3(A_o-x_c)(B_o-x_c-2x_d)}{(F)(100)^2(1-x_c-x_d)^2} \qquad \text{E-4}$$

$$\frac{d(100x_d)}{d\theta} = \frac{(k_2)(f_b)^2(w)(100)^3(B_o-x_c-2x_d)^2}{(F)(100)^2(1-x_c-x_d)^2} \qquad \text{E-5}$$

Combining the constants we let

$$H = \frac{(k_1)(f_a)(f_b)(100)(w)}{(F)} \text{ and } U = \frac{(k_2)(f_b)^2(100)(w)}{(F)}$$

Therefore

$$\frac{d(100x_c)}{d\theta} = \frac{(H)(100)(A_o-x_c)(100)(B_o-x_c-2x_d)}{(100)^2(1-x_c-x_d)^2} \qquad \text{E-6}$$

$$\frac{d(100x_d)}{d\theta} = \frac{(U)(100)^2(B_o-x_c-2x_d)^2}{(100)^2(1-x_c-x_d)^2} \qquad \text{E-7}$$

Equations E-6 and E-7 are now programed for the analog computer as shown in Figure (23).

The operating procedure used in obtaining the analog solution was as follows. The timing circuit shown at the bottom of Figure (23) was adjusted to give a solution time of three seconds. This was arbitrary and any pre-determined value could have been used. The coefficient pots $A_o$ and $B_o$, corresponding to the input data, were then adjusted. The computer was set for repeated operation and then started. Coefficient pots H and U, corresponding to the unknown rate constants, were adjusted until the values of $x_c$ and $x_d$ obtained from the analog solution were equal to the

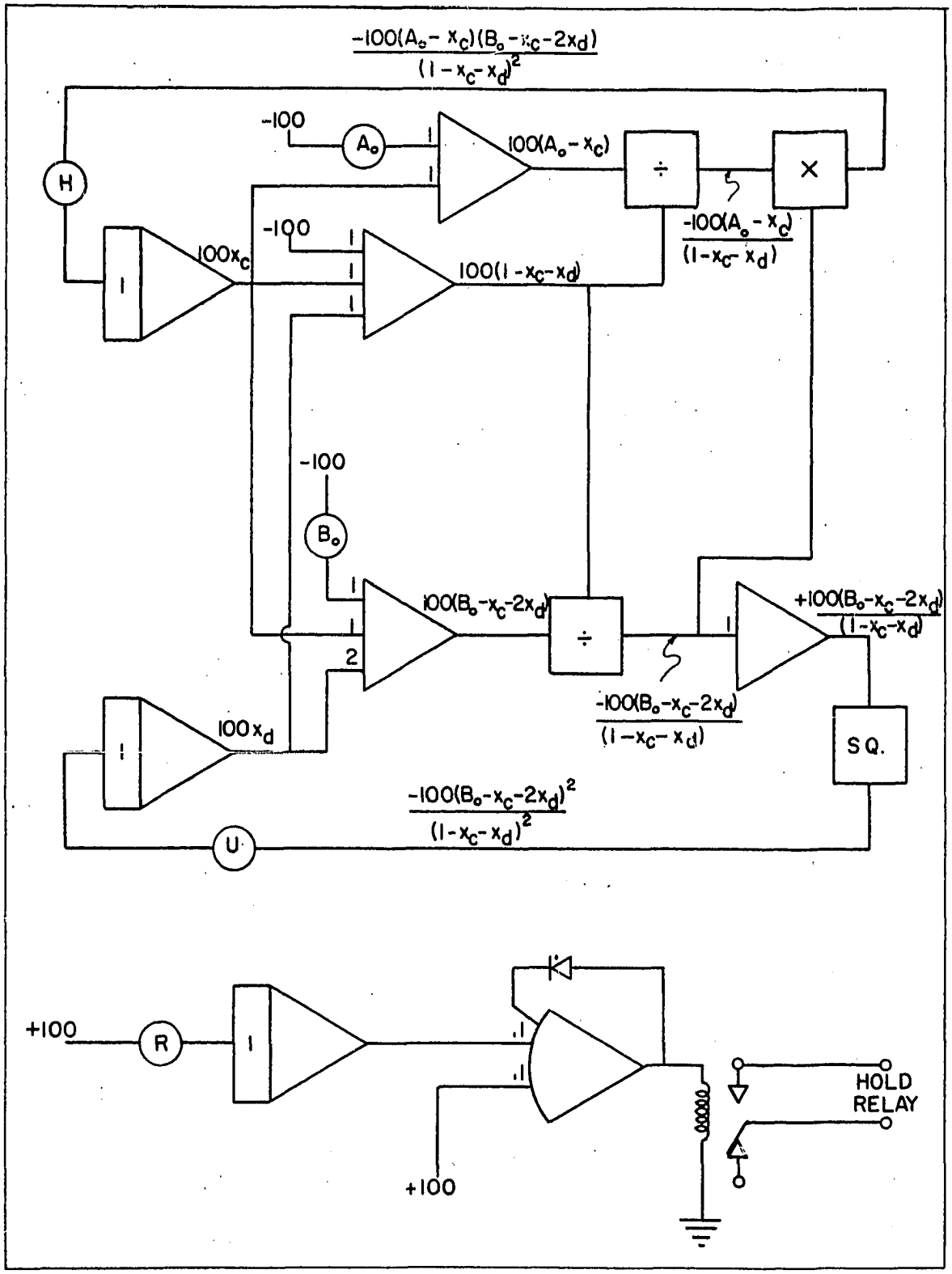


Figure 23 - Analog Computer Program for Solution of Differential Rate Equations

experimental values. Accurate values of H and U were determined from which subsequently the rate constants were obtained.

# APPENDIX F

# ANALYTICAL SOLUTION OF DIFFERENTIAL RATE EQUATIONS

1. Solution of Rate Equations for Determining the Rate Constants Based on Fugacities.

The differential rate equations to be solved for the raction rate constants are

$$\frac{dx_c}{dV_r} = \frac{(k_1)(f_a)(f_b)(A_o-x_c)(B_o-x_c-2x_d)}{(F)(1-x_c-x_d)^2} \qquad F\text{-}1$$

$$\frac{dx_d}{dV_r} = \frac{(k_2)(f_b)^2(B_o-x_c-2x_d)^2}{(F)(1-x_c-x_d)^2} \qquad F\text{-}2$$

For convenience let $K = (k_1)(f_a)(f_b)/F$ and $L = (k_2)(f_b)^2/F$ Therefore

$$\frac{dx_c}{dV_r} = \frac{(K)(A_o-x_c)(B_o-x_c-2x_d)}{(1-x_c-x_d)^2} \qquad F\text{-}3$$

$$\frac{dx_d}{dV_r} = \frac{(L)(B_o-x_c-2x_d)^2}{(1-x_c-x_d)^2} \qquad F\text{-}4$$

Rather than solving the two simultaneous differential equations, divide Equation F-4, by Equation F-3 and solve for the ratio of the rate constants. Therefore

$$\frac{dx_d}{dx_c} = \frac{(L)(B_o-x_c-2x_d)}{(K)(A_o-x_c)} \qquad F\text{-}5$$

With a slight rearrangement of Equation F-5 one obtains

$$\frac{dx_d}{dx_c} + \left(\frac{2L}{K}\right)\left(\frac{x_d}{A_o-x_c}\right) = \frac{(L)(B_o-x_c)}{(A_o-x_c)} \qquad F\text{-}6$$

Now, for simplicity, let $S = \frac{A_o-x_c}{A_o}$, $\epsilon = B_o-A_o$ and $N = \frac{2L}{K}$.

With this change in variable, the differential Equation F-6 may be written as

$$-\frac{dx_d}{dS} - \frac{(N)(x_d)}{S} = -\left(\frac{N}{2}\right)\frac{(\epsilon + A_o S)}{S} \qquad \text{F-7}$$

Using the integration factor $e^{\int -N/S\, dS} = \frac{1}{S^N}$, the analytical solution to this equation is

$$x_d = \frac{1}{2}\left[(\epsilon)(1-S^N) + \left[\frac{(N)(A_o)(S)}{(1-N)}\right]\left(S^{N-1}-1\right)\right] \qquad \text{F-8}$$

With a rearrangement and the substitution $\Pi = 2x_d - \epsilon$, the following equation is obtained.

$$S^N - (A\ )(S)\left(\frac{N}{(B\ )(N)-\epsilon}\right) + \frac{(\Pi\ )(N-1)}{(B\ )(N)-\epsilon} = 0 \qquad \text{F-9}$$

The only unknown in Equation F-9 is N since all the remaining quantities are known from experimental data. To solve for N break up Equation F-9 as follows

$$S^N = \frac{(A_o)(S)(N)}{(B_o)(N)-\epsilon} - \frac{(\Pi)\ (N-1)}{(B_o)(N)-\epsilon} \qquad \text{F-10}$$

Taking the natural logarithm and solving for N

$$N = \frac{\ln\left(\frac{(A_o)(S)(N)}{(B_o)(N)-\epsilon} - \frac{(\Pi)(N-1)}{(B_o)(N)-\epsilon}\right)}{\ln S} \qquad \text{F-11}$$

The value for N is obtained from this equation.

Now that the ratio of the reaction rate constants is known, it is possible to express $x_d$ in terms of $x_a$, or its equivalent S. Therefore, Equation F-3 may be expressed as

$$KdV_r = \frac{-(N-1)\left(1+S^N\left(B_o+\frac{A_o}{N-1}\right)+\frac{(A_o)(S)(N-2)}{N-1}\right)^2}{(4)(S)\left(S^N\left[B_o(N-1)+A_o\right]-(A_o)(S)\right)}\,dS \qquad F\text{-}12$$

Integrating the above expression with the appropriate limits of integration, one obtains

$$\int_o^{V_r} KdV_r = \int_1^S \frac{-(N-1)\left\{1+S^N\left(B_o+\frac{A_o}{N-1}\right)\frac{(A_o)(S)(N-2)}{N-1}\right\}^2}{(4)(S)\left(S^N\left[(B_o)(N-1)+A_o\right]-(A_o)(S)\right)}\,dS \qquad F\text{-}13$$

Denoting the value of the right side by C, then

$$KV_r = C \qquad F\text{-}14$$

$$k_1 = \frac{(C)(F)}{(V_r)(f_a)(f_b)} \qquad F\text{-}15$$

$$k_2 = \frac{(N)(F)(C)}{(2)(V_r)(f_b)}2 \qquad F\text{-}16$$

The reaction rate constants obtained from Equations F-15 and F-16 are the results of the analytical solution of the differential rate Equations F-1 and F-2.

The IBM 650 digital computer was used in the actual solution of the above equations. The method of successive substitution was used to determine N in Equation F-11. If N were equal to one then Equation F-11 would be identically satisfied. This was the solution obtained using Newton's method for finding the root of the equation. The integral in Equation F-13 was evaluated using Simpson's rule of integration.

2. Solution of Rate Equations for Determining the Rate Constants Based on Concentrations.

The differential equations to be solved are

$$\frac{dx_c}{dV_r} = \frac{(k_{1c})(P)^2(A_o-x_c)(B_o-x_c-2x_d)}{(F)(Z_m)^2(R)^2(T)^2(1-x_c-x_d)^2} \qquad \text{F-17}$$

$$\frac{dx_d}{dV_r} = \frac{(k_{2c})(P)^2(B_o-x_o-2x_d)^2}{(F)(Z_m)^2(R)^2(T)^2(1-x_c-x_d)^2} \qquad \text{F-18}$$

Assuming additive volumes then

$$Z_m = X_aZ_a+X_bZ_b+X_cZ_c+X_dZ_d \qquad \text{F-19}$$

where $Z_a$, $Z_b$, $Z_c$, and $Z_d$ = compressibility factors for ethylene, butadiene, cyclohexene and vinylcyclohexene respectively at the pressure and temperature in question.

Let $K_c = \frac{(k_{1c})(P)^2}{(F)(R)^2(T)^2}$ and $L_c = \frac{(k_{2c})(P)^2}{(F)(R)^2(T)^2}$.

Therefore by substitution

$$\frac{dx_c}{dV_r} = \frac{(K_c)(A_o-x_c)(B_o-x_c-2x_d)}{\left[(A_o-x_c)Z_a+(B_o-x_c-2x_d)Z_b+x_cZ_c+x_dZ_d\right]^2} \qquad \text{F-20}$$

$$\frac{dx_d}{dV_r} = \frac{(L_c)(B_o-x_c-2x_d)^2}{\left[(A_o-x_c)Z_a+(B_o-x_c-2x_d)Z_b+x_cZ_c+x_dZ_d\right]^2} \qquad \text{F-21}$$

Dividing Equation F-21 by Equation F-20 and integrating as previously shown gives

$$N' = \frac{\ln\left(\frac{(A_o)(S)(N')}{(B_o)(N')-\epsilon} - \frac{(\Pi)(N'-1)}{(B_o)(N')-\epsilon}\right)}{\ln S} \qquad \text{F-22}$$

where $N' = \frac{(2)(L_c)}{K_c}$, $S = \frac{A_o - x_c}{A_o}$, $\epsilon = B_o - A_o$

$\Pi = (2)(x_d) - \epsilon$.

Knowing the ratio of the reaction rate constants from the above equation, $x_d$ can be expressed in terms of $x_c$. Therefore Equation F-20 can be integrated with proper limits of integration to give

$$\int_o^{V_r} K_c dV_r = \int_1^S \frac{\left[(A_o)(S)(Z_a)+(Q)(Z_b)+A_o(1-S)Z_c+(M)Z_d\right]^2 (A_o)}{(A_o)(S)(Q)} dS \qquad \text{F-23}$$

where $Q = S^{N'}\left(\epsilon + \frac{(N')(A_o)}{N'-1}\right) - \frac{(A_o)(S)}{N'-1}$

and $M = \frac{(N')(A_o)(S)}{(2)(N'-1)} - \frac{(S^{N'})\left[(B_o)(N')-\epsilon\right]}{(2)(N'-1)} + \frac{\epsilon}{2}$

Denoting the value of the right side of Equation F-23 by C', then

$$K_c V_r = C' \qquad \text{F-24}$$

$$k_{1c} = \frac{(C')(F)(R)^2(T)^2}{(P)^2(V_r)} \qquad \text{F-25}$$

$$k_{2c} = \frac{(N')(C')(F)(R^2)(T^2)}{(2)(V_r)(P)^2} \qquad \text{F-26}$$

Equations F-25 and F-26 are the solutions for the reaction rate constants based on concentrations. The IBM 650 digital computer was used in the actual solution of these equations as previously described.

# APPENDIX G

# REACTION RATE CONSTANTS DETERMINED FROM THE ANALYTICAL SOLUTION OF THE DIFFERENTIAL RATE EQUATIONS

TABLE 3

REACTION RATE CONSTANTS DETERMINED FROM THE ANALYTICAL SOLUTION OF THE DIFFERENTIAL RATE EQUATIONS

| Run # | $k_1$ | $k_2$ | $k_{1c}$ | $k_{2c}$ |
|---|---|---|---|---|
| | mole/hr.-lb./sq.in.-cu.ft. | mole/hr.-lb./sq.in.-cu.ft. | cu.ft./-mole hr. | cu.ft./-mole hr. |
| 77 | 5.23 | 20.1 | 7.33 | 26.5 |
| 78 | 5.27 | 21.1 | 7.36 | 27.8 |
| 79 | 5.38 | 26.3 | 7.35 | 33.8 |
| 80 | 4.88 | 15.9 | 6.92 | 21.1 |
| 81 | 4.41 | 19.0 | 5.60 | 21.3 |
| 82 | 5.06 | 20.2 | 6.47 | 22.7 |
| 83 | 4.60 | 17.2 | 5.90 | 19.4 |
| 84 | 1.04 | 4.01 | 1.17 | 4.09 |
| 85 | 0.99 | 3.80 | 1.12 | 3.90 |
| 86 | 1.20 | 7.20 | 1.09 | 5.69 |
| 87 | 1.06 | 5.76 | 0.995 | 4.43 |
| 88 | 1.04 | 5.00 | 1.03 | 4.00 |
| 89 | 1.04 | 5.13 | 1.00 | 4.04 |
| 90 | 1.02 | 5.45 | 1.02 | 4.49 |
| 91 | 1.10 | 6.90 | 1.06 | 5.47 |
| 92 | 0.944 | 2.71 | 1.14 | 3.15 |
| 93 | 1.38 | 7.63 | 1.02 | 3.98 |
| 94 | 1.49 | 9.15 | 1.03 | 4.48 |
| 95 | 1.24 | 6.01 | 0.97 | 3.36 |
| 96 | 1.25 | 6.56 | 0.93 | 3.47 |
| 97 | 1.58 | 8.83 | 1.20 | 4.03 |
| 98 | 1.69 | 9.16 | 1.32 | 4.31 |
| 99 | 1.60 | 9.07 | 1.22 | 4.14 |
| 100 | 0.156 | -- | 0.106 | -- |
| 101 | 0.164 | 0.753 | 0.106 | 0.364 |
| 102 | 0.163 | 0.751 | 0.105 | 0.362 |
| 103 | 0.171 | 0.882 | 0.116 | 0.437 |
| 104 | 0.278 | 1.95 | 0.125 | 0.540 |
| 105 | 0.292 | 2.29 | 0.121 | 0.582 |
| 106 | 0.370 | 2.80 | 0.142 | 0.661 |
| 107 | 0.316 | 2.35 | 0.132 | 0.600 |
| 108 | 0.282 | 2.04 | 0.128 | 0.568 |
| 109 | 0.541 | 4.49 | 0.234 | 1.03 |
| 110 | 0.498 | 3.95 | 0.222 | 0.938 |
| 111 | 0.504 | 3.91 | 0.217 | 0.897 |
| 112 | 0.471 | 2.78 | 0.389 | 1.81 |

TABLE 3--Continued

| Run # | $k_1$ | $k_2$ | $k_{1c}$ | $k_{2c}$ |
|---|---|---|---|---|
| | mole/hr.-lb./sq.in.-cu.ft. | mole/hr.-lb./sq.in.-cu.ft. | cu.ft./-mole hr. | cu.ft./-mole hr. |
| 113 | 0.470 | 2.51 | 0.375 | 1.58 |
| 114 | 0.356 | 2.12 | 0.346 | 1.83 |
| 115 | 0.370 | 2.16 | 0.365 | 1.89 |
| 116 | 0.368 | 2.20 | 0.360 | 1.92 |
| 117 | 0.361 | 2.94 | 0.364 | 2.63 |
| 118 | 0.500 | 2.65 | 0.393 | 1.64 |
| 119 | 0.425 | 2.61 | 0.353 | 1.71 |
| 120 | 0.475 | 2.65 | 0.382 | 1.68 |
| 121 | 0.477 | 3.64 | 0.363 | 2.18 |
| 122 | 0.750 | 5.48 | 0.435 | 2.16 |
| 123 | 0.783 | 5.81 | 0.452 | 2.27 |
| 124 | 0.697 | 4.39 | 0.418 | 1.78 |
| 125 | 0.754 | 5.14 | 0.419 | 1.93 |
| 126 | 0.647 | 4.83 | 0.394 | 1.99 |
| 127 | 1.05 | 8.44 | 0.630 | 2.98 |
| 128 | 0.998 | 6.66 | 0.602 | 2.38 |
| 129 | 0.913 | 6.32 | 0.561 | 2.30 |
| 130 | 1.02 | 7.14 | 0.621 | 2.56 |
| 131 | 0.668 | 4.88 | 0.393 | 1.94 |
| 132 | 0.546 | 4.60 | 0.242 | 1.04 |
| 133 | 0.412 | 3.16 | 0.184 | 0.754 |
| 134 | 1.24 | 0.698 | 0.104 | 0.503 |
| 135 | 0.261 | 0.212 | 0.114 | 0.567 |
| 136 | 0.467 | 4.01 | 0.205 | 0.937 |
| 137 | 0.611 | 4.40 | 0.367 | 1.79 |
| 138 | 0.611 | 4.15 | 0.386 | 1.77 |
| 139 | 1.27 | 9.92 | 0.997 | 5.51 |
| 140 | 1.39 | 9.89 | 1.06 | 5.33 |